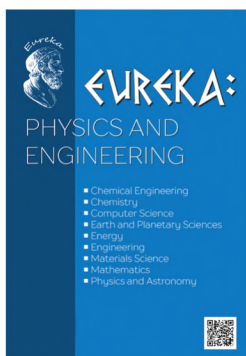# EUREKA:

PHYSICS AND ENGINEERING

- Chemical Engineering
- Chemistry
- Computer Science
- Earth and Planetary Sciences
- Energy
- Engineering
- Materials Science
- Mathematics
- Physics and Astronomy

SCIENTIFIC JOURNAL

EUREKA: Physics and Engineering – scientific journal whose main aim is to publish materials allowed to see *new discoveries at the intersection of sciences.*

- Chemical Engineering
- Chemistry
- Computer Science
- Earth and Planetary Sciences
- Energy
- Engineering
- Material Science
- Mathematics
- Physics and Astronomy
- Technology Transfer

EUREKA: Physics and Engineering publishes
4 types of materials:
　　– review article,
　　– progress reports,
　　– original Research Article
　　– reports on research projects

CONTENT

DEVELOPMENT OF INFORMATION VISUALIZATION METHODS FOR USE IN MULTIMEDIA APPLICATIONS

Yevhen Hrabovskyi
Department of Computer Systems and Technologies[1]
maxmin903@gmail.com

Natalia Brynza
Department of Informatics and Computer Engineering[1]
natalia.brynza@hneu.net

Olga Vilkhivska
Department of Informatics and Computer Engineering[1]
grom_o@i.ua

[1]*Simon Kuznets Kharkiv National University of Economics*
9-a Nauky ave., Kharkiv, Ukraine, 61166

Abstract

The aim of the article is development of a technique for visualizing information for use in multimedia applications. In this study, to visualize information, it is proposed first to compile a list of key terms of the subject area and create data tables. Based on the structuring of fragments of the subject area, a visual display of key terms in the form of pictograms, a visual display of key terms in the form of images, and a visual display of data tables are performed. The types of visual structures that should be used to visualize information for further use in multimedia applications are considered. The analysis of existing visual structures in desktop publishing systems and word processors is performed.

To build a mechanism for visualizing information about the task as a presentation, a multimedia application is developed using Microsoft Visual Studio software, the C# programming language by using the Windows Forms application programming interface. An algorithm is proposed for separating pieces of information text that have key terms. Tabular data was visualized using the "parametric ruler" metaphorical visualization method, based on the metaphor of a slide rule.

The use of the parametric ruler method on the example of data visualization for the font design of children's publications is proposed. Interaction of using the method is ensured due to the fact that the user will enter the size of the size that interests for it and will see the ratio of the values of other parameters. The practical result of the work is the creation of a multimedia application "Visualization of Publishing Standards" for the visualization of information for the font design of publications for children. The result of the software implementation is the finished multimedia applications, which, according to the standardization visualization technique in terms of prepress preparation of publications, is the final product of the third stage of the presentation of the visual form.

Keywords: information visualization, multimedia application, visual display, key terms.

1. Introduction

In the process of development of modern society, the computer era has begun – the era of information and informatization. Hundreds of terabytes of information appear annually in local and global networks. Mechanisms are being introduced to search for the necessary information, however, these tools are effective when users have a specific goal and understand what information is stored. In other cases, methods for visualizing information can help the user.

The main objective of visualization is the use of human visual perception of information to enhance its cognitive abilities. The human visual system is capable of quickly processing visual signals, and advanced information technology has turned the computer into a powerful tool for managing digital information. Visualization is a bridge connecting the human visual system and the information system, helping to identify images, hypothesize and extract ideas from huge data sets, and contributes to scientific research and forecasting. The main purpose of visualization is the use of human visual perception of information to enhance its cognitive abilities.

To date, there are a large number of techniques that are devoted to the visualization of various information [1–5]. In a variety of information it is possible to understand objects that

have a physical nature (scientific visualization), program codes, software (software visualization), etc.

According to various methods of visualizing information in specialized literature [6–10], mechanisms for controlling the quality of content and optimizing the interface of multimedia applications are proposed.

The most effective application of information visualization in various multimedia applications will facilitate the perception of a large amount of text information and facilitate its visual representation in multimedia systems.

2. Materials and Methods

The research methods are as follows. Analysis and synthesis are used at all stages of the study. Induction and deduction methods are used to study the theoretical foundations of the design of multimedia applications and determine the subject area of information visualization. Logical analysis is applied to study the principles of information visualization existing in theory and practice in the process of designing multimedia applications.

3. Experimental procedures

The first stage of the information visualization technique for use in multimedia applications should consist of two steps:

1) formation of a list of key terms of the subject area;

2) formation of data tables.

Step 1. 1. Formation of a list of key terms.

Raw data can be presented in any form, starting with spreadsheets and ending with unstructured texts. Key terms will be used as raw data to be used in the process of visualization of publishing standards.

Step 1. 2. Formation of data tables.

The second stage of the standardization visualization technique consists of the following steps:

1) visual display of key terms in the form of pictograms;

2) visual display of key terms in the form of images;

3) visual display of data tables.

Visual structures are images that fully convey the content of the keyword. To visualize information with a view to further use in multimedia applications, it is necessary to apply three types of visual structures:

1) the first type is pictograms that schematically depict the content of the key term;

2) the second type is an image, which is an example of the use of key terms in practice;

3) the third type is the interactive infographics of parameter ruler, with the help of which tabular data is presented.

It is important to choose the most expressive visual structure that reflects all the data without loss, which can easily and quickly be interpreted by a person with the least number of errors and to the maximum transfers all the differences in the data. The visual structures of the first type are developed in accordance with existing examples of the use of key terms of a multimedia publishing house. The second type of visual structures is also developed independently, but some structures have already been developed and are used in desktop multimedia publishing systems. The third type of visual structures is the parameter ruler interactive infographic, which refers to one of the visualization methods, namely metaphor visualization, with which the data will be visualized.

Programs of the electronic publishing house QuarkXPress, Adobe InDesign, Adobe PageMaker have already developed visual structures regarding key terms in the field of prepress preparation of publications, in particular in terms of general concepts, design and execution of the publication page and printing performance of the publication. Visual structures refer to pictograms that are used as interface elements of desktop publishing systems – these are buttons that convey the contents of a key term in the field of multimedia publishing. Visual structures that convey the content of key terms in the field of prepress publications, in particular, are used not only in desktop publishing systems,

4

but also in a regular text editor such as Microsoft Word. A set of pictograms is formed on the basis of pictograms distributed in desktop publishing systems and word processors (**Table 1**).

Table 1

Analysis of existing visual structures in desktop publishing and word processors

Key term	Desktop publishing & word processor			
	Adobe PageMaker	**Adobe InDesign**	**QuarkXPress**	**Microsoft Word**
Edition page	▯	▯	▯	▯
Font group				
Indent		☰	☰	Absent
Initial	Absent	A☰	A☰	A☰
Illustration	⊠	⊠	🖼	
Table	▦	▦	▦	
Text	T	T	T	T
Mark	N**B***I*	Absent	**B***I*	**Ж***К*Ч
Fields	Absent	Absent	Absent	▯
Publication format	Absent	Absent	Absent	▯

The analysis of existing visual structures will help to develop all other structures that have no analogues in desktop publishing. The visual structures that were discovered during the analysis, some will be used without changes, some will be amended. The selected and developed pictograms have a different display style, some flat and some voluminous, in order to present them in a single style, a "flat design" was chosen.

"Flat" design – a minimalistic approach to the design of objects, which emphasizes ease of use, it is more focused on the end user.

As a result of applying a "flat" design with respect to the pictograms, the following results were obtained (**Table 2**).

Table 2

Pictograms in flat design style

Edition block	Edition	Main page	Text
▢	▤	▥	T
Complex notebook	**Notebook**	**Borderless edition page format**	**Font group**
📖	📖	▯	T
Compiled cover	**Base**	**Frontispiece**	**Title**
Тип 4	▯	▯	▤

The third stage of the methodology consists of 3 steps:

1) development of a general concept of presentation;

2) development of the constituent elements of the presentation;

3) implementation of navigational interaction of presentation elements.

Step 3. 1. Determine in what form the data tables and visual structures will be reflected.

Relative to the task, a multimedia application based on Microsoft Visual Studio software, the C# programming language, using the Windows Forms application programming interface is being developed as a presentation.

Step 3. 2. Implementation of navigational interaction of presentation elements.

Navigation through the multimedia application for the visualization of information should be performed according to the following scheme (**Fig. 1**).

Fig. 1. Navigation through the multimedia application for the visualization of information

The navigation of elements of a visual form is implemented directly by writing code for each form and each of its elements.

Presentation of a visual form interactively changes and complements visual structures in order to get visualization from a static presentation by setting graphic parameters – to get a representation of the visual structure. The multimedia application developed using the C # programming language using XML (the standard for constructing markup languages for hierarchically structured data for exchanging between different applications) acts as a visual form.

4. Results

The formation of data tables takes place in two stages.

The first stage is the formation of the data Table "terms – determination".

The second stage is the formation of the data Table "term – a piece of information" based on the use of a piece of information, which is visualized.

The formation of the data Table "terms – fragments of information" consists in isolated fragments of the text of the source information containing the key term (**Fig. 2**).
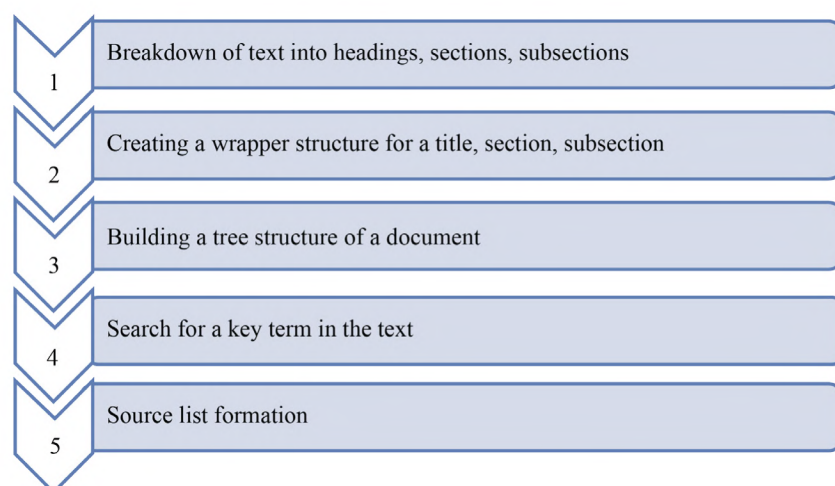
Fig. 2. The algorithm for separating text fragments of information that have key terms

Relative to each key term, visual structures are developed, and data tables are also supplemented – these are pictograms and images.

It is proposed to use interactive infographics to create visualized tabular data.

6

To visualize tabular data in publishing standards, it is proposed to select a method from the "metaphorical visualization" group. Visual metaphors have a dual function: firstly, they present information in graphical form in order to organize and structure it, and secondly, they convey an idea of the information presented through the key characteristics of the metaphor that is used. Metaphors are useful because they allow to explain an abstract concept in specific conditions, which makes it easier to understand. They can also cause an emotional reaction.

Tabular data can be visualized using the metaphorical visualization method "parametric ruler". This interactive method is based on a metaphor of a slide rule that allows users to move the scales to analyze various combinations of parameter values. "Parametric ruler" refers to interactive infographics, because the user has the opportunity to interact with the information display system and observe its reaction.

Alternative methods for solving the tasks are indexing and using classification and clustering algorithms.

Indexing is necessary to extract some attributes of visualization objects; they convey the meaning and content of the objects themselves. It is necessary the different indexing algorithms depending on the nature of the data: for example, natural language processing algorithms (dictionaries of keywords, key phrases, group of names, parts of speech) for collections of texts; image processing algorithms (segmentation by color, brightness, structure) for image collections; audio processing algorithms (by sound and pitch) for collections of audio files; video processing algorithms (scene segmentation) for video collections.

Classification algorithms distribute visualization objects into certain categories (groups) using machine learning algorithms, for example, Bayes algorithm, k-nearest neighbor algorithm, neural network algorithms, etc.

Clustering algorithms dynamically divide visualization objects into groups by calculating some degree of similarity between them, for example, the k-average algorithm, Kohonen self-organizing maps, hierarchical algorithms, etc. As a result, matrices are obtained that describe objects and the relationships between them and their groups.

However, the methods of indexing and using classification and clustering algorithms do not provide opportunities to facilitate the perception of a large amount of textual information and to ensure its presentation in multimedia systems.

Let's consider the use of the metaphorical visualization method "parametric ruler" on the example of data visualization for the font design of publications for children.

The parameters will include: font size, leading increase, minimum line length, maximum line length, font group, font capacity on the Cyrillic graphic basis, font capacity on the Latin graphic basis, styles. Horizontal scales with possible parameter values, sorted from small to large, should move relative to each other. Interactivity is realized due to the fact that the user will enter the size of the size that interests for it and will see the ratio of the values of other parameters (**Table 3, Fig. 3**).

Table 3
Font design of publications for children

Font size, at least, points	Leading increase, not less, points	Line length				Font group	Font capacity, no more sign/sq.	Mark
		minimal		maximal				
		squares	mm	squares	mm			
20 and more	2	6 1/2	117	9 1/2	171	Sans-serif (grotesque) or with serif	5,0 (5,5)*	Normal or wide bright direct
16–18	4	6 1/2	117	9 1/4	167	Sans-serif (grotesque) or with serif	6,0 (6,6)*	Normal or wide bright direct
14	4	6	108	8 1/2	153	Sans-serif (grotesque)	6,7 (7,4)*	Normal or extra wide bright direct
12**	2	5	90	8 1/2	153	Sans-serif (grotesque)	7,7	Normal, wide or extra wide bright direct

*Note: * – for a font on a Latin graphic basis; ** – for additional text that is over 200 characters per page*
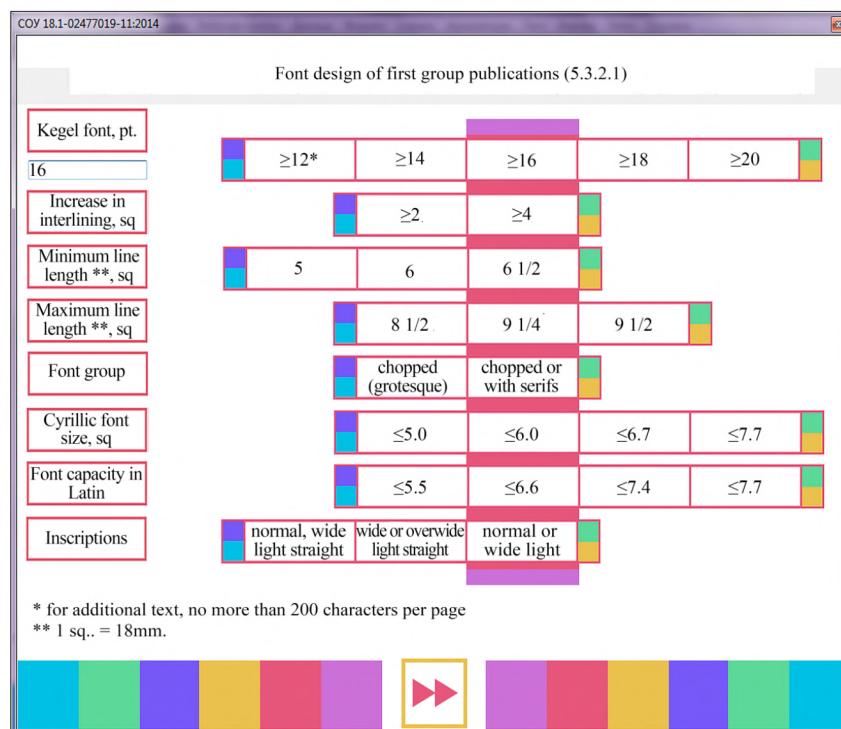
Fig. 3. The Table and the result of its visualization

Tables visualized in this way will help simplify the process of covering a large amount of information, as well as reduce the cost of finding the necessary data and consolidate them at the visual level.

The existing data Table "term – definition – standard fragment – visual structures" has the following data set: key term, definition, standard fragments, and visual structures. The grouped data of the table, namely key terms, their definitions and visual structures will be presented in the form of a kind of database, namely in the form of an xml-file (keywords.xml) (**Fig. 4**).

```xml
<?xml version="1.0" encoding="utf-8" ?>
<keywords>

<chapter name="...">
 <keyword name="..." image="..." icon="...">...</keyword>
</chapter>

</keywords>
```

Fig. 4. The structure of the xml file that contains the elements of the data Table "term – definition – visual structures"

The structure of the xml file consists of tags. In principle, xml is a database with a tree structure (**Fig. 5**).

The root tag <keywords> ... </ keywords>, it lists the entire list of grouped key terms. The <chapter> ... </ chapter> tag represents each group of key terms (General concepts, Design and implementation of a publication's page, Design and implementation of a publication's block, Design and implementation of a publication's cover, Target design of a publication, and Polygraphic execution of a publication). This tag has the attribute name="...", in which it is necessary to declare the name of the group of key terms in quotation marks. The <keyword> ... </ keyword> tag is responsible for the safety of elements from the data Table "term - definition – visual structures", namely the key term, definition, visual structure of the first and second type. This tag has three attributes name="...", image="...", icon="...". The attribute name="..." is responsible for the preservation of the

8

key term, the name of which must be placed in quotation marks after the declaration of the attribute. The attribute image="..." is responsible for the preservation of the visual structure of the first type, in the blots of this attribute, it is necessary to specify the path of the corresponding image, the attribute icon="..." is responsible for the preservation of the visual structure of the second type, in the blots of this attribute it is necessary to register the path of the corresponding icon. The term definition is placed between the <keyword> ... </ keyword> tags.
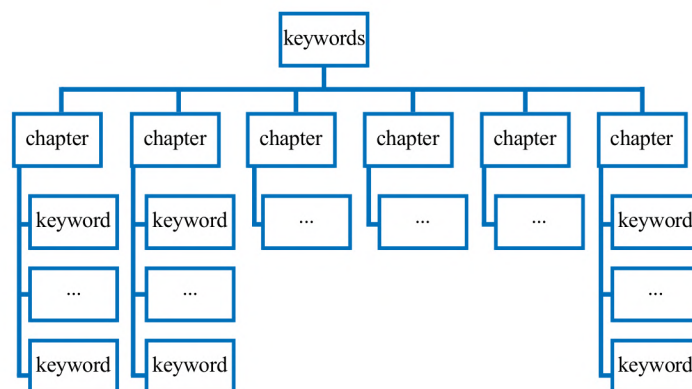
Fig. 5. The tree structure of the xml file that contains the elements of the data Table "term – definition – information fragment – visual structures"

The existing structure of the xml-file is filled with elements from the data Table "term – definition – visual structures" (keywords.xml) (**Fig. 6**).

```xml
<keywords>
    <chapter name=" General concepts ">
    <keyword     name="Edition     block"     image="images\zagal1.jpg"
icon="images\z2.png">
    a set of printed sheets or notebooks, enclosed at the root, containing all
pages of a future edition.
    </keyword>
    <keyword          name="Edition"          image="images\zagal.jpg"
icon="images\z.png">
    a printed product intended for the dissemination of information contained
therein, has undergone editorial and publishing work, is self-printed and has
original information.
    </keyword>
    <keyword          name="Cover"          image="images\zagal2.jpg"
icon="images\z3.png">
    the outer cover of the edition that connects to the unit without the
flywheels.
    </keyword>
    <keyword          name="Bookbinding"          image="images\zagal3.jpg"
icon="images\z4.png">
    the outer covering of the product that connects to the block with or without
the two flywheels and the core material.
    </keyword>
    </chapter>
</keywords>
```

Fig. 6. The xml file filled with elements of the data Table "term – definition – visual structures"

The xml-file filled with elements of the data Table is responsible for the safety of the data that will be used in the future developed by the multi-dairy edition.

5. Discussion

Microsoft Visual Studio, the C# programming language using Windows Forms, was chosen as a tool for developing an electronic publication.

9

The practical result of this work is the creation of a multimedia application "Visualization of Publishing Standards" for the visualization of information for the font design of publications for children. The design of this multimedia application was developed according to new trends in the field of design – the "flat" design (flat design), as evidenced by the colors and navigation elements used in the multimedia application.

Basic principles of Flat design:

1) lack of unnecessary effects;

2) simplicity of the elements;

3) accurate work with fonts. The use of simple elements increases the importance of typography in design. Working with fonts should be done very carefully. The nature of the font should complement, and not contradict, the general design scheme. A font in a "flat" design is an important navigation element. The simplicity of the elements does not mean that complex fonts cannot be used. Simply, everything should be sustained in the style of minimalism;

4) minimalism. In a "flat" design, it is possible to avoid unnecessary "bells and whistles", complex approaches to the visualization of elements.

The structure of the application "Visualization of Publishing Standards" has four component forms, each of which has corresponding elements (which perform the corresponding navigation and interactive tasks) and performs functional tasks. The general concept of the multimedia application is presented in **Fig. 7**.
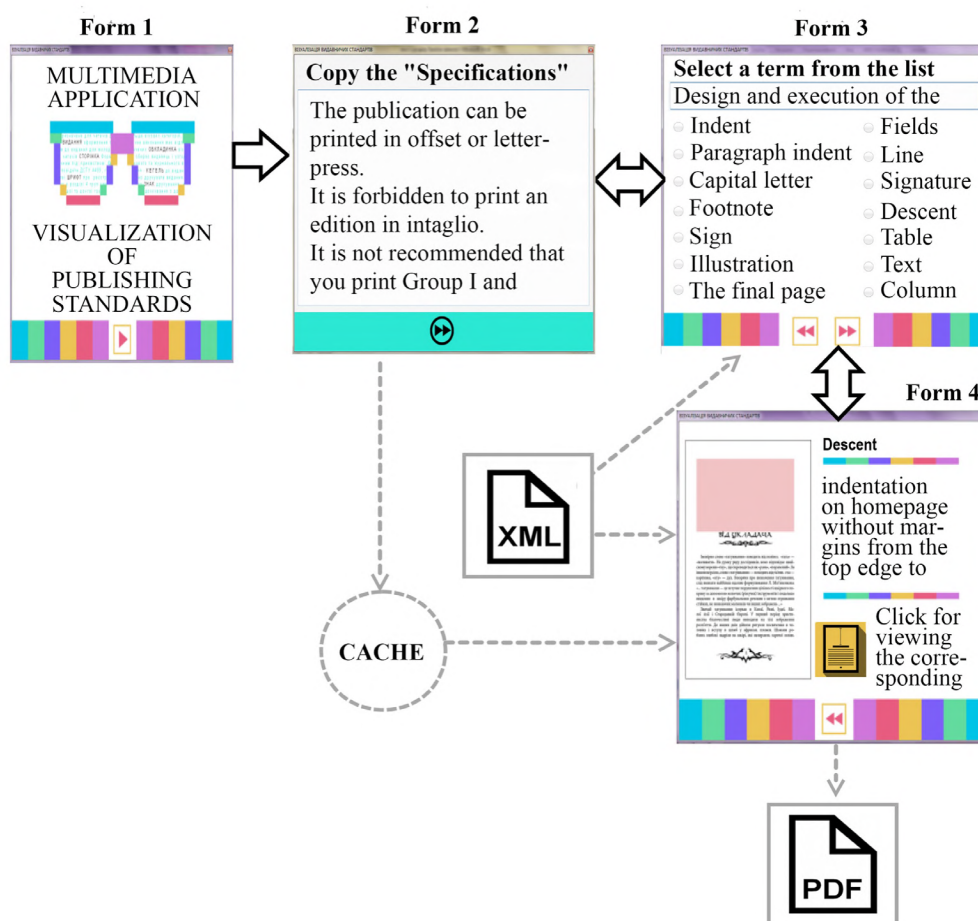
Fig. 7. The work scheme of the "Visualization of publishing standards" multimedia application

The software implementation of a multimedia application begins with the creation of a new project in the Microsoft Visual Studio environment, namely the WindowsFormsApplication proj-

ect, which will allow to begin creating windows (form) of the future multimedia application. At the beginning of the creation of forms, let's determine the size of the future publication and the ability to change the size of the form. In order to set the sizes of future forms, the application needs to specify the sizes in pixels in the properties of the forms in the Size section: 900; 754. The future multimedia application has fixed form sizes, therefore, in the form properties in the FormBorder-Style section, specify the value FixedToolWindow. It is also necessary to enter a name for the future publication and fix the icon, in the Text section let's mark "Visualization of information", and in the Icon section let's define an icon for the future multimedia application. For each form, a developed background image is loaded using the section in the properties of the BackgroundImage forms.

Form 1 of the application has only one element – this is the navigation element – the button (button1), which is responsible for switching to relatively (**Fig. 8**).

This code is in the class Form1.cs.

```
private void button1_Click(object sender, EventArgs e)
{
    // At the click of a button go to form 2
    var form2 = new Form2();
    form2.Show();
    this.Hide();
}
```

Fig. 8. The program code of the button, which makes the transition to Form 2

Form 2 has three elements: the first label1 – does not have any navigation and interactive functions, it is just an inscription, informs the user about what needs to be done in this form, the second element is textBox1, the field into which it is necessary to copy a fragment of the standard text (section "Technical requirements") and the third element is button1, which is responsible for saving the text that was entered into textBox1 by activating the corresponding class, as well as for switching to the next form (**Fig. 9**).

This code is in the class Form2.cs.

```
private void button1_Click(object sender, EventArgs e)
{
    // Memorizes the entered text
    Program.State.Text = textBox1.Text;

    // Press the button to go to form 3
    var form3 = new Form3();
    form3.Show();
    this.Hide();
}
```

Fig. 9. The program code of the button, performs the operation of saving text and transition to Form 3

The code that declares the State class, which is responsible for saving the entered text, is in the Program.cs class (**Fig. 10**).

```
// A global object for storing information
public static State State { get; private set; }
```

Fig. 10. State class declaration

The description of the State class is found in State.cs (**Fig. 11**).

```csharp
using System.Collections.Generic;
using System.Linq;
using System.Xml.Linq;

namespace PublicationStandartsVisualization
{
    ///<summary>
    /// A class that stores the state of an application at runtime
    /// It also has a database of key terms
    ///<summary>
    public class State
    {
        public string Text { get; set; }
        public Chapter SelectedChapter { get; set; }
        public Keyword SelectedKeyword { get; set; }
        public IEnumerable<Chapter> Chapters { get; set; }
        public static State Load()
    {
        // Creating an empty status object
        var result = new State();
        try
        {
            // Open keywords file
            var keywordsDocument = XDocument.Load("keywords.xml");

            // Handling groups of key terms for the drop-down list
            result.Chapters = keywordsDocument
            .Descendants("chapter")
            .Select(c => new Chapter
                {
                    Name = c.Attribute("name").Value,
                    Keywords = c.Elements("keyword")
                        .Select(ParseKeyword).ToArray()
                }).ToArray();
        }
        catch
        {
        }
        return result;
    }
    // Processing each keyword from a configuration file
    private static Keyword ParseKeyword(XElement el)
    {
        var imageAttr = el.Attribute("image");
        var iconAttr = el.Attribute("icon");
        return new Keyword
            {
            Name = el.Attribute("name").Value,
            Image = imageAttr != null ? imageAttr.Value : null,
            Icon = iconAttr != null ? iconAttr.Value : null,
            Description = el.Value
            };
    }
    }
}
```

Fig. 11. State class program code

Form 3 has five elements: the first label1 does not have any navigation and interactive functions, it is just an inscription that informs the user about what needs to be done in this form, the second comboBox1 element is a drop-down list of terms group names, the third flowLayoutPanel1 element reflects the list key terms using the RadioButton elements, the fourth element of button1 is the transition to Form 2, the fifth element of button2 is the transition to Form 3.

The second and third elements are related to each other, because when to select one of the group names options presented in comboBox1, the set of key terms that are part of the flowLayout-Panel1 element will change (**Fig. 12**).

This code is in the class Form3.cs.

12

```
private void comboBox1_SelectedIndexChanged(object sender, EventArgs e)
    {
        // Check whether events can be processed from the drop-down list
        if (!isInitialized) return;

        // Cleaning the panel with RadioButton
        flowLayoutPanel1.Controls.Clear();

        // Memorizes the selected item from the list
        var chapter = comboBox1.SelectedItem as Chapter;
        if (chapter == null) return;
        Program.State.SelectedChapter = chapter;

        // Fill in the RadioButton panel from the key terms associated with the drop
down box
        bool hasSelection = false;
        foreach (var k in chapter.Keywords)
        {
            // Creating a RadioButton with a key term name
var rb = new RadioButton {Text = k.Name, Margin = new Padding(5), Tag = k,
Width = 300, Height=28};
            // If this is the last selected key term (the user has returned to form 4) mark
it as selected
            if (Program.State.SelectedKeyword == k)
            {
                hasSelection = true;
                rb.Checked = true;
            }
            flowLayoutPanel1.Controls.Add(rb);
        }
        // If no key terms are selected, select the first term in the list
        if (!hasSelection)
        {
        (flowLayoutPanel1.Controls[0] as RadioButton).Checked = true;
        }
    }
}
```

Fig. 12. The program code of the comboBox1 (flowLayoutPanel1) elements

Buttons button1 and button2 navigate – go to Form 2 and Form 4 (the code is also in the file Form3.cs) (**Fig. 13**).

```
private void button1_click( object senter, EventArgs e)
    {
        // click buttons to go to form 2
        var form2 = new Form2();
        form2.Show();
        this.Hide();
    }
        private void button1_click( object senter, EventArgs e)
    }
        // searching for RadioButton favorites and memorizing the associated
        key term
        foreach (var rb in
flowLayotPanel1.Controls. 0fType< RadioButton>())
            if (rb.Checked)
            {
                Program.State.SelectedKeyword = rb. Tag as Keyword;
            }
        }
        // click buttons to go to form 4
        var form4 = new Form4();
        form4.Show();
        this.Hide();
```

Fig. 13. Program code for button1 and button2

13

Form 4 has six elements: label 1 – display of the key term, piturebox – reflection of the first type of visual structures, richtextbox – reflection of the definition of the key term, button1 – transition to Form 3, button 2 – opening a pdf file with a visual structure of the second type, label 2 – an inscription corresponding to the task of Button 2 (**Fig. 14**).

This code is in the class Form 4.cs.

```csharp
public Form4 ()
{
    InitializeComponent();
    // The key term chosen on Form3
    var keyword = Program.State.SelectedKeyword;
    if (keyword !=null)
    {
        // Displays an image related to a key term
        // If there is no image, show the default image
        if(string.IsNullOrEmpty(keyword.Image))
        {
            pictureBox1.Image = Properties.Resources.no_image;
        }
        else
        {
            pictureBox1.Image = Bitmap(keyword.Image);
        }
        // Display the key term related icon on the PDF output button
        // If there is no icon, show the default icon
        if (string.IsNullOrEmpty(keyword.Icon))
        {
            button2.Image = Properties.Resources.no_icon;
        }
        else
        {
        button2.Image = new Bitmap(keyword.Icon);
        }
        // Output the name of the key term
        label1.Text = keyword.Name;
    // Output of key term description
        richTextBox1.Clear();
        richTextBox1.SelectAll();
        var i = richTextBox1.SelectionLength;
        richTextBox1.AppendText((keyword.Description ?? "").Trim(new[] {
' ', '\r', '\n', '\t' }));
        }
    }
private void button2_click( object senter, EventArgs e)
{
    // search in the text typed in Form 2 for the key term selected in Form 3
    var chapters = TextSearch.FindString(Program.State.Text,
Program.State.SelectedKeyword.Name).ToArray();

    // if not found, show the message
    If (chapters.Length == 0)
    {
        messageBox.Show("No matching snippets were found!");
        return;
    }
    // create a temporary file to burn a PDF document
    var file = Path.GetTempFileName();
    file = Pats.ChangeExtension(file, "pdf");

    // Generate a PDF document in a temporary file
    PDFHelper.CreatePDF(file, chapters);
    // wait for the operation to complete
    System.Threading.Thread.Sleep(1800);
    // open pdf document
    Process.Start(file);
}
private void button1_click( object senter, EventArgs e)
{
    // click buttons to go to form 3
    var form3 = new Form3();
    form3.Show();
    this.Hide();
}
```

Fig. 14. Program code for Form 4

14

In the process of writing code for Form 4, two auxiliary classes were added – TextSearch.cs, which searches for fragments of text that was entered in Form 2, which contains the key term that is selected on Form 3 and PDFHelper.cs, which generates PDF-document.

The structure of the application "SOU 22.2-02477019-11: 2014 Printing. Edition for children. General Technical Requirements" has eight component forms, each of which has corresponding elements (which perform the corresponding navigation and interactive tasks) and performs functional tasks. The general concept of the multimedia application is presented in **Fig. 15**.
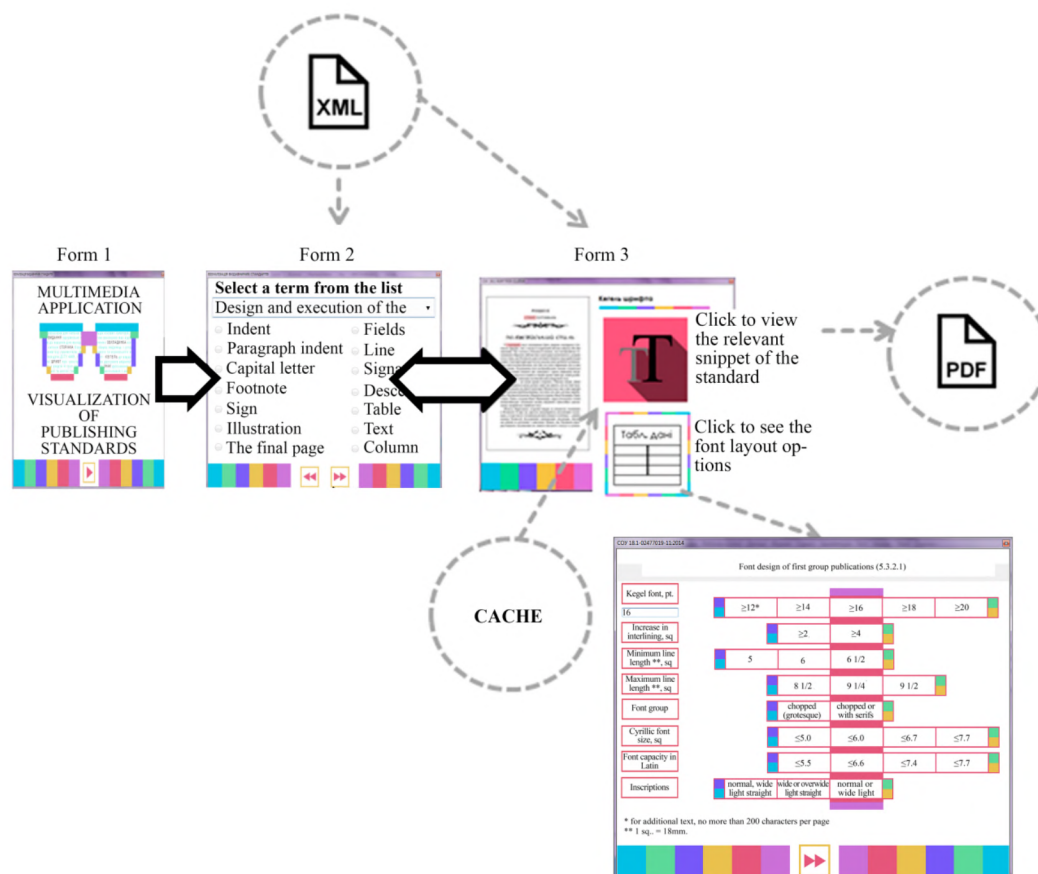
Fig. 15. The work scheme of the "Visualization of publishing standards" multimedia application

In general, the functionality remained from the previous application, but the new one is supplemented with a button that opens a window with visualized data tables. This button appears at the moment when the user has selected at least one key date, which is part of the tabular data. Regarding functionality, a textBox element was added, which allows the user to enter the value of the font size parameter and depending on what value is entered, the ratio of other parameters relative to the entered value changes. The element also implements the interactivity of the multimedia application, depending on the parameter entered, the font size of the font changes the appearance of the rendered data tables.

The textbox element code is shown in **Fig. 16**.

The result of the software implementation is the finished multimedia applications, which, according to the standardization visualization technique in terms of prepress preparation of publications, is the final product of the third stage of the presentation of the visual form.

Another example of the implementation of the metaphorical visualization method "parametric ruler" is a multimedia didactic complex in the discipline "Technological processes of publishing and printing" (Air Force TP), developed by the authors as part of the e-learning system (**Fig. 17**).

```csharp
private void textBox_TextChanged(object sender, EventArgs e)
    { try
     {
        if (double.Parse(textBox1.Text) < 14 &&
double.Parse(textBox1.Text) >=12)
          {
            pictureBox1.Image =
PublicationStandartsVisualization.Properties.Resources._3_1;
          }
        if (double.Parse(textBox1.Text) < 16 &&
double.Parse(textBox1.Text) >= 14)
          {
            Clear();
            pictureBox1.Image =
PublicationStandartsVisualization.Properties.Resources._3_2;
          }
        if (double.Parse(textBox1.Text) < 18 &&
double.Parse(textBox1.Text) >= 16)
          {
            Clear();
            pictureBox1.Image =
PublicationStandartsVisualization.Properties.Resources._3_3;
          }
        if (double.Parse(textBox1.Text) < 20 &&
double.Parse(textBox1.Text) >= 18)
          {
            Clear();
            pictureBox1.Image =
PublicationStandartsVisualization.Properties.Resources._4_2;
          }
        else
          {
            if (double.Parse(textBox1.Text) >= 20)
             {
                Clear();
                pictureBox1.Image =
PublicationStandartsVisualization.Properties.Resources._4_3;
```

Fig. 16. Program code for the textbox element
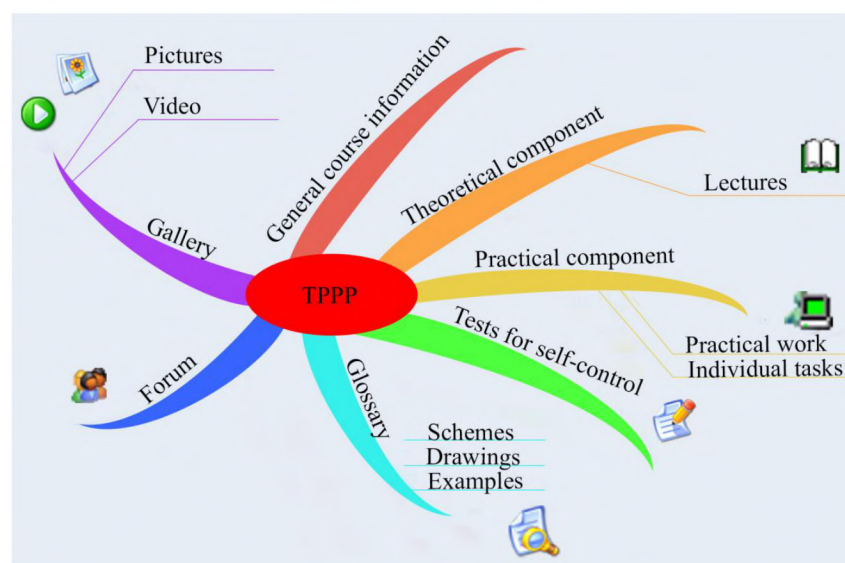
Fig. 17. General structure of the multimedia didactic complex in the discipline "Technological processes of publishing and printing" (TPPP)

16

For the created multimedia didactic complex, the following types of interactive infographic objects were used:

– infographic stories for building interesting and visual practical exercises;

– interactive test systems in the form of infographic tables;

– interactive maps for the organization and administration of the educational process, scheduling, student accounting and their performance;

– infographic tables that allow students to perform common tasks or consult on their implementation.

As possible limitations of using the proposed methodology for visualizing information for use in multimedia applications, there are individual characteristics of the user's mental activity formed under the influence of personal and situational factors. In particular, the proposed visualization technique can be effectively used by users of visual-effective and visual-figurative types of thinking. But objective difficulties with the use of visualization techniques may arise in users with a verbal-logical type of thinking.

6. Conclusions

Thus, as a result of research, a technique is proposed for visualizing information for use in multimedia applications, which facilitates the perception of a large amount of text information and ensures its presentation in multimedia systems. Using this technique allows to more fully cover a large amount of information for presentation in multimedia applications, reduce the cost of finding the necessary information and fix it at the visual level.

This study allows the user to explore the space of objects with their parameters, resulting in the possibility of optimizing the functionality of multimedia applications. The results of this research can be used in the design of multimedia applications both at the design stage to support decision-making on the choice of information presentation method, and to analyze the degree of optimization of the functionality of an already developed publication.

References

[1] Cerdas, F., Kaluza, A., Erkisi-Arici, S., Böhme, S., Herrmann, C. (2017). Improved Visualization in LCA Through the Application of Cluster Heat Maps. Procedia CIRP, 61, 732–737. doi: https://doi.org/10.1016/j.procir.2016.11.160

[2] Ahn, J., Brusilovsky, P. (2013). Adaptive visualization for exploratory information retrieval. Information Processing & Management, 49 (5), 1139–1164. doi: https://doi.org/10.1016/j.ipm.2013.01.007

[3] Corchado, E., Herrero, Á. (2011). Neural visualization of network traffic data for intrusion detection. Applied Soft Computing, 11 (2), 2042–2056. doi: https://doi.org/10.1016/j.asoc.2010.07.002

[4] Ben, X., Beijun, S., Weicheng, Y. (2013). Mining Developer Contribution in Open Source Software Using Visualization Techniques. 2013 Third International Conference on Intelligent System Design and Engineering Applications. doi: https://doi.org/10.1109/isdea.2012.223

[5] Chaolong, J., Hanning, W., Lili, W. (2016). Research on Visualization of Multi-Dimensional Real-Time Traffic Data Stream Based on Cloud Computing. Procedia Engineering, 137, 709–718. doi: https://doi.org/10.1016/j.proeng.2016.01.308

[6] Zhang, F., Tourre, V., Moreau, G. (2014). Using metrics to evaluate and improve text-based information visualization in 3D urban environment. WSCG2014 Conference on Computer Graphics, Visualization and Computer Vision, 375–382.

[7] Frey, G., Jurkschat, A., Korkut, S., Lutz, J., Dornberger, R. (2019). Intuitive Hand Gestures for the Interaction with Information Visualizations in Virtual Reality. Progress in IS, 261–273. doi: https://doi.org/10.1007/978-3-030-06246-0_19

[8] Vultur, O.-M., Pentiuc, S.-G., Lupu, V. (2016). Real-time gestural interface for navigation in virtual environment. 2016 International Conference on Development and Application Systems (DAS). doi: https://doi.org/10.1109/daas.2016.7492592

[9] Teras, M., Raghunathan, S. (2015). Big data visualisation in immersive virtual reality environments: embodied phenomenological perspectives to interaction. ICTACT Journal on Soft Computing, 05 (04), 1009–1015. doi: https://doi.org/10.21917/ijsc.2015.0141

[10] Hrabovskyi, Y., Fedorchenko, V. (2019). Development of the optimization model of the interface of multimedia edition. EUREKA: Physics and Engineering, 3, 3–12. doi: https://doi.org/10.21303/2461-4262.2019.00902

DEVELOPMENT OF BASIC CONCEPT OF ICT PLATFORMS DEPLOYMENT STRATEGY FOR SOCIAL MEDIA MARKETING CONSIDERING TECTONIC THEORY

Ivan Demydov[1]
ivan.v.demydov@lpnu.ua

Najm Ahmad Baydoun[1]
najem.b@iptpowertech.com

Mykola Beshley[1]
beshlebmi@gmail.com

Mykhailo Klymash[1]
mykhailo.m.klymash@lpnu.ua

Oleksiy Panchenko[1]
oleksij@gmail.com

[1]*Department of Telecommunications*
Lviv Polytechnic National University,
12 S. Bandery str., Lviv, Ukraine, 79013

Abstract

This paper presents authors analytical view on social impacts as targeted advertisement into the network environment using Omori tectonic theory for description the processes of audience response evolution. This could be extremely important and useful in the modern world to realize desirable e-Gov informational policy in the circumstances of hybrid treats emergence that is especially relevant for the informational space and reaching a cyber-supremacy. Some mathematical and algorithmic basics were contributed for narrative description of information and communications technologies (ICT) architectural deployment could be used for outer regulation of audience response character by Social Media Marketing (SMM) principles. That could be performed by controlled distribution of specified digital content that contains respective key phrases, for example social advertisements and analyzing respective feed-backs. Some results of the empiric study of live audience response dependence on controlled impacts are discussed. Election processes data and recent media recordings for preliminary proof of the contributed concept feasibility have been analyzed. There were shown using gathered empiric data sets, that the extent of impacts to targeted audience response intensity could be the subject of outer regulation. The index has been contributed for assessment the efficiency of the impact's propagation inside the audience by calculation of row correlation of keyword occurrence and audience response intensity. The approaches suggested in the article can be useful both for building effective interactive systems of state-society interaction and for detecting manipulative traits when influencing a specific audience.

Keywords: controlled social impact, SMM, ICT, targeted content advertising, e-Gov strategy, cyberspace, tectonic theory.

1. Introduction

Many of us heard about earthquakes and their forecasting. Current models for stresses forecasting are not precise, due to long term character of earthquakes recurrence and relatively low volumes of statistics. But, some of them are mathematically suitable to describe the distribution of the information activity peaks intensity in the blogosphere [1], especially while applying SMM procedures actively. Other works, such as [2, 3], investigate the distribution of message lengths and dependence of its parameters on informational events excitation and excitation wave propagation in a homogeneous scale-free network features respectively. The distribution of the information activity peaks intensity turned out to be similar to the distribution of the intensity of underground shocks in the earth's crust – aftershocks (small stresses following the main stresses), the number of aftershocks decreases inversely in proportion to the time elapsed since the moment of the main

18

stress, and this law is the name of the Japanese scientist Omori, which at the end of the nineteenth century observed aftershocks of a strong earthquake in central Japan and foreshocks (small shocks preceding the main blow) [4].

In [1] two types of information shocks were distinguished, the "seismograms" of which differ radically. A graph similar to a bell for an *endogenous* (internal) stress present a peak preceded by a curve that fixes the gradual increase in the frequency of informational events (i. e. targeted informational activities intensity), followed by a near-symmetrical form of attenuation. The moments of stresses it fixes are induced by information circulating in the blogosphere of informational space for a long time, both before and after the peak. An example of the endogenous event is elected President's inauguration after final declaration of the poll.

The authors of the article also point out that the peak and post-peak reaction of the informational space correlates with the behavior of key word markers preceding an endogenous shake, that is, in a certain sense, predictable. Hence the hypothesis is reasonable that knowing the behavior of precursors can even control this reaction, to build a predictable SMM automated system. As of 2011, by the keywords there were revealed about 150 of individual endogenous events, but exogenous (that is, caused from the outside) – about 1000 [1]. In fact, it was shown that exogenous events are an order of magnitude greater than endogenous, and one media event generally corresponds to events in several word frequencies (occurrences) of related keywords.

Obviously, the blogosphere, while being a part of the information space, is at the same time a highly-strung environment that loses equilibrium in two main scenarios. According to the first one, endogenous (**Fig. 1, *b***), in part of this medium, the gradual ordering of information begins (participants in the information environment, bloggers show increasing interest in a particular topic), reaching at some point the least entropy (the maximum of discussion), followed by a gradual relaxation and loss of information (interest in the subject of information impact disappears). This is an oscillating process, and it is important that the information involved in it is contained in the oscillating system itself, that is, endogenous.
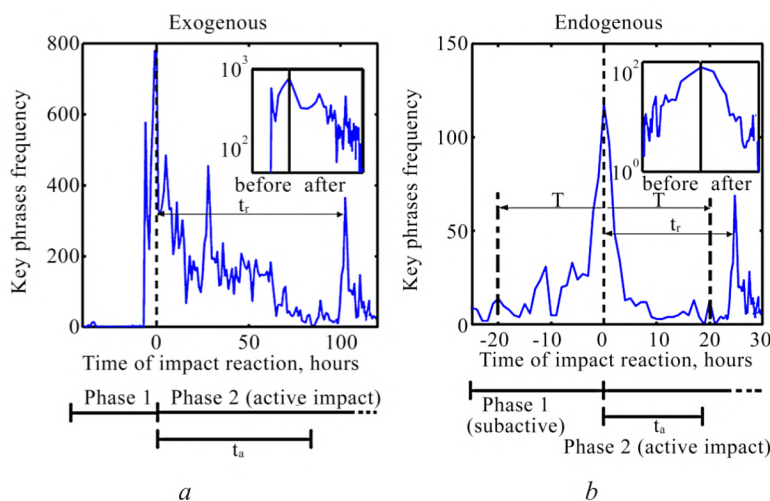
Fig. 1. The two basic scenarios of impact evolution through informational events into cyberspace: *a* – exogenous; *b* – endogenous (by [1], modified by authors)

The second, *exogenous*, scenario is quite different: despite the lack of information in the system, it instantly arranges (many participants in the information environment begins to discuss a topic unexpectedly) (**Fig. 1, *a***). It is clear that the sources of low entropy are the information here from the outside or being under SMM impact. An apologist of the Next Generation of "Media 2.0 concept" is obliged to object that in this case, the source of external information does not necessarily have to be traditional media that themselves are excited by the same pattern, responding to some events (the same nomination to candidates Sarah Palin in former 2008 US Vice-President's Elections or Volodymyr Zelenskiy nomination in recent 2019 Ukrainian President's Elections).

Social media – Twitter, Facebook, and various blogs – are built on the similar principle, as opposed to traditional media with their hierarchical editorial policy [5].

This is a peer-to-peer, non-hierarchical info communication network with peer-to-peer agent nodes (individual users' interaction of the P2P type), as shown in [6]. The processes of ordering/excitement are one-sided, so it is safe to assert with a high degree of certainty that exogenous events (most often found to be frequent for the blogosphere) are induced by traditional media just like long-lived trends, for example, in Twitter. Otherwise, it will have to divide the blogosphere into "true new media" and "untrue", which already contradicts the non-hierarchical ideology concept of "Media 2.0".

The problem statement. That is, knowing basic principles of these two evolutional processes it is possible to try to impact the informational, or, more correctly, cyber space with inducing and/or controlling desirable informational events as a part of state or commercialized SMM strategy. And, introducing, configuring, adoption of info communication platforms to deploy appropriate technologies of such impacts' automation is not known to authors from open literature sources of very last years. This work is intended to describe possible scenarios of informational impacts in cyberspace and draw the ways of their efficiency increasement. On our opinion, in the modern world this kind of informational impacts is very important to save the leadership of the state, commercial presence, cyber supremacy using modern ICT environment appliance.

The structure of the paper. Chapter 2 of this paper is dedicated to the brief theoretical description of possible scenarios of informational impacts propagation in cyberspace using Omori tectonic theory. Subchapter 2.1 describes pure endogenous information event with controlled post-impact; subchapter 2.2 is dedicated to the support of quasi-endogenous information events with hidden pre-impact and controlled post-impact; and, finally, subchapter 2.3 briefly describes quasi-exogenous information event with no pre-impact and controlled post-impact case. After that in the chapter 3 let's make generalization of algorithmic basics for the implementation of the strategy of controlled social impacts in the information space. A visual algorithmic description of SMM kind information operations associated with both the target distribution of a given information content and the collection of data on response changes in the preferences and sentiments of various user groups has been given. Subchapter 3.1 is dedicated to the statement of the classification problem for audience profiling procedures into ICT environment that supports informational space to reach the targeted groups of electronic services consumers effectively. The hierarchical classification of the target audience profiling levels for ICT content distribution platforms that sharing key messages in e-government platforms over the information space has been contributed. And subchapter 3.2 describes the authors opinion on features of SMM technique implementation applicable to the strategy of managed social impacts based on e-government ICT platforms. Chapter 4 is devoted to the brief analytical case study of audience response dependence on some events, including controlled impacts and declared approaches feasibility preliminary assessment. Subchapter 4.1 shows the qualitative comparison of presented in the paper dependences with statistical processes, available from existent literature sources. And subchapter 4.2 presents the empiric study results discussion of live audience response dependencies on controlled impacts and their efficiency. The discussion and conclusions are also presented in the chapters 5 and 6 respectively.

2. Some theoretical basics of the Omori tectonic theory and description of the options for scenarios of informational impacts propagation in cyberspace

Let's make a hypothesis that, evidently, it is possible to create a public resonance over short period of time, with the given amplitude, both with the help of the right endogenous precursors (key elements of the information presence or SMM strategy), and to manage it using a sequence of influences, while fixing how they affect in a feedback system on the basis of which allows to describe the moments of the compensating influences that lead the whole segment of system to a state of quasi-constant resonance (both for the endogenous and for the exogenous reaction of the target groups of society). Let's describe these processes on the basics of Omori tectonic theory for earthquakes shocks intensity description applicable to the targeted audience response.

Works [4, 7] give the description of Omori's law, as:

$$n(t) = \frac{K}{(t+c)^p},$$ (1)

where t is time; K, c and p are constants, and cumulative number of aftershocks after the main stress (or informational event peak size) could be defined by integral:

$$N(t) = \int_0^t n(s)\,\mathrm{d}s = \frac{K\left[c^{(1-p)} - (c+t)^{(1-p)}\right]}{p-1}.$$ (2)

By [8] and equations (3), (4) from [7] the seismicity rate as a function of time after the stress step is expressed as:

$$R(t) = \frac{r\dot{\tau}/\dot{\tau}_r}{\left[\dfrac{\dot{\tau}}{\dot{\tau}_r} e^{\left(-\frac{t_r}{t_a}\right)} - 1\right] e^{\left(-\frac{t}{t_a}\right)} + 1},$$ (3)

where, conditionally, t_a is the characteristic relaxation time; t_r is peak impact recurrence time; r is the reference seismicity rate, proportional to the reached peak-event intensity level (the maximal frequency of key words occurrence) into informational space (**Fig. 1**).

By [1] the endogenous events' cumulative distribution of event-size E is similar to the Gutenberg-Richter law with a parameter β of 0.574, that is typical for earthquakes (attenuation of social influences and inflammation of these effects by after and foreshocks), and for an exogenous case it could be fitted by this law with exponent 1.003 (when a contribution of introduced external impacts prevails).

Gutenberg-Richter law, where events' intensity E is proportional to radiated seismic energy (discussion intensity propagation of an event within some targeted group):

$$P_r\left(E^* > E\right) \propto E^{-(\beta+1)}.$$ (4)

Let's also give the Omori law interpretation within view of (4) for intensities of fore- and aftershocks while informational events evolve within certain audience inside a cyberspace. For exogenous events and impacts equation (6) exists only:

$$w_i\left(t < t_0\right) \propto \left(t_0 - t\right)^{-\alpha_g},$$ (5)

$$w_i\left(t > t_0\right) \propto \left(t - t_0\right)^{-\alpha_d}.$$ (6)

Here $w_i(t)$ is the frequency (occurrence) of i-th key words at the time t (or nearest time interval). Let's follow with considering scenarios of informational impacts in the cyberspace while maintaining SMM automation by ICT means.

2. 1. Scenario 1. Pure endogenous information event with controlled post-impact response

With this scenario, first it is necessary to detect new trend in the society or targeted social group, and to define right key words to impact this group, late to decide about expediency of controlled impact support after event peak size time moment ($t=0$, **Fig. 1, b**). This could be performed by monitoring algorithm presented in **Fig. 2** (key messages monitoring in the informational space and probably by using certain kind of deep learning algorithms, neural networks etc.). This algorithm could be realized by means of implementing the scalable metadata fixation

platform, applicable approaches are described in the works [9–11]. An additional keywords injection process is depicted in **Fig. 3**. If controlled endogenous aftershock impact is desirable, it is possible to implement (voidable) algorithms in **Fig. 4, 8** (key messages injection process to support controlled social impact and to stabilize the impact intensity during t_a aftershock period), where $f_{msg.inj.}$ is proposed, as equivalent of corrective (compensation) key messages injection intensity (at the time t) within aftershock active impact period (up to t_a time) and could be assessed in respect to (1)–(3) as:

$$f_{msg.inj.} = w_i(t_0)\left(1 - \frac{w_i(t)R(t)}{w_i(t_0)R(t_0)}\right),$$ (7)

and event-size for key words set i at peak-time t_0 ($t_0 = 0$) is taken by [1]:

$$E_{i,t_0} = \frac{1}{2T+1}\frac{w_i(t_0)}{\sum\limits_{t=t_0-T}^{t_0+T} w_i(t)},$$ (8)

where $w_i(t)$ is the frequency (occurrence) of key word i at the time t. For our informational impact's propagation, it is possible to put a relaxation time $t_a \approx T$ (**Fig. 1, b**).

In the case of possible negative compensation intensity appearance, it means, that it is necessary to apply lawful interception and filtering measures for key messages on the state level or try to introduce new impact to the targeted groups and snuff out current superfluous resonance in the cyber space. In any case, the duration and expediency of influence is determined by the volume of allocated resources, as well as by the criterion of accomplishing the goals set of SMM strategy.

Let's note that it is necessary to choose $t_a > t_r$ to extinguish or change the subject of impact in a managed system with social influence and $t_r \gg t_a$ for long-term maintenance of the level of managed social impact with injection of key messages considering (7), (8); where t_r, as recurrence time could be calculated by solved equation (3) (where $\dot{\tau}_r$ and $\dot{\tau}$ are the stressing rate prior to and following the stress step, and r is proportional to $E_{i,t0}$, and taking $t_a \approx T$):

$$t_r = T\ln\left(\frac{\frac{\dot{\tau}}{\dot{\tau}_r}\cdot R(t)}{R(t)\left[1 - e^{\frac{t}{T}}\right] + r\frac{\dot{\tau}}{\dot{\tau}_r}e^{\frac{t}{T}}}\right).$$ (9)
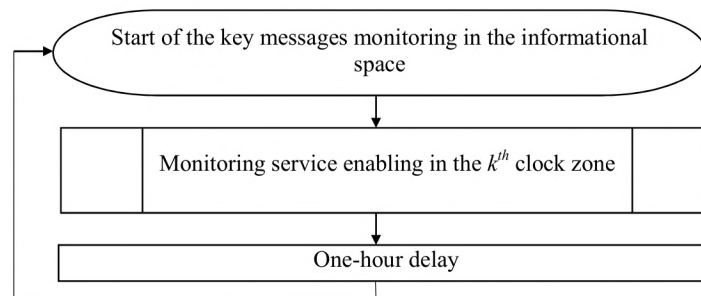
Fig. 2. The basic algorithm of key messages monitoring in the informational space

The difference between **Fig. 2, 3** is that first one is intended for passive monitoring of informational space or digital media resources, and the second one is intended to realize controlled (hidden) pre-impact, to reach, respectively, defined event peak intensity in some SMM strategy activities' profile. Time-zones are also featured in the case if scalable strategies are realizing.
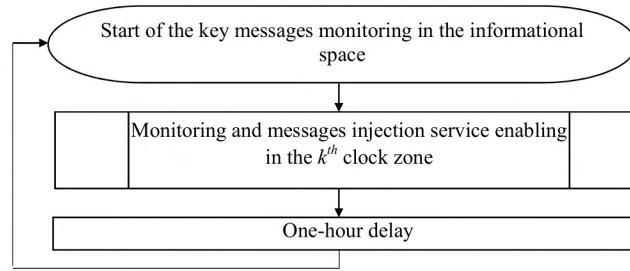
Fig. 3. The basic algorithm of monitoring and injection of the key messages to informational space

2. 2. Scenario 2. Quasi-endogenous information event with hidden pre-impact and controlled post-impact response

Within this scenario, it is firstly necessary to determine hidden pre-impact beacons for preparation the society (or audience) to react on some informational event very intensively (**Fig. 1, b**). Calculations of the necessary time profile for intensities of hidden preliminary pre-impacts (sub active phase) should be performed using (7) and (8) and considering desirable event-size $E_{i,t0}$, T – the period for preparation, and, accordingly to the used algorithm of monitoring and injection of the key messages to informational space, involving ICT mechanisms (**Fig. 3**). If controlled aftershock impact is desirable, it is possible to implement algorithms in **Fig. 3, 5** applied mandatory by **Fig. 7**, using **Fig. 4** after reaching of pre-defined event peak size limit $E_{i,t0}$ into the cyber (informational) space to stabilize the impact intensity during T aftershock period.
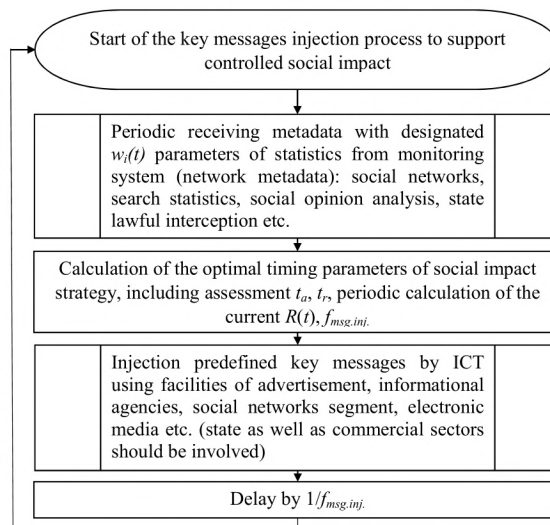
Fig. 4. The algorithm of the key messages injection process to support controlled social impacts
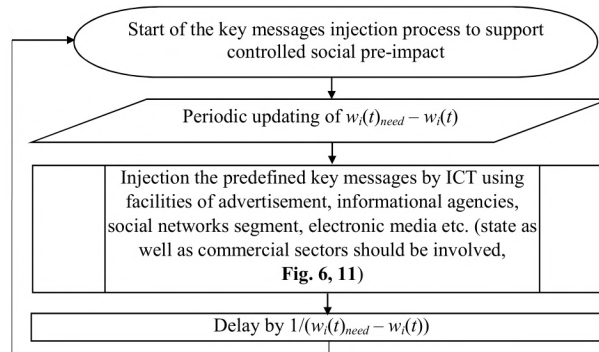
Fig. 5. The algorithm of the key messages injection process to support controlled social pre-impact

Fig. 6 presents a means set of ICT platforms and their deployment process to support informational impacts in the targeted cyber space segments. Thus, for endogenous influences scenarios it is necessary to evaluate amplitude of influence and make selection of t_a, t_r in order to maximize (to reach desirable amount of) $E_{i,t0}$ and $R(t)$ in real time based on the results of feedback analysis of statistical indicators, in particular statistics for dedicated keywords $w_i(t)$, for example by feedback from the infocommunication environment by metadata fixation system, **Fig. 6.**

The designing features of cloud messaging protocol for content distribution as a service is studied in [12], and respective architectural concepts are presented in [13], and also in [14]. Let's also note that all social networks and media distribution platforms use cloud engines to operate with higher resource efficiency.

It is important to determine correctly targets and targeted geographical regions/audience for social impact informational injection by ICT and intensity timing profile of social informational impact (chosen SMM strategy) that supported by ICT to calculate the features and scalability potential of such technical platforms in the future works. That is, the further researches on ICT distributed platforms adaptation (feedback collection features, maximal load in specialized architecture for impact propagation assessments) should be performed in the future. Mentioned architectural features should consist of e-services plurality, and servers configuring, impact propagation in networks flowcharts, results of proposed techniques implementing and automation.

2. 3. Scenario 3. Quasi-exogenous information event with no pre-impact and controlled post-impact response

For this case scenario implementing (**Fig. 1, *a***) it is necessary to define initial key event to determine the most effective moment for implementing the exogenous impact using **Fig. 2,** and mandatory by **Fig. 8, 4** algorithms. Let's note that this is very simplified approach and do not consider deep learning algorithms formalization procedures here, as it could be the subject of special and stand-alone investigation. The algorithm in **Fig. 4** is used after reaching of pre-defined event peak size limit E_{limit} into the cyber (informational) space to stabilize and control the impact intensity during t_a exogenous aftershock period. The rest features of implementation were described in the first scenario. All these presented algorithms consider separate impacts within pre-defined clock zones during ongoing SMM strategy realization. Let's note, the respective effects to the targeted audience could be got using commercial messaging services (**Fig. 6**), for example by Viber commercial solutions, Google Adds, Facebook, Telegram services etc.
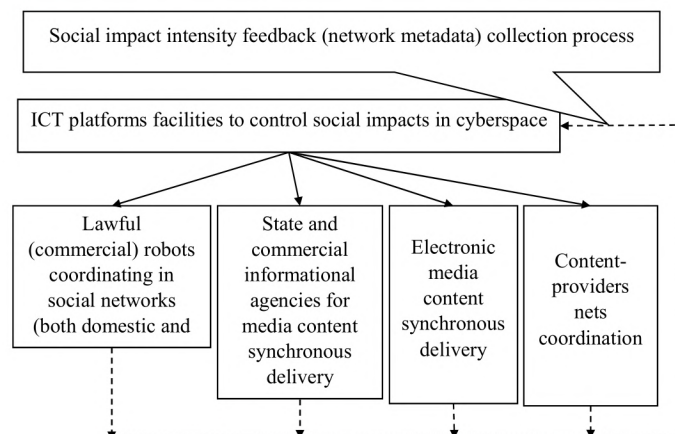
Fig. 6. A means of ICT platforms and their deployment process to support informational impacts in cyber space during ongoing SMM strategy realization

Fig. 7 depicts the algorithm of key messages monitoring service enabling in the kth clock zone to be realized within proposed scenario described in subchapter 2.2.
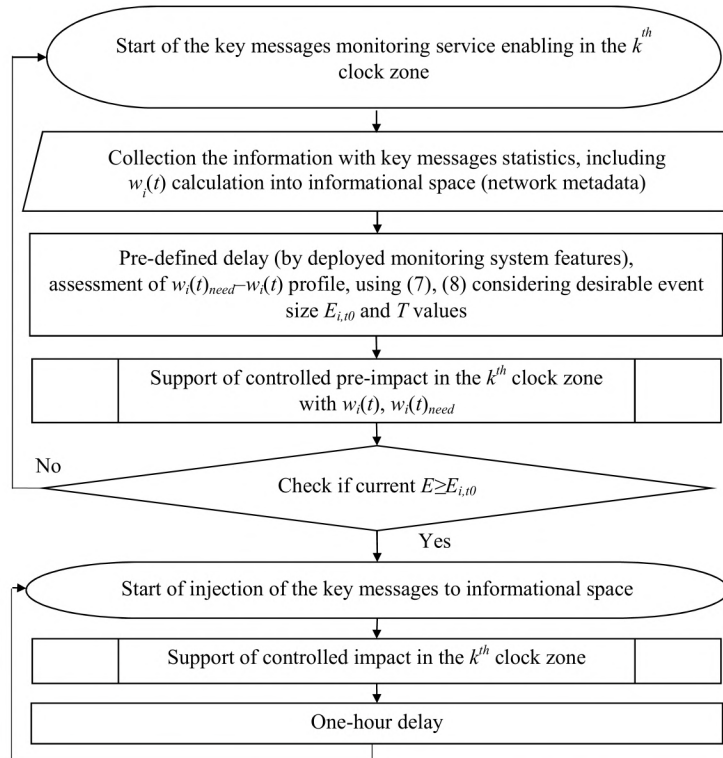
Fig. 7. The algorithm of key messages monitoring service enabling in the kth clock zone
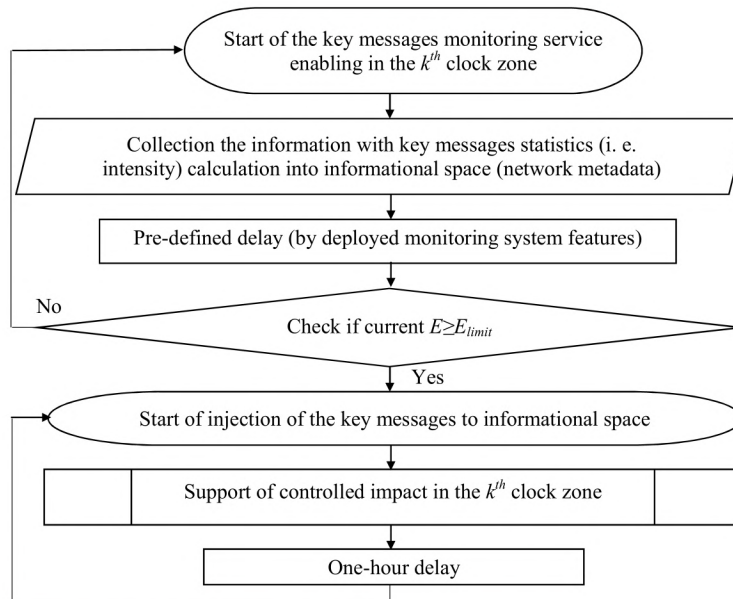
Fig. 8. The algorithm of the key messages monitoring service enabling in the kth clock zone for exogenous impact preparation strategy

In **Fig. 7, 8** module "Support of controlled impact in the kth clock zone" could be realized using facilities that have been described and depicted in the following section 3 of this paper.

3. The generalized approach to the implementation of the strategy of controlled social impacts in the information space

To date, the data on user activity in the world information space has become a valuable information resource. Hidden, but credible reports (from casual life practice) about leading glob-

al IT companies such as Google, Facebook, Twitter, Microsoft, MasterCard, VISA, booking and reservation services and many others involved, probably make possible to postulate that them use their products to provide B2B collaboration between different companies in order to get the most complete profile of the persons who consuming their or third-party digital services. The purpose of obtaining such information is not only the selection of a content for its personalized preferences and sentiments [15, 16], for SMM introducing but also realization of unprecedented cases of information operations related to both targeted advertising [5, 17], as products, goods and services, and political forces, social programs of the state, as well as with the manipulation of the opinion of representatives of certain social groups, that is, the creation of targeted social influences, in some special cases operations of cyber-fight on the territory of the enemy, etc. Information and telecommunication platforms, with the help and on the basis of which the above-mentioned activities are realizing, as a rule, are simultaneously platforms of state e-governance or incorporated. Support for information operations and SMM automation on their new ones becomes most effective in the case of targeted segments of an audience, which profiled and integrated into target groups based on the characteristics that are posed when implementing a strategy of managed social impacts (**Fig. 9**).
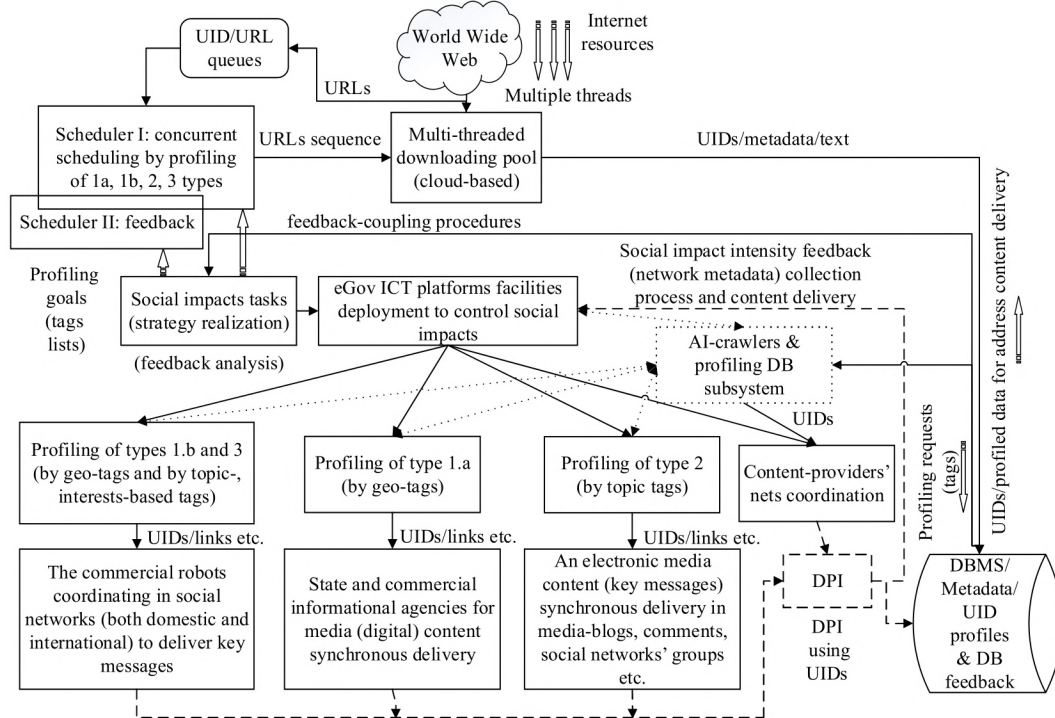
Fig. 9. The generalized approach for implementing the strategy of controlled social impacts into the information space

In **Fig. 9** the DBMS/Metadata/UIDs profiles module should perform the UIDs collection and storing process (under respective State DB Administration advising); and late binding the collected metadata to collected UIDs, which data space is organized under UID's unification policy (by format) for e-mail addresses, web-addresses, links to additional content, users' pages links to social networks/forums etc. This forming DPI and web-crawling results that could be used furtherly in feedback analysis process.

3. 1. The statement of the problem of SMM automation into ICT environment
According to [18–20], typical examples of information impact generators are:
– Social networking groups;
– Small forums with the community of their participants;

– Sections or topics of large forums with a community of forum members who are active in a section or topic;

– Thematic interactive sites or blogs and the commentators' communities;

– Thematic sections of the online media and the commentators' communities.

Thus, profiling levels of the target audience for infocommunication complexes for delivering key messages in e-government platforms in the process of managing social impacts (or while realizing SMM strategy) could be classified and presented as following (ordered by decreasing the performance):

1a. Managed broadcasting of key media messages (in mass media), broadcasting targeted advertising messages and content in the media, for example, social advertising, for which the necessary coverage area should be determined, or certain geographic areas.

1b. Managed broadcast of commercial advertising and content or social content in social networks, for which it is necessary to determine the target audience based on the territorial principle, using the meta-information collection (geo-tagging) in the database (DB) of the electronic communication platform of the e-government Artificial Intelligence (AI) subsystems using web crawlers (web-spiders) – programs that are part of search engines. And, respectively, Internet-driven web pages analyzing to enter information about them (key-words) to a database (**Fig. 10**) [21]. According to the definition of Wikipedia, spider programs perform a general search of information on the Internet. They report the contents of the found document, index it and extract the summary information. They also read headers, some links, and submit the indexed information to the search engine database. The prototype of powerful crawler architecture that could be implemented in the cloud environment is presented, for example in [22].

2. Group distribution within the framework of implementing the strategy of managed social impacts of key informational messages (target media content) to members of social networking groups and forums, their sections, commentator communities of thematic interactive sites, including sections of electronic mass media. To determine and create a target audience database, it is necessary to use artificial intelligence subsystems (AIs) using web crawlers that search for relevant topics, key words, etc.

3. Individual targeted mailing of key messages to profile users of social networks and other ICT systems whose UIDs lists are determined by a set of keywords (subject topics, user interests) that are captured by the web crawler AI subsystem for the implementation of a certain SMM strategy for managed social impacts.
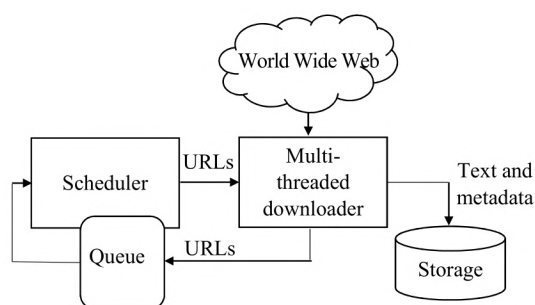
Fig. 10. The basic architecture of the typical Web-crawler software tool (by Wikipedia), by [21, 22]

For the implementation of all three proposed levels of profiling of target audiences for infocommunication delivery systems of key messages in e-government platforms, it is possible to use metainformation fixation systems with the use of DPI (Deep Packet Inspection) technologies (**Fig. 11**). This architectural direction in relation with inter-cloud messaging protocol development for content distribution as a service (of CoDaaS type) over Future Internet is for example investigated and discussed in [12]. Algorithms and generalized strategies for the implementation of computer-aided SMM influences are developed by the authors of this publication and could easily be automated by IT companies.
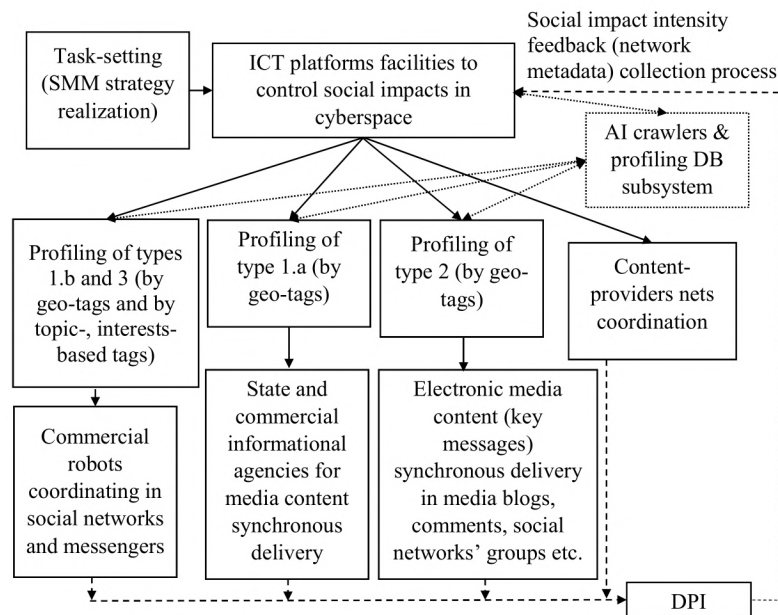
Fig. 11. Means of eGov (ICT systems) platforms and their deployment to support information impacts into social and communication space, with proper targeting the audience (performed by the authors)

The algorithms that improving the storage efficiency of DPI technological applications and respective database management principles are discussed in [32], and semantic principles of such analysis are also given and developed in the works [18, 20].

3. 2. The features of implementation of the strategy of managed social impacts based on E-Government ICT platforms

An important aspect of the functioning of e-government platforms for managing information impacts is the monitoring of metadata in the Internet space [1] (particularly, in the socio-infocommunication environment) (**Fig. 9**, **11**). Content providers operating within the existing national legal field may be required to configure their networks in such a way as to elaborate the concepts of the introduction of e-government systems and provide secured data-based services in accordance with the processes of the operation of the established infocommunication platform (**Fig. 10**). Feedback-coupling mechanisms are also needed to control the effect of the implementation of certain information operations and the possible automated adjustment of the implementation of the strategy of e-government or advertising campaigns of SMM kind on selected groups of users of certain information resources. An important feature of searching through search engines is the need to create a single informational field with unique identifiers of these or other user profiles (global UIDs). But this, in turn, requires the creation of a reliable information storage and information security measures that should be developed at the state level on the hybrid ICT platform (**Fig. 9, 11**). Relevant robotic crawling devices should have a special mode of access to Internet-based traffic points due to the specifics of their operation and the large number of consistent requests [22]. Distribution of commercial or other type of information in such socio-communication environments as social networks is rather complicated process [2, 3], therefore its course should be managed using means of artificial intelligence. Accordingly, the development of such tools is one of the priorities for the creation of e-governance systems for the future. Their application will facilitate the coordination of efforts of various organizations of commercial and public character within the framework of established systems for controlled social impacts and their protection in the national information space as automated SMM strategy realization, including from potentially hostile multinational corporations.

28

4. A brief analytical case study of audience response dependencies on controlled and casual impacts

Authors should note that analytical (statistical) proof of the dependencies (**Fig. 1**), presented in this work faces with difficulties due to different reasons. And, to some extent, these difficulties highlight the partially debating character of the paper, which scope was to present idea and draw narrative ICT approach of the controlled impacts realization (of SMM kind) under specified targeting audience, being used as a part of state informational policy implementation within respective e-Gov services deployment. The main difficulty (**Fig. 9**) is using the specialized technique, named DPI or lawful interception. It means that effective realization of such ICT platforms, regardless of their commercial or state ownership, faces with specified law constraints, being a kind of data intelligence process [23] and obtained data, regardless of its volume are as usual classified (as by the US regulations, as well as in EU, PRC, and another countries). It means also that data sets, collected using such approaches are in the property of state or commercial structures and cannot be published without their permission, even for scientific purposes. But authors could strongly agree with readers that this situation does not satisfactory, and providing in this paper result of their own alternative study.

4. 1. The comparison with statistical processes, known from existent literature sources

First, let's compare character of dependencies in **Fig. 1** [1] with results of Twitter crawling that were made in [24] and [25]. These works represent the information propagation (twits' volumes) about Abu Dhabi double-crime event (2014) and Sebastian Vettel victory in Formula 1 (2013), respectively. The correlation of time synchronized curves from [25] and of **Fig. 1, a** gives the correlation index 0.3802 and respective index 0.4416 to **Fig. 1, b**. For this case, the intensity growth of audience response was smooth. It means **Fig. 1, b**, that discussion was growth inside the society (is more endogenous), being ad initium quasi exogenous. Therefore, it is suddenly that the event of Sebastian's Vettel victory in F1 competitions (2013), studied in [24] is much more endogenous (correlation indexes are 0.62 versus 0.1, respectively), as the attributes of hidden advertisement and publicity hooks are, evidently, were presented during that campaign. It could be concluded from this that used material by [1] in general is correct and could be used for further scientific investigation process.

4. 2. The empiric study of live audience response dependence on controlled impacts and its efficiency evaluation

Secondly, let's analyze 50 data sets, generated from certain video files which contain recordings of Ukrainian TV talk-shows with the echo of the indexes of positive/negative reaction of the auditorium is made, according to the topic of the discussion. It is postulated that a sample of more than 300 viewers present in the television studio is representative of all sections of society to a sufficient extent (justified by TV-channel sociologists), and their moods and preferences are aggregated and become an anonymous echo of the audience in the running echo graph (using also remote interactive ICT means), and the audience fairly adequately represents certain target groups that would be formed in the Internet space by topic and preferences, in relation to the topics covered in a particular television program. Let's detect the typical time profile of the audience response during all the program [26] (the properties of analyzed materials are substantially equivalent to the retrieved from mentioned media), **Fig. 12** (accomplished by authors, empirical data, no simulation was used).

Authors specially do not show the process of data retrieving, as this is out of scope for this paper's topic but interested readers could contact authors personally to get some data set in the table format. Let's note that this process could be automated using Microsoft Azure toolset and appropriate software deployment, to detect necessary keywords. As for this case the keywords used were the following (in Ukrainian): "president, system, responsibility, referendum, reform". The endogeneity of the audience's reaction prevails (the correlation index to the **Fig. 1, b** is about 0.30 versus 0.18 for this index to **Fig. 1, a**). The keywords usage occurrence profile is quasi-exog-

enous (the correlation index to the **Fig. 1, _a_** is about −0.03 versus −0.23 for this one to **Fig. 1, _b_**). The efficiency of the impact's propagation inside the audience by row correlation index of keyword occurrence and audience response intensity is 0.17. For the reaction intensity the t_r index value is about 40–48 minutes, and $t_r \gg t_a$, $t_a \approx 5$–6 minutes.
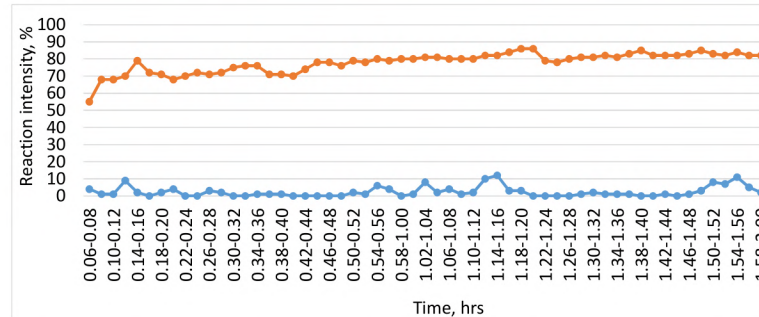
Fig. 12. The temporal profile of audience response intensity against keywords' usage occurrence (the empiric data are gathered)

A data from **Fig. 12** could show that the medium reaction level is 80 %. This case is studied with condition of controlled impacts absence.

The next case is more interesting, as one from the authors of this paper could be represented in the editorial office during the TV program recording (the properties of analyzed materials are substantially equivalent to the retrieved from recorded media [27]) and conditionally could made hidden advices to the linkman how often to control the discussion, using certain calculations, based on the pre-collected dataset. So, hypothesis, postulated in this paper were put under verification by respective series of experiments.

The respective temporal profile of audience response intensity against keywords' usage occurrence is shown in **Fig. 13** (accomplished by authors, empirical data, no simulation was used).
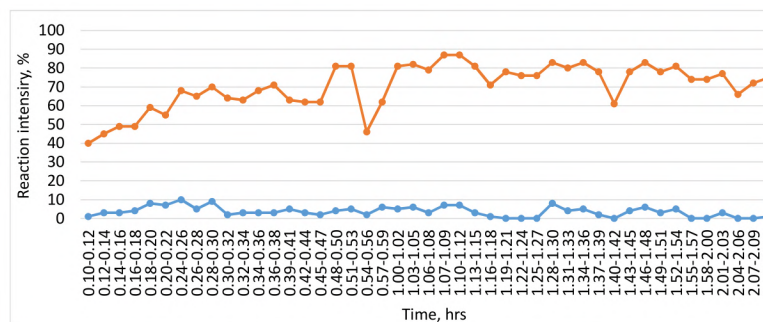
Fig. 13. The temporal profile of audience response intensity against keywords' usage occurrence in the case of controlled impact realization (the empiric data are gathered)

This TV program recordings were analyzed and for this case the keywords used were the following (in Ukrainian): "demarcation (peace), peace, negotiations, conflict, invasion, Minsk treaties, fight (protect), corruption". Analyzing **Fig. 13** let's note that there are signs of exogeneity of the audience's reaction (which is cardinally different to previous case and typical for hidden impacts in more than 80 % of such cases) at the level of informative (and partly emotional) attitudes from the participants of the discussion (the correlation index to the **Fig. 1, _a_** is about −0.06, but this index to the **Fig. 1, _b_** is less than −0.03, so this is ambivalent situation, or hidden exogeneous reaction). The keywords usage occurrence profile is endogenous (the correlation index to the **Fig. 1, _b_** is about 0.21 versus −0.18 for this one to **Fig. 1, _a_**). The efficiency of the impact's propagation inside the audience by row correlation index of keyword occurrence and audience response intensity is 0.31 (that is up to 45 % (!) greater, than for previous case, **Fig. 12**). And the times for impacts ac-

tivization were assessed by (9), t_r index value is chosen and implemented (retrieved from **Fig. 13**) as about 12–14 minutes, and $t_a \geq t_r$, $t_a \approx 16$–20 minutes. Thus, scenario 2 was implemented (using appropriate time scaling).

A data from **Fig. 13** could show that the medium reaction level is 74 %, so the energy of audience response is more constant, being "smeared" over time, accordingly to (4). The controlled reaction overcomes the negative expressions about the subject of discussion, making the disputing more constructive.

5. Discussion of the development features of the Basic Concept for ICT Platforms Deployment Strategy for Social Media Marketing

As for disclaimer, this work could be partially considered as positional authors' look. It was not performed as a part of project, supported by any organization/government. All investigation should be considered as the private initiatives of authors. But all described processes of informational impacts are considering to be realized and automated into the models of specialized ICT infrastructure for further investigations. Being highly significant for the developing of the partnership between business, government and citizens, a part of this work could be transformed on the commercialization basis, especially in SMM automation field.

Let's note that high informational impact intensity stabilizing during t_a aftershock period by means of ICT (**Fig. 6**) is a sort of cyber operation and should be performed carefully under control of respective state services and in the interests of the state due to its potentially destructive character [28–30]. Especially, when significant targeted resonance is created within short period of time. It is very important to define goals, subject and components of informational cyber impact correctly, as well as targeted geographical region and audience coverage, including traditional media, and by means of state or commercial advertisement agencies' resources (as for example), depending on amount of allocated resources. Ways of ICT means effective application, including cloud resources virtualization and scaling is also very important question in the national scale systems [31] to be investigated in the future.

Interesting is also approach with creation of countermeasures to the undesirable hidden informational impacts while they are not appeared in the form of highly resonance informational peak-event, by setting some "sematic jamming" with specially adopted contrary key words or lawful interception (of DPI kind) traffic filtering. In the active phase, while resonance into informational space is undesirable and is high it should be considered inspiring a new exogenous impact using inequality $t_a > t_r$ and assessments by (9) to extinguish or change the subject of current impact (or to struggle current strategic trend) in a managed system with targeted social influence in some region or social group. But this technique could be the subject of further study.

As was already noticed, correct determining of targets and targeted geographical regions/audience for social impacts informational injection by ICT and intensity assessment of such impacts by ICT to calculate the features and necessary scalability potential of the respective info-communication architectures are mutually significant tasks. Nearest investigations will be also addressed to the technical side of the proposed approaches realization with support of their automation by means of ICT.

The necessity of attention of the state to the issues raised in this work is undoubted, since the benefits from active interaction with society consists not only in carrying out of certain information campaigns, but its consequence, in essence, is the achievement of the top of the process of society informatization in the postindustrial era, which will directly contribute to the consolidation of a single monolithic nations.

6. Conclusions

Therefore, in this paper, the general statement of the problem of implementing the strategy of controlled social impacts in the information space based on hybrid intelligence ICT platforms is considered. Thus, as a result of investigations conducted within this work, it is possible to conclude the following.

A generalized visual algorithmic description of information operations (of SMM sort) related to both the targeted distribution of the given information content and the collection of feedback data on reactionary changes in the preferences and sentiments of certain groups of users in the relevant social and informational environments is presented (three scenarios were depicted).

The classification of types of users' profiling of digital services in the information space has been contributed (three types were described), which can be practically useful in the development of e-government systems on the basis of modern ICT tools. A brief characteristic of the profiling process to arrange a target audience for the purpose of carrying out the above-mentioned information operations on the basis of infocommunication platforms operating in an open Internet space is given. Authors find an effective the transition to hybrid cloud information and communication technologies for the implementation of the processes shown in **Fig. 9.**

As could be concluded from **Fig. 12, 13** (using empirically collected data) the approaches that presented in this article could significantly improve the efficiency of the impact's propagation inside the targeted audience using controlled social impacts (SMM-based) technique. It is possible to contribute, as a result of empiric experimental data sets analysis, an efficiency evaluation index of the impact's propagation inside the audience by row correlation calculating of keyword occurrence and audience response intensity (in the conditions of pre-defined impacts absence this index is about 0.17, otherwise it was increased up to 0.31, or by 45 %).

Developed mathematical description helped to assess the timing parameters for live impact propagation control purposes. It has been empirically shown that it is necessary to choose $t_a > t_r$ to extinguish or change the subject of impact in a managed system with social influence and $t_r \gg t_a$ for long-term maintenance of the level of managed social impact with injection of key messages (from **Fig. 12**: t_r=40–48 min, t_a=5–6 mins; and from **Fig. 13**: t_r=12–14 min, t_a=16–20 mins).

The authors are planning to conduct a further and deeper analytical empiric study to confirm in more accurate manner the postulated in this paper target audience reaction intensity dependencies on the keyword occurrences which used to impact on this reaction character. For this purpose, more issues of information-analytical television programs will be taken, during which the echo of the indexes of positive / negative reaction of the auditorium is made, according to the topic of the discussion. Social networks data dynamics study is also planned to be used.

References

[1] Klimek, P., Bayer, W., Thurner, S. (2011). The blogosphere as an excitable social medium: Richter's and Omori's Law in media coverage. Physica A: Statistical Mechanics and Its Applications, 390 (21-22), 3870–3875. doi: https://doi.org/10.1016/j.physa.2011.05.033

[2] Shinyaeva, T. S., Tarasevich, Y. Y. (2016). Virtual network as excitable medium. Journal of Physics: Conference Series, 681, 012008. doi: https://doi.org/10.1088/1742-6596/681/1/012008

[3] Szell, M., Grauwin, S., Ratti, C. (2014). Contraction of Online Response to Major Events. PLoS ONE, 9 (2), e89052. doi: https://doi.org/10.1371/journal.pone.0089052

[4] Utsu, T., Ogata, Y., S, R., Matsu'ura (1995). The Centenary of the Omori Formula for a Decay Law of Aftershock Activity. Journal of Physics of the Earth, 43 (1), 1–33. doi: https://doi.org/10.4294/jpe1952.43.1

[5] Yoo, S.-C., Shin, I. (2018). Digital Signage Media Creative : A Study for the Media Typology and Advertising Creative Strategy for Digital Signage. The Korean Journal of Advertising, 29 (6), 81–108. doi: https://doi.org/10.14377/kja.2018.8.31.81

[6] Dunbar, R. I. M., Arnaboldi, V., Conti, M., Passarella, A. (2015). The structure of online social networks mirrors those in the offline world. Social Networks, 43, 39–47. doi: https://doi.org/10.1016/j.socnet.2015.04.005

[7] Correig, A. M., Urquizú, M., Vila, J., Manrubia, S. C. (1997). Aftershock series of event February 18, 1996: An interpretation in terms of self-organized criticality. Journal of Geophysical Research: Solid Earth, 102 (B12), 27407–27420. doi: https://doi.org/10.1029/97jb02487

[8] Dieterich, J. (1994). A constitutive law for rate of earthquake production and its application to earthquake clustering. Journal of Geophysical Research: Solid Earth, 99 (B2), 2601–2618. doi: https://doi.org/10.1029/93jb02581

[9] Poniszewska-Maranda, A., Matusiak, R., Kryvinska, N., Yasar, A.-U.-H. (2019). A real-time service system in the cloud. Journal of Ambient Intelligence and Humanized Computing. doi: https://doi.org/10.1007/s12652-019-01203-7

[10] De la Prieta, F., Bajo, J., Rodríguez, S., Corchado, J. M. (2016). MAS-based self-adaptive architecture for controlling and monitoring Cloud platforms. Journal of Ambient Intelligence and Humanized Computing, 8 (2), 213–221. doi: https://doi.org/10.1007/s12652-016-0434-8

[11] Mladenow, A., Kryvinska, N., Strauss, C. (2012). Towards cloud-centric service environments. Journal of Service Science Research, 4 (2), 213–234. doi: https://doi.org/10.1007/s12927-012-0009-y

[12] Kaddouri, A., Guezouri, M., Mbarek, N. (2017). A new inter-cloud service-level guarantee protocol applied to space missions. International Journal of Grid and Utility Computing, 8 (2), 152. doi: https://doi.org/10.1504/ijguc.2017.085909

[13] Jiang, L., Feng, G., Qin, S. (2015). Content Distribution for 5G Systems Based on Distributed Cloud Service Network Architecture. KSII Transactions on Internet and Information Systems, 9 (11), 4268–4290. doi: https://doi.org/10.3837/tiis.2015.11.001

[14] Krishna, M. (2019). User-Centric and Information-Centric Networking and Services. CRC Press, 310. doi: https://doi.org/10.1201/9781315207650

[15] Molnár, E., Molnár, R., Kryvinska, N., Greguš, M. (2014). Web intelligence in practice. Journal of Service Science Research, 6 (1), 149–172. doi: https://doi.org/10.1007/s12927-014-0006-4

[16] Peköz, Ü. G. (2018). Product Usage Data Collection and Challenges of Data Anonymization. Lecture Notes on Data Engineering and Communications Technologies, 117–136. doi: https://doi.org/10.1007/978-3-319-94117-2_6

[17] Bauer, C., Kryvinska, N., Strauss, C. (2016). The Business with Digital Signage for Advertising. Lecture Notes in Information Systems and Organisation, 285–302. doi: https://doi.org/10.1007/978-3-319-28907-6_19

[18] Korzh, R., Peleshchyshyn, A. (2013). Formalization of process of forming university's information image in the social environments on the internet. Eastern-European Journal of Enterprise Technologies, 5 (3 (65)), 4–8.

[19] Korzh, R., Fedushko, S., Peleshchyshyn, A. (2015). Methods for forming an informational image of a higher education institution. Webology, 12 (2).

[20] Korzh, R., Peleshchyshyn, A. (2016). Forming University's Information Image Based on Image Information Generator. Journal of Multidisciplinary Engineering Science and Technology, 3 (1), 3621–3624.

[21] Witten, I., Frank, E., Hall, M., Pal, C. (2011). Data mining. Burlington, MA: Morgan Kaufmann.

[22] Lehtonen, J. (2011). Characterizing the deep Web. University of Turku.

[23] Cadwalladr, C., Graham-Harrison, E. (2019). Revealed: 50 million Facebook profiles harvested for Cambridge Analytica in major data breach. Available at: https://www.theguardian.com/news/2018/mar/17/cambridge-analytica-facebook-influence-us-election

[24] Alsaedi, N., Burnap, P. (2015). Arabic Event Detection in Social Media. Lecture Notes in Computer Science, 384–401. doi: https://doi.org/10.1007/978-3-319-18111-0_29

[25] Burnap, P., Williams, M. L., Sloan, L., Rana, O., Housley, W., Edwards, A. et. al. (2014). Tweeting the terror: modelling the social media reaction to the Woolwich terrorist attack. Social Network Analysis and Mining, 4 (1). doi: https://doi.org/10.1007/s13278-014-0206-4

[26] Pravo na vladu season 6 issue 39 online on 1+1 video (2019). Available at: https://www.youtube.com/watch?v=AyfZ9EO9qEM

[27] Pravo na vladu season 6 issue 36 online on 1+1 video (2019). Available at: https://1plus1.ua/1plus1video/pravo-na-vlast/6-sezon/36-vypusk-pravo-na-vladu-za-4-lipnya-2019-roku#player

[28] Narayanan, A., Shmatikov, V. (2008). Robust De-anonymization of Large Sparse Datasets. 2008 IEEE Symposium on Security and Privacy (sp 2008). doi: https://doi.org/10.1109/sp.2008.33

[29] Salas, J., Domingo-Ferrer, J. (2018). Some Basics on Privacy Techniques, Anonymization and their Big Data Challenges. Mathematics in Computer Science, 12 (3), 263–274. doi: https://doi.org/10.1007/s11786-018-0344-6

[30] Weber, R. H. (2010). Internet of Things – New security and privacy challenges. Computer Law & Security Review, 26 (1), 23–30. doi: https://doi.org/10.1016/j.clsr.2009.11.008

[31] Klymash, M., Demydov, I., Beshley, M., Shpur, O. (2016). Features of the cloud services implementation in the national network segment of Ukraine. Information and Telecommunication Sciences, 1, 31–38. doi: https://doi.org/10.20535/2411-2976.12016.31-38

[32] Yu, Q., Huo, H.-W. (2011). Algorithms Improving the Storage Efficiency of Deep Packet Inspection. Journal of Software, 22 (1), 149–163. doi: https://doi.org/10.3724/sp.j.1001.2011.03724

DEVELOPMENT OF METHODS FOR DETERMINING THE CONTOURS OF OBJECTS FOR A COMPLEX STRUCTURED COLOR IMAGE BASED ON THE ANT COLONY OPTIMIZATION ALGORITHM

Hennadii Khudov
Department of Radar Troops Tactic[1]
2345kh_hg@ukr.net

Igor Ruban
Department of Electronic Computers[2]
ruban_i@ukr.net

Oleksandr Makoveichuk
Department of Electronic Computers[2]
omakoveychuk@gmail.com

Hennady Pevtsov
Deputy Head in Science[1]
pevz_gv@ukr.net

Vladyslav Khudov
Department of Information Technology Security[2]
vladkhudov@gmail.com

Irina Khizhnyak
Department of Mathematical and Software Automated Control Systems[1]
khizh_ia@ukr.net

Sergii Fryz
Department of Telecommunications and Radioengineering
Zhytomyr Military Institute named after S. P. Korolyov
22 Myr ave., Zhytomyr, Ukraine, 10023
sfriz_69@ukr.net

Viacheslav Podlipaiev
Department of the ontological systems and applied algebraic combinatorics
Institute of Telecommunications and Global Information Space
25 Chokolivskiy bulv., Kyiv, Ukraine, 02000
pva_hvu@ukr.net

Yurii Polonskyi
Department of Physics and Radioelectronics[1]
upol_71@gmail.com

Rostyslav Khudov
Department of Theoretical and Applied Informatics
Kharkiv National University named after V. N. Karazin
4 Svobodyi sq., Kharkiv, Ukraine, 61022
rhudov@gmail.com

[1]Ivan Kozhedub Kharkiv National Air Force University
77/79 Sums'ka str., Kharkiv, Ukraine, 61023
[2]Kharkiv National University of Radio Electronics
14 Nauky ave., Kharkiv, Ukraine, 61166

Abstract

A method for determining the contours of objects on complexly structured color images based on the ant colony optimization algorithm is proposed. The method for determining the contours of objects of interest in complexly structured color images based on the ant colony optimization algorithm, unlike the known ones, provides for the following. Color channels are highlighted. In each color channel, a brightness channel is allocated. The contours of objects of interest are determined by the method based on the ant colony optimization algorithm. At the end, the transition back to the original color model (the combination of color channels) is carried out.

A typical complex structured color image is processed to determine the contours of objects using the ant colony optimization algorithm. The image is presented in the RGB color space. It is established that objects of interest can be determined on the resulting image. At the same time, the presence of a large number of "garbage" objects on the resulting image is noted. This is a disadvantage of the developed method.

A visual comparison of the application of the developed method and the known methods for determining the contours of objects is carried out. It is established that the developed method improves the accuracy of determining the contours of objects. Errors of the first and second kind are chosen as quantitative indicators of the accuracy of determining the contours of objects in a typical complex structured color image. Errors of the first and second kind are determined by the criterion of maximum likelihood, which follows from the generalized criterion of minimum average risk. The errors of the first and second kind are estimated when determining the contours of objects in a typical complex structured color image using known methods and the developed method. The well-known methods are the Canny, k-means (k=2), k-means (k=3), Random forest methods. It is established that when using the developed method based on the ant colony optimization algorithm, the errors in determining the contours of objects are reduced on average by 5–13 %.

Keywords: contour, object, color image, ant colony optimization algorithm, color space.

1. Introduction

Many branches of technology related to the receipt, processing, storage and transmission of information are currently largely oriented towards the development of systems in which information has the character of color images. A large number of color images are obtained in geology, mineralogy, biology, metallurgy, medicine, ecology, agriculture, military affairs, cartography, etc. [1–4].

The current trend in the development of technical systems is the production of complex structured color images presented in heterogeneous color spaces. Folding structure of color images of modern technical systems is determined by the resolution of the sensors, their sensitivity, and also due to [5]:

– presence of a large number of heterogeneous objects;
– objects in the image belong to various structural and spatial elements;
– each type of object has its own significant characteristics, it must be taken into account;
– objects are morphologically complex structures;
– objects are compact and low contrast compared to the background.

In such systems, it is important to ensure the accuracy of determining the contours of objects of interest. The accuracy of determining the contour of an object is understood as ensuring the continuity of the contour. This is especially important in automated image processing in order to develop and use machine learning methods using deep neural networks, convolutional deep neural networks, recurrent neural networks, etc. [1, 2]. Machine learning methods are used in computer vision systems, decoding of aerospace images, medicine, bioinformatics, automatic speech recognition, etc. [1, 2, 5, 6].

Existing methods for determining the contours of objects in color images provide for the preliminary conversion of a color image into a tonal image [1, 5, 6] and the further use of well-known methods for determining the contours of objects in tone images [1, 7, 8]. A study of the use of well-known methods for determining the contours of objects in color images indicates the following disadvantages [1, 5–8]:

– conversion of a complex structured color image into a tonal image leads to a break in the contour of the object, loss of the share of information, and, as a result, some decoding features of objects of interest;

– definition of the contours of objects is carried out sequentially in the "sliding" window leads to breaks in the contours of the objects when combining the information of the "sliding" windows;

– accuracy of determining the contours of objects substantially depends on the selected initial parameters of known methods;

– complicated procedure for adapting well-known methods to the current situation (methods work according to a "hard" program);

– accuracy of determining the contours of objects by known methods does not satisfy the quality requirements for solving problems that are assigned to technical systems and the like.

So, the development of a method for determining the contours of objects of interest in complexly structured color images is relevant.

The aim of research is increasing the accuracy of determining the contours of objects of interest in complexly structured color images through the use of an ant colony optimization algorithm.

To achieve the aim, the following objectives:

– to develop a method (set of actions) to determine the contours of objects in a typical complex structured color image based on an ant colony optimization algorithm;

– to determine the contours of objects in a typical complex structured color image by the method based on the ant colony optimization algorithm;

– to evaluate the accuracy of determining the contours of objects in a typical complex structured color image by the method based on the ant colony optimization algorithm.

2. Review of problem

In [9], it is proposed to determine the contours of regions in a color image using the method of maximum likelihood (expectation-maximization). The method uses colored signs of regions, spatial coordinates of points, texture signs (anisotropy, polarity, contrast, etc.). The method [9] is effective only for determining the contours of large regions (forest of various textures, field, lake, sea, ocean, city, etc.) in color images.

In [10], a method for searching scenes in color images (WAveLetbased Retrieval of User-specified Scenes) is proposed. Scenes are understood as large territories – forests, agricultural fields, wetlands, rivers, lakes, seas, oceans, urban landscape and the like. At the first stage of the method, the Haar wavelet transform is carried out, the coefficients of which form the scene feature vector. At the second stage, scenes are highlighted in a color image by clustering local areas in the feature space. The feature vector is the result of averaging the local feature vectors of the areas included in the corresponding scene. The main disadvantage of the method [10] is the possibility of its application only for determining the contours of large territories.

In [11], a method based on wavelet-based Indexing of Images Using Region Fragmentation was proposed to determine the contours of objects in color images. The method uses the global Haar transform wavelet for the image in the Hue-Saturation-Value (HSV) color space (hue-saturation-brightness). The determination of the color uniformity of the region is performed by comparing the trace of the covariance matrix of the image. It follows the covariance matrix of the image is calculated by the coefficients of the wavelet transform with an empirically selected threshold value. For regions with a heterogeneous color, the wavelet-perturbation coefficients are partitioned into 2–10 clusters. Better breakdowns are determined by the value of the evaluation function, taking into account only large regions. The main disadvantage of the method [11] is its effectiveness for determining the contours of only large regions, the consumption of significant time for conducting wavelet image analysis.

Methods for determining the contours of color images [1, 5–8] provide for the preliminary conversion of a color image into a tonal one. After conversion, in the future, well-known methods for determining the contours of objects on tone images are used. Briefly consider the known methods for determining the contours of objects in tone images.

36

In [1], methods are proposed for determining the contours of objects in images based on the use of a two-dimensional differential scalar Laplace operator. The main disadvantages are the impossibility of determining the direction of the border, not highlighting, but only emphasizing the difference in brightness. This leads to breaks in the contours of objects.

In [2], gradient methods are proposed in which the full image gradient vector is calculated. The main disadvantages are the difficulty of solving the Bayesian problem, the need for a priori knowledge of conditional probabilities of gradient values.

In [6, 7], heterogeneous methods of spatial differentiation are used (Sobel, Prewitt, Roberts, Wallace methods, sequential masking, etc.). The main disadvantages of the methods are the presence of gaps, points, and strokes forming an interfering background, the need to know the initial approximation to the desired boundary, and significant computational costs. The disadvantage of sequential masking methods [7] is the reduction in image contrast, image blur. The disadvantage of the Laplacian – Gausian (LoG) method [7] is the non-directionality of the Laplace and Gauss operators, which leads to the appearance of contour breaks.

In [8], the Canny boundary extraction method is used to determine the contours in an image. The Canny method provides a high probability of detection, high localization accuracy. The disadvantage of the Canny method is the destruction of boundaries at the connection points.

In [12], a method for determining closed loops in images based on a piecewise optimization strategy is proposed. The main disadvantage of the method [12] is the possibility of using it only for contours consisting of Bezier curves.

In [13], the active contour method is proposed. The disadvantages of the method are: high accuracy of the initial approximations, the presence of gaps, significant computational costs.

In [14], the use of neural networks is proposed to determine the contours. Neural networks are certainly suitable for determining the contours of objects in complexly structured color images, but require lengthy preliminary training.

In [15], the use of neural networks for mapping and land cadaster using images from the WorldView-2 system (DigitalGlobe, United States of America) was proposed. The methods proposed in [15] solve problems in rural areas. The application of the methods [15] to the determination of contours in complexly structured color images without a preliminary high-quality learning process is difficult.

Methods [16–18] are based on the fact that objects consist of geometric primitives (straight lines, circles, etc.). The work of such methods is based on the integral vector Radon transform [16] and the Hough transform [17]. These methods provide a qualitative definition of geometric primitives in images, for example, when revealing a power line in a forest area [17]. The use of the Radon and Hough transforms [18] is advisable only in the case of determining the geometric primitives of simple objects. It can be images of forests, agricultural fields, rivers, seas, oceans and the like. In conditions of complex structured images, the Radon and Hough transforms do not ensure the integrity of the contours of objects of interest, leading to the appearance of a large number of "garbage" objects. This significantly affects the quality of further decryption of images.

In [5], in the processing of medical tone images when determining geometric primitives, the well-known methods for determining contours and the Radon and Hough transforms are successively used. The results [5] make it possible to qualitatively determine the geometric primitive in medical images. More complex contours of objects in medical images, especially in bioinformatics systems, are destroyed.

Thus, the methods for determining the contours of objects in images have certain drawbacks, and their application to determining the contours of objects in complexly structured color images does not ensure the continuity of the contours of objects.

In [19], the use of evolutionary methods is proposed for segmenting medical images. The main attention in [19] is given to the genetic method of segmenting a medical image. The main drawback [19] is the use of the method only for segmenting simple objects on medical images. This is due to the strict binding to the conditions for the formation of the medical image and the information component, which is presented in the medical image.

In recent years, swarm methods for solving heterogeneous optimization problems have been rapidly developing. So, in [20], to find global extrema of complex functions (the function of a sphere, Rastrigin, Schwefel, and others), the method of artificial bee colony is used. The main advantages of the method are the non-susceptibility of looping at local optima; multiagency implementation; ability to adapt to environmental changes; the possibility of using for solving both discrete and continuous optimization problems.

In [21], the use of the ant colony optimization algorithm is proposed to solve the traveling salesman problem and heterogeneous transportation problems. The main advantages of the ant colony optimization algorithm are ensuring the continuity of the transport path, the possibility of efficient separation into parallel processes, adaptation, high speed, optimization of control, independence from unsuccessful initial solutions, primer search for the best solution in the solutions of all agents (ants).

The appearance of swarm methods does not go unnoticed by image processing specialists either. In [5], the use of swarm methods for segmenting tone images was proposed. The features of the ant method, the artificial bee colony method, the particle swarm method, and the like are considered. But the fact of using swarm methods in [5] is not investigated, but only postulated.

In [22], the well-known k-means method was proposed for segmenting a medical image. To select the optimal number of segments k and calculate the Euclidean distance between the segments, the use of the ant colony optimization algorithm is proposed. The sequence of operations of the ant colony optimization algorithm in general is given in [21]. In [22], in contrast to [21], an objective function is introduced that takes into account the features of calculating the Euclidean distance between segments, an optimization problem is formulated and solved, which consists in minimizing this distance. The results of [22] are applied to optimize the choice of k domains of the k-means method.

In [23], the application of the ant colony optimization algorithm to determine the contours of objects in tone images is presented. In [23], the objective function is introduced taking into account the peculiarities of the formation of an aerospace image. Applying the results of [23] to determining the contours of objects in complexly structured color images leads to a loss of the share of information and some decoding features of objects of interest. Also, the quality of determining the contours of objects of interest does not satisfy the requirements for the quality of problem solving.

To conduct further research in order to increase the accuracy of determining the contours, let's pose the problem of developing a method for determining the contours of objects of interest in complexly structured color images based on an ant colony optimization algorithm.

3. Materials and methods

It is known [21, 23] that the ant colony optimization algorithm provides for the determination of the inextricable path of each agent (ant). The continuity of the path of agents along the contour of objects, in turn, will lead to the continuity of the contour of the object of interest in the image. By the method of determining the contours of objects of interest in complexly structured color images based on an ant colony optimization algorithm, let's mean the set of actions leading to the solution of the problem [24]. When developing a method for determining the contours of objects on complexly structured color images, let's take into account the color space of the image representation. The most difficult in terms of processing is the processing of color images presented in the Red-Green-Blue (RGB) color space [1, 5, 7, 8]. So, for further study of the definition of the contours, let's carry out in each color channel of the color spaceRGB. It is known [1, 5, 7, 8] that the quality of determining the contours of objects depends more on the brightness of the pixels in the picture and less on the hue and saturation. In this regard, in each color channel, it is advisable to highlight the brightness channel. In view of the above, the method for determining the contours of objects of interest in complexly structured color images based on the ant colony optimization algorithm, in accordance with the definition of the term "method" [24], can be represented in the following form (**Fig. 1**).

38

```
                        ⬭ Begin ⬭

              ▱ Initial data input:
                f(X), S, α, β, ρ, F₀ ▱

         ▭ Highlighting color channels in the original imagef(X):
              fR(X), fG(X), fB(X) ▭

         ▭ Highlighting the luminance channel in each color channel
              of the original imagef(X) ▭

         ▭ Determining the contours of objects of interest by the
              method based on the ant colony optimization
              algorithm [22, 23], obtaining images for each color
              channel: fsR(X), fsG(X), fsB(X) ▭

         ▭ Reverse to RGB color model (color channel merging) ▭

              ▱ fs(X) ▱

                        ⬭ End ⬭
```

Fig. 1. A set of actions (method [24]), which leads to the solution of the problem of determining the contours of objects of interest in complexly structured color images based on an ant colony optimization algorithm

1. Input data:

$-f(\mathbf{X})$ – initial complex structured color image, $\mathbf{X}(x, y)$ – coordinates of points on the image;

$-\mathbf{S} = \begin{pmatrix} S_\mathrm{R} \\ S_\mathrm{G} \\ S_\mathrm{B} \end{pmatrix}$ – a vector that determines the total number of agents in color channels (S_R – in the color channel Red, S_G – in the color channel Green, S_B – in the color channel Blue);

$-\alpha = \begin{pmatrix} \alpha_\mathrm{R} \\ \alpha_\mathrm{G} \\ \alpha_\mathrm{B} \end{pmatrix}$ – a vector that determines the weight of the pheromone in the color channels;

$-\beta = \begin{pmatrix} \beta_\mathrm{R} \\ \beta_\mathrm{G} \\ \beta_\mathrm{B} \end{pmatrix}$ – a vector that determines the "greed" of the method in color channels;

$-\rho = \begin{pmatrix} \rho_\mathrm{R} \\ \rho_\mathrm{G} \\ \rho_\mathrm{B} \end{pmatrix}$ – a vector that determines the rate of pheromone evaporation in color channels;

39

$$- \mathbf{F}_0 = \begin{pmatrix} F_{0R} \\ F_{0G} \\ F_{0B} \end{pmatrix} - \text{a vector that determines the initial level of pheromone concentration in}$$

color channels.

2. Highlighting color channels in the original image $f(\mathbf{X})$: $f_R(\mathbf{X})$, $f_G(\mathbf{X})$, $f_B(\mathbf{X})$ (where $f_R(\mathbf{X})$, $f_G(\mathbf{X})$, $f_B(\mathbf{X})$ – the images on the color channels Red, Green, Blue, respectively).

3 The allocation of the brightness channel in each color channel of the output image: $f_R(\mathbf{X})$, $f_G(\mathbf{X})$, $f_B(\mathbf{X})$.

4. Determination of the contours of objects of interest by the method based on the ant colony optimization algorithm [22, 23], obtaining images for each color channel: $fs_R(\mathbf{X})$, $fs_G(\mathbf{X})$, $fs_B(\mathbf{X})$ (where $fs_R(\mathbf{X})$, $fs_G(\mathbf{X})$, $fs_B(\mathbf{X})$ – an image with certain contours of objects of interest in the color channels Red, Green, Blue, respectively).

5. Return to the RGB color model (combining color channels).

6. Obtaining the resulting image $fs(\mathbf{X})$.

Thus, the novelty of the method for determining the contours of objects of interest in complexly structured color images based on the ant colony optimization algorithm, in contrast to the known ones, consists in:

– highlighting color channels;

– highlighting in each color channel of the brightness channel;

– determination of the contours of objects of interest by the method based on the ant colony optimization algorithm;

– reverse transition to the original color model (combination of color channels).

4. Experiments on processing conventional color images

4. 1. Determination of the contours of objects on a typical complex structured color image by the method based on the ant colony optimization algorithm

As a typical output of a complex structured color image, let's use a color image from the on-board optical-electronic surveillance system based on the Ikonos spacecraft (GeoEye, USA) (**Fig. 2**) [25]. This is the territory of the Donetsk airport in 2015. The image is presented in the RGB color space. Image size – (868×847) pixels.

Fig. 2. Initial color image [25]

Image Processing of complex structured color image for determining the contours of objects will be carried out by the method based on the ant colony optimization algorithm (**Fig. 1**).

Fig. 3 shows the images of the brightness channel of each color channel of the RGB color space of the original image (**Fig. 2**).

In the brightness channel of each color space, the ant colony optimization algorithm is used to determine the contours of objects. The ant colony optimization algorithm, taking into account the results of [21, 23], is represented by the following sequence of actions.
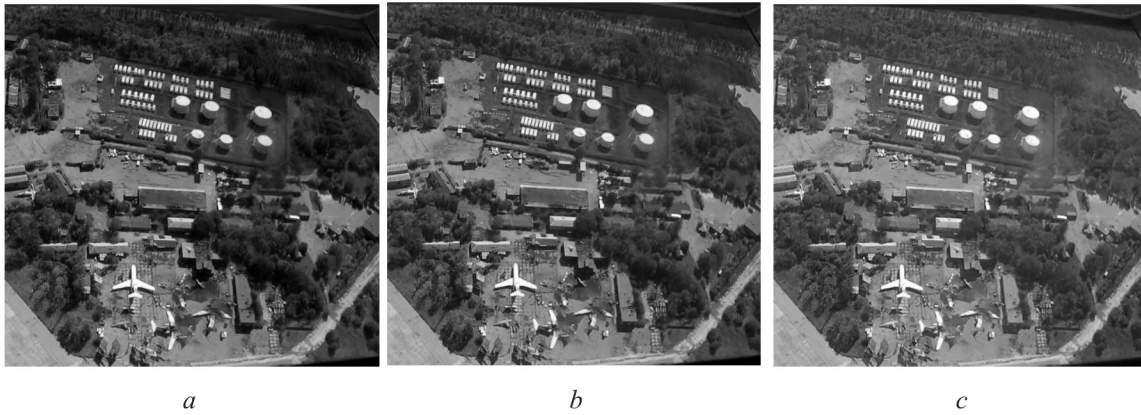
Fig. 3. Images of the brightness channel of the original color image (**Fig. 2**) in the color channels:
a – Red; *b* – Green; *c* – Blue

1. Initialization of the initial positions of the agents in the picture at the first iteration (*j*=1). $\mathbf{X}_{i1}(x_{i1}, y_{i1})$ – the vector of agent positions at the first iteration, *i*=1, 2, …, *S*; *S* – the total number of agents. The total number of agents *S* is equal to the number of pixels in the original image.

2. Calculation of the objective function $\varphi_j(\mathbf{X})$ at the *j*-th iteration. As the objective function at the *j*-th iteration, let's define function (1):

$$\varphi_j(\mathbf{X}) = \sum_{m=1}^{S}\sum_{i=1}^{N}\left(P_i^m(j)D_i^m(j)\right), \tag{1}$$

where *m* – the current number of the agent; *N* – the image size; $P_i^m(j)$ – the probability of transition of the *m*-th agent to the *i*-th turning point of the route at the *j*-th iteration (2):

$$P_i^m(j) = \frac{\left(F_i^m(j)\right)^{\alpha}\left(L_i^m(j)\right)^{\beta}}{\sum\limits_{r=1}^{R}\left(F_r^{\alpha}(j)\cdot L_t^b(j)\right)}, \tag{2}$$

where α and β – parameters specifying the weight of the pheromone and the "greed" of the method, respectively;

– *R* – the number of possible turning points of the route;

– $L_i^m(j)$ – the attractiveness of the route section for the *m*-th agent at the *i*-th image point at the *j*-th iteration;

– $F_i^m(j)$ – pheromone concentration of the *m*-th agent at the *i*-th point of the image at the *j*-th iteration;

– $D_i^m(j)$ function determines the length of the route section taking into account the difference in brightness of neighboring pixels for the *m*-th agent at the *i*-th image point at the *j*-th iteration and is determined by the expression (3):

$$D_i^m(j) = \left|\triangle x_i^m(j)\right| + \left|\triangle y_i^m(j)\right| + k\left|\triangle f_i^m(j)\right|, \tag{3}$$

where $\left|\triangle x_i^m(j)\right|$, $\left|\triangle y_i^m(j)\right|$ – the elementary displacements of the m-th agent at the i-th image point at the *j*-th iteration along the *x* and *y* axes, respectively;

– *k* – coefficient taking into account the difference in scales along the *x* and *y* axes and the brightness of the image pixels and various units of measurement of elementary displacements and brightness. If the brightness takes values from the range [0..255], then *k*=1;

– $\left|\triangle f_i^m(j)\right|$ – the difference in brightness of neighboring points for the *m*-th agent in the *i*-th image point at the *j*-th iteration – (4):

41

$$\left| \triangle f_i^m (j) \right| = \left| \begin{matrix} f\left(x_i^m (j), y_i^m (j) \right) - \\ -f\left(x_{i-1}^m (j), y_{i-1}^m (j) \right) \end{matrix} \right|. \tag{4}$$

3. Movement of agents. In the ant colony optimization algorithm in each iteration of the iterative process, m agents search for a solution and update pheromones along the found route. Each m-th agent starts the path from the starting point of the route, successively passes the turning points of the route selected by the method and ends the path at one of the end points of the route. The movement of agents is carried out according to the criterion of the minimum of the objective function (1), which, taking into account the quadruple connection of the movement of agents (5):

$$\left| \triangle x_i^m (j) \right| + \left| \triangle y_i^m (j) \right| = 1, \tag{5}$$

has the form (6):

$$\varphi_j (\mathbf{X}) = \sum_{m=1}^{S} \sum_{i=1}^{N} \left(P_i^m (j) \left(1 + k \left| \begin{matrix} f(x_i^m (j), y_i^m (j) - \\ -f(x_{i-1}^m (j), y_{i-1}^m (j) \end{matrix} \right| \right) \right) \to \min. \tag{6}$$

Let's believe that the attractiveness of the route $L_i^m (j)$ section for the m-th agent at the i-th image point at the j-th iteration inversely depends on the length of the route segment, for example (7):

$$L_i^m (j) = \frac{1}{1 + e^{\frac{D_i^m (j)}{D_0}}}, \tag{7}$$

where D_0 – a parameter that takes into account the image scale.

At the beginning of the iterative process, the amount of pheromone in the sections of the route is taken equal to and equal to some small number F_0. After each iteration, the concentration of pheromones in the areas selected by the agents is updated according to the rule (8):

$$F_i^m (j+1) = (1-\rho) F_i^m (j) + \sum_{m-1}^{M} \triangle F_i^m, \tag{8}$$

where $\rho \in [0, 1]$ – the evaporation rate of pheromone; $\triangle F_i^m$ – the concentration of the pheromone on the i-th section of the route is created by the passage of the m-th agent.

As a result of a certain number of iterations, the most attractive routes are determined by the chosen criterion, the concentration of pheromone on which is maximum. Pheromone gradually "evaporates" on unattractive routes, and unattractive routes disappear. At α=0, the agents at each step go to the nearest turning point of the route, and the ant colony optimization algorithm turns into the "greedy" method of the classical optimization theory. When β=0, only the effect of pheromones is taken into account will quickly lead to a suboptimal solution.

4. Verification of the fulfillment of the stopping condition. If the condition is met, then the original image with certain contours of the objects is obtained. Otherwise – the transition to the second paragraph.

Thus, in the ant colony optimization algorithm for determining the contours of objects, it is reduced to calculating the objective function, the totality of the areas of movement of agents, and the concentration of pheromone on the routes of movement of agents.

The method parameters are the same for the brightness channel of each color channel and are equal to: **S**=735,196 agents (the number of pixels in the picture), α=2; β=1; ρ=10⁻³; **F₀**=10⁻². The number of iterations in each color channel is the same and equal to 50.

The return to the RGB color model is carried out by combining color channels using the well-known rules for mixing colors and the laws of mathematical logic [1].

42

The result of determining the contours in a typical complex structured color image using the ant colony optimization algorithm is shown in **Fig. 4**. Objects of interest are also identified in the resulting image (**Fig. 4**), for example, containers with oil or fuel for airplanes; airplanes that survived after striking; aircraft that have been damaged or destroyed and the like. Decryption of these objects of interest, recognition, thematic classification, and more is the subject of further research and remains outside the scope of this work.
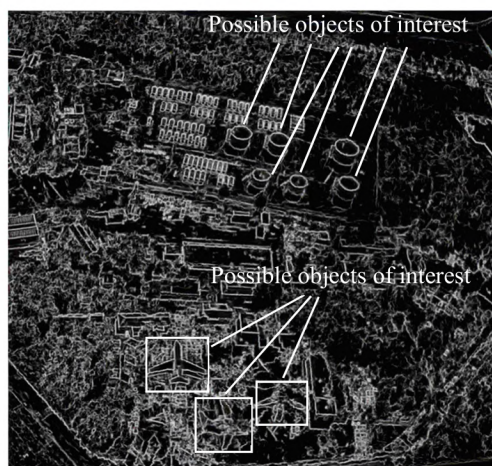
Fig. 4. The result of determining the contours of objects in a typical complex structured color image by the method based on the ant colony optimization algorithm

It should be noted that there is a large number of "garbage" objects in the resulting image (**Fig. 4**). This is a disadvantage of the developed method.

4. 2. Assessment of the accuracy of determining the contours of objects

Let's conduct a comparative visual assessment of the accuracy of determining the contours of objects by the developed method and known methods. As well-known methods for determining the contours of objects, let's consider the Canny method [8], the k-means method (with different k values) [22, 26], and the Random forest method [19, 22].

Fig. 5 shows the results of determining the contours of objects by known methods (Canny, k-means ($k=2$, $k=3$), Random forest). From visual analysis of **Fig. 5, *a*** it is possible to state that the Canny method has significant gaps in the contours of objects. This is especially true for fuel tanks and small airport infrastructure. Visual analysis of **Fig. 5, *b*, *c*** indicates a low visual quality of determining the contours of objects using the k-means method. The Random forest method determines a large number of false paths (**Fig. 5, *d***).

a   *b*   *c*   *d*
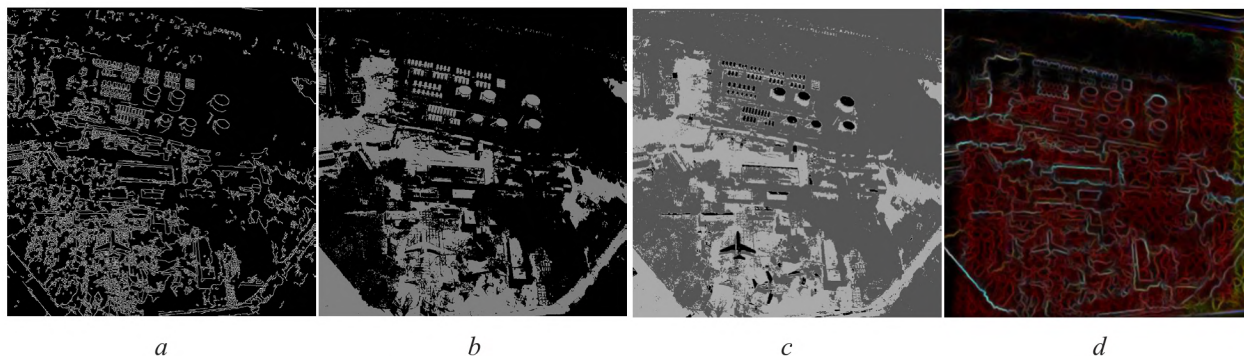
Fig. 5. The resulting image with certain contours:
a – by the Canny method; *b* – by the *k*-means method ($k=2$); *c* – by the *k*-means method ($k=3$);
d – by the Random forest method

In well-known works [1, 2, 5, 6, 10], various quantitative indicators are used to evaluate the quality of image processing. Such indicators take into account the type of image, the presence or absence of a priori information about objects of interest, etc. and characterize the quality of image processing. To quantify the accuracy of determining the contours of objects of interest in practice, errors of the first and second kind are widely used [2, 5, 23, 27]. Therefore, let's choose the errors of the first and second kind as indicators of the quality of determining the contours of objects in a typical complex structured color image.

Errors of the first (α_1) and second (β_2) kind are determined by the criterion of maximum likelihood, which follows from the generalized criterion of minimum average risk [2, 5, 23, 27]. Errors in determining the first-kind contours α_1 and second-kind β_2 are calculated using expressions (9), (10), respectively [2, 5, 23, 27]:

$$\alpha_1 = \frac{N_1\left(fs(\mathbf{X})\right)}{N_2\left(f(\mathbf{X})\right)}, \tag{9}$$

$$\beta_2 = 1 - \frac{N_3\left(fs(\mathbf{X})\right)}{N_4\left(f(\mathbf{X})\right)}, \tag{10}$$

where $N_1(fs(\mathbf{X}))$ – the number of pixels in the background, erroneously assigned to the contours of objects in the image fs(X); $N_2(f(\mathbf{X}))$ – the number of pixels in the background of the original image $f(\mathbf{X})$; $N_3(fs(\mathbf{X}))$ – the number of pixels correctly assigned to the contours of objects in the image fs(X); $N_4(f(\mathbf{X}))$ – the number of points that belong to the contours of the objects in the original image $f(\mathbf{X})$.

Calculations by expressions (9), (10) will be carried out under the same conditions, the same signal-to-noise ratio for the methods for determining the contours of objects by known methods. The well-known methods were the Canny methods, the k-means method ($k=2$), the k-means method ($k=3$), and the Random forest method. The sample size is equal to the number of pixels in the image. In this case, it is 735,196 pixels. The variability of observation is equal to the time of obtaining a color image. Calculated by the expressions (9), (10), the values of errors of the first and second kind for various methods are given in **Table 1**.

Table 1
Evaluation of errors of the first and second kind of determining the contours of objects in a typical complex structured color image by various methods

Method for determining the contours of objects	α_1, %	β_2, %
Canny	25	30
k-means (*k*=2)	31	36
k-means (*k*=3)	27	31
Random forest	24	29
Method for determining the contours of objects based on ant colony optimization algorithm	19	21

The calculations are carried out using a high-level programming language and an interactive environment for programming, numerical calculations and visualization of the results of MATLAB R2017b. **Table 1** and **Fig. 6** show a part of program code.

Analysis of data in **Table 1** indicates a reduction in the errors of the first and second kind of edge detection in a typical complex structured color image using the developed method based on the ant colony optimization algorithm. Errors in determining the contours of objects are reduced on average by 5–13 %.

44

```
close all
clear all
clc

srcPath='src\';
files=dir([srcPath 'vl*.png']);

k0=2.5;
n=1;
src=single(imread([srcPath files(n).name]))/255;
g0=rgb2gray(src);
th=mean2(g0)+k0*std2(g0);
bw0=g0>th;

method={ 'ACO', 'k-means_2', k-means_3', Randon forest'};

for n=1:length(files)

  srcName=[srcPath 'res\' files(n).name(1:end-4)];

  for m=1:length(method)
    fileName=sprintf(' %s\\ %s- %04d-u.png', srcName, method{m}, 8);
    res=imread(fileName);
    res=double(res)/255;
    g1=rgb2gray(res);
    th=mean2(g1)+k0*std2(g1);
    bw1=g1>th;
    s{m,n}(1,1)=mean2(double(bw0==0 & bw1==0));
    s{m,n}(2,1)=mean2(double(bw0==1 & bw1==0));
    s{m,n}(1,2)=mean2(double(bw0==0 & bw1==1));
    s{m,n}(2,2)=mean2(double(bw0==1 & bw1==1));

    fileName=sprintf(' %s\\ %s- %04d-bw.png', srcName, method{m}, 8);
    imwrite(bw1, fileName);
  end

end
fileName=sprintf(' %s\\bw0.png', srcName);
imwrite(bw0, fileName);
```

Fig. 6. A fragment of the program code for calculating the data in Table 1

5. Discussion of results

The method for determining the contours of objects of interest in complexly structured color images based on the ant colony optimization algorithm, unlike the known ones, provides for the following (**Fig. 1**). Color channels are highlighted. In each color channel, a brightness channel is allocated. The contours of objects of interest are determined by the method based on the ant colony optimization algorithm. At the end, the transition back to the original color model (the combination of color channels) is carried out.

The contours of objects are determined on a typical complex structured color image (**Fig. 2**) by the method based on the ant colony optimization algorithm. In the resulting image (**Fig. 4**), objects of interest can be identified, for example, containers with oil or fuel for aircraft; airplanes that survived after striking; aircraft that have been damaged or destroyed and the like. Decryption of these objects of interest, recognition, thematic classification, and more is the subject of further research and remains outside the scope of this work. The presence of a large number of "garbage" objects on the resulting image (**Fig. 4**) is noted. This is a disadvantage of the developed method.

A visual comparison of the application of the developed method and the known methods for determining the contours of objects is carried out. It is established that the developed method improves the accuracy of determining the contours of objects. Errors of the first and second kind were chosen as quantitative indicators of the accuracy of determining the contours of objects in a

45

typical complex structured color image. Errors of the first and second kind are determined by the criterion of maximum likelihood, which follows from the generalized criterion of minimum average risk (expressions (9), (10)). The errors of the first and second kind are estimated when determining the contours of objects in a typical complex structured color image using known methods and the developed method (**Table 1**). The well-known methods are the Canny, k-means (k=2), k-means (k=3), Random forest methods. It is established that when using the developed method based on the ant colony optimization algorithm, the errors in determining the contours of objects are reduced on average by 5–13 %.

When conducting further research, it is necessary to:

– develop a method to reduce "garbage" objects;

– conduct a comparative assessment of the quality of the developed methods with known using information quality indicators (for example, image entropy, Kullback-Leibler distance, etc.).

6. Conclusions

1. The method for determining the contours of objects in complex color images based on the ant colony optimization algorithm has been improved. Unlike the known methods, the method provides for: the allocation of color channels, in each color channel the allocation of the brightness channel, the determination of the contours of objects of interest by the method based on the ant colony optimization algorithm, the reverse transition to the original color model.

2. The determination of the contours of objects on a typical complex-structured color image by the method based on the ant colony optimization algorithm has been carried out. It is established that objects of interest can be determined on the resulting image. At the same time, the presence of a large number of "garbage" objects on the resulting image is noted. This is a disadvantage of the developed method.

3. A visual comparison of the application of the developed method and known methods for determining the contours of objects. It is established that the developed method improves the accuracy of determining the contours of objects. The errors of the first and second kind are estimated when determining the contours of objects in a typical complex structured color image using known methods and the developed method. It is established that when using the developed method based on the ant colony optimization algorithm, the errors in determining the contours of objects are reduced on average by 5–13 %.

References

[1] Gonzalez, R., Woods, R. (2017). Digital Image Processing. Prentice Hall, Upper Saddle Rever, 1192.

[2] Richards, J. (2013). Remote Sensing Digital Image Analysis. An Introduction. Springer. doi: https://doi.org/10.1007/978-3-642-30062-2

[3] Vysotska, V., Lytvyn, V., Burov Y., Gozhyj, A., Makara, S. (2018). The consolidated information web-resource about pharmacy networks in city. CEUR, 239–255.

[4] Stryzhak, O., Prychodniuk, V., Podlipaiev, V. (2019). Model of Transdisciplinary Representation of GEOspatial Information. Advances in Information and Communication Technologies, 34–75. doi: https://doi.org/10.1007/978-3-030-16770-7_3

[5] El-Baz, A., Jiang, X., Jasjit, S. (Eds.) (2016). Biomedical image segmentation. Advances and trends. CRC Press, 546. doi: https://doi.org/10.4324/9781315372273

[6] Karamti, H., Tmar, M., Gargouri, F. (2017). A new vector space model for image retrieval. Procedia Computer Science, 112, 771–779. doi: https://doi.org/10.1016/j.procs.2017.08.202

[7] Gupta, V., Singh, D., Sharma, P. (2016). Image Segmentation Using Various Edge Detection Operators: A Comparative Study. International Journal of Innovative Research in Computer and Communication Engineering, 4 (8), 14819–14824.

[8] Kabade, A., Sangam, V. (2016). Canny edge detection algorithm. International Journal of Advanced Research in Electronics and Communication Engineering (IJARECE), 5 (5), 1292–1295.

[9] Carson, C., Thomas, M., Belongie, S., Hellerstein, J. M., Malik, J. (1999). Blobworld: A System for Region-Based Image Indexing and Retrieval. Lecture Notes in Computer Science, 509–517. doi: https://doi.org/10.1007/3-540-48762-x_63

[10] Natsev, A., Rastogi, R., Shim, K. (1999). WALRUS. ACM SIGMOD Record, 28 (2), 395–406. doi: https://doi.org/10.1145/304181.304217

[11] Bartolini, I., Patella, M., Stromei, G. (2011). The windsurf library for the efficient retrieval of multimedia hierarchical data. Proceedings of the International Conference on Signal Processing and Multimedia Applications. doi: https://doi.org/10.5220/0003451701390148

[12] Yang, M., Chao, H., Zhang, C., Guo, J., Yuan, L., Sun, J. (2016). Effective Clipart Image Vectorization Through Direct Optimization of Bezigons. IEEE Transactions on Visualization and Computer Graphics. Available at: https://arxiv.org/pdf/1602.01913.pdf

[13] Sum, K., S. Cheung, P. (2006). A Fast Parametric Snake Model with Enhanced Concave Object Extraction Capability. 2006 IEEE International Symposium on Signal Processing and Information Technology. doi: https://doi.org/10.1109/isspit.2006.270844

[14] Karamti, H., Tmar, M., Gargouri, F. (2014). Vectorization of Content-based Image Retrieval Process Using Neural Network. Proceedings of the 16th International Conference on Enterprise Information Systems. doi: https://doi.org/10.5220/0004972004350439

[15] Nyandwi, E., Koeva, M., Kohli D., Bennett, R. (2019). Comparing Human Versus Machine-Driven Cadastral Boundary Feature Extraction. Remote Sens, 11, 1662. doi: https://doi.org/10.20944/preprints201905.0342.v1

[16] Ramlau, R., Scherzer, O. (2019). The Radon Transform. Berlin/Boston: Walter de Gruyter GmbH. doi: https://doi.org/10.1515/9783110560855

[17] Li, Z., Liu, Y., Walker, R., Hayward, R., Zhang, J. (2009). Towards automatic power line detection for a UAV surveillance system using pulse coupled neural filter and an improved Hough transform. Machine Vision and Applications, 21 (5), 677–686. doi: https://doi.org/10.1007/s00138-009-0206-y

[18] Manzanera, A., Nguyen, T. P., Xu, X. (2016). Line and circle detection using dense one-to-one Hough transforms on greyscale images. EURASIP Journal on Image and Video Processing, 2016 (1). doi: https://doi.org/10.1186/s13640-016-0149-y

[19] Faroogue, M. Y., Raeen, M. S. (2014). Latest trends on image segmentation schemes. International journal of advanced research in computer science and software engineering, 4 (10), 792–795.

[20] Karaboga, D., Gorkemli, B., Ozturk, C., Karaboga, N. (2012). A comprehensive survey: artificial bee colony (ABC) algorithm and applications. Artificial Intelligence Review, 42 (1), 21–57. doi: https://doi.org/10.1007/s10462-012-9328-0

[21] Dorigo, M., Stützle, T. (2018). Ant Colony Optimization: Overview and Recent Advances. International Series in Operations Research & Management Science, 311–351. doi: https://doi.org/10.1007/978-3-319-91086-4_10

[22] Choudhary, R., Gupta, R. (2017). Recent Trends and Techniques in Image Enhancement using Differential Evolution- A Survey. International Journal of Advanced Research in Computer Science and Software Engineering, 7 (4), 106–112. doi: https://doi.org/10.23956/ijarcsse/v7i4/0108

[23] Ruban, I., Khudov, H., Makoveichuk, O., Chomik, M., Khudov, V., Khizhnyak, I. et. al. (2019). Construction of methods for determining the contours of objects on tonal aerospace images based on the ant algorithms. Eastern-European Journal of Enterprise Technologies, 5 (9 (101)), 25–34. doi: https://doi.org/10.15587/1729-4061.2019.177817

[24] Gauch, H. (2002). Scientific Method in Practice. Cambridge University Press. doi: https://doi.org/10.1017/cbo9780511815034

[25] Ikonos Satellite Image Gallery. Available at: https://www.satimagingcorp.com/gallery/ikonos/

[26] Pelleg, D., Moore, A. (2000). X-means: Extending k-means with efficient estimation of the number of clusters. Proceeding of the 17th International Conference on Machine Learning. San Francisco, 727–734.

[27] Gonzaga, A. (2009). Method to Evaluate the Performance of Edge Detector. The XXII Brazilian Symposium on Computer Graphics and Image Processing, 87–91.

IMPROVEMENT OF PROJECT RISK ASSESSMENT METHODS OF IMPLEMENTATION OF AUTOMATED INFORMATION COMPONENTS OF NON-COMMERCIAL ORGANIZATIONAL AND TECHNICAL SYSTEMS

Alexander Androshchuk
Educational and Scientific Institute of Management Training[1]
asa_20_1968@ukr.net

Serhii Yevseiev
Department of Cyber Security and Information Technology
Simon Kuznets Kharkiv National University of Economics
9-A Nauky ave., Kharkiv, Ukraine, 61166
serhii.yevseiev@hneu.net

Victor Melenchuk
Department of repair and operation of automotive and special equipment
Military Academy (Odessa)
10 Fontanskaya road str., Odessa, Ukraine, 65009
viktor.melenchuk1976@i.ua

Olga Lemeshko
Department of English[1]
lemeshkolia@ukr.net

Vladimir Lemeshko
Department of Border Guard Tactics[1]
lem-73@ukr.net

[1]National Academy of the State Border Guard Service of Ukraine named after Bohdan Khmelnytskyi
46 Shevchenko str., Khmelnitsky, Ukraine, 29007

Abstract

The results of a study using the methodological apparatus of the theory of fuzzy logic and automation tools for analyzing input data for risk assessment of projects for the implementation of automated information components of organizational and technical systems are presented. Based on the model of logistics projects for motor transport units, the method for assessing the risks of projects implementing automated information components of non-commercial organizational and technical systems has been improved. To do this, let's analyze the peculiarities of implementing ERP projects as commercial ones and investigate the specifics of the activities of state institutions, when successful tasks, and not economic indicators, lay the foundation for the assessment. It is considered that it is possible to formulate a system of risk assessment indicators for reducing the effectiveness of projects for implementing automated information systems in non-commercial organizational and technical systems. A meaningful interpretation of the fuzzy approach is carried out regarding the formalization of the risk assessment process for projects of automated information systems of public institutions. A tree of fuzzy inference is constructed based on the results of a study of the description of indicators and expert assessments on the risk assessment of the implementation of the project of such an automated information system.

The improved method differs from the known ones by the use of hierarchical fuzzy inference, which makes it possible to quantify, reduce the time to evaluate project risks and improve the quality of decisions. An increase in the number of input variables leads to an increase in complexity (an increase in the number of rules) for constructing a fuzzy inference system. The construction of a hierarchical system of fuzzy inference and knowledge bases can reduce complexity (the number of rules). The development of a software module based on the algorithm of the method as part of corporate automated information systems of non-commercial organizational and technical systems will reduce the time for risk assessment of projects for the implementation of automated information systems.

Keywords: organizational and technical system, implementation project, risk management, fuzzy logical conclusion.

1. Introduction

The development of the state and society involves solving the issue of improving the quality of tasks by organizational (socio) technical systems (hereinafter referred to as OTS) that are part of them. Including these are the following systems: unit management, logistics, personnel learning (training), etc. A significant role in solving this question is given to informatization – the implementation of automated information systems (hereinafter – AIS). An analysis of activities over the past decade indicates that project-oriented OTSs are becoming more effective with respect to vertically integrated OTSs with their functional organization of activities [1–3]. Therefore, the current period of OTS development is characterized by a transition to a project-oriented management principle. At the same time, the activities of most OTSs have certain specifics, when the main criterion for the implementation of AIS is successfully completed tasks, and not economic indicators. For example, implementation projects of AIS material and technical support of state institutions are non-commercial in nature. The activities of most of them have significant elements of uncertainty and danger. The functioning of military and law enforcement agencies is generally impossible without risk. Therefore, one of the most important elements of project management of the implementation of AIS of such OTSs is risk management [4, 5]. Existing approaches to risk management in projects, including their assessments, are defined in the following standards: AS/NZS 4360:2004, COSO-ERM, ISO 26500:2012, FERMA, PMBoK, P2M, PRINCE, PSPRM, RMI and the like. They describe risk management approaches in projects related to financial, economic, technical systems, etc., as a rule, in deterministic and stochastic conditions. However, the management and risk assessment of AIS projects in the activities of such non-commercial (specific) OTS included in state institutions is carried out in conditions of uncertainty. As a result, most of these projects are a failure. Therefore, the improvement of the method of risk assessment of AIS projects of non-commercial OTS and the like is an urgent scientific and applied task.

The general problems of the project management study are the subject of [6]. It addressed the general issues of project management, which, as a rule, did not take into account the specifics of nonprofit OTS and similar systems. The issue of developing risk management methods in projects is presented in the following works: [7] – an organizational model for project risk management is developed while assessing project risks in the face of uncertainty; no attention is paid; [8] – a method for managing the cost of projects of scientific institutions taking into account risks has been developed, while a qualitative risk assessment is not carried out; [9] – classification of deviations in projects with respect to risks, problems, changes; [10] – methods for structuring, evaluating, and controlling project risks have been developed for the efficient implementation of projects by the enterprise at minimal cost. At the same time, in the considered works, a quantitative risk assessment of the AIS implementation projects in particular and in general other projects under conditions of uncertainty was not given attention. In [11], the Accelerated SAP Methodology (ASAP) is considered, which was developed by SAP in order to improve the implementation of information systems risk management. In [12], general issues of risk management are considered. The paper [13] presents a model for assessing the risks of logistics projects for motor units of the Armed Forces of Ukraine using three linguistic variables, taking into account the conditions of uncertainty, but it is clearly not enough to evaluate complex projects.

It should be noted that the most common approach to the implementation of commercial AIS can be considered the implementation of an ERP system, therefore, to improve the risk assessment method for projects implementing AIS of nonprofit OTS, let's consider in more detail the features of ERP implementation [14].

"ERP is an AIS implementation technology, it contains a set of coordination, organizational, investment, economic, analytical and research, information technology and production activities, the purpose of which is to inform the organization, increase the effect and optimize the management of its resources" [15].

To assess the risks of projects implementing a logistics AIS (implementation of ERP systems) of OTS to reduce the effectiveness (not achieving the desired efficiency) of a project or a project failure when implementing a project is quite problematic due to its complexity. This is due to the fact that, for example, the risks of logistic automated information system (hereinafter referred

to as LAIS) logistics projects are characterized by a system of indicators that are usually weak and informal. These indicators reflect the ratio of the effect and costs of the project from the point of view of its participants.

Most scientists most often use the types of risk analysis and assessment that can be applied to the implementation of the AIS material and technical support of the OTS with the corresponding indicators [14–17]:

1) standard according to the method in investment analysis (Cost Benefit Analysis – CBA);

2) Activity Based Costing (ABC) – a method that performs a functional analysis of expenses;

3) set of methods in the analysis that use integrated service planning and planning of the information sphere;

4) methods, carrying out a system analysis of the project;

5) methods of expert assessment (methods of "experience, intuition of brainstorming"), etc.

When assessing the risk of projects regarding the achievement of benefits at certain costs in existing studies, in most cases, it is proposed to use indicators of an economic and informational nature.

The economic component is estimated using methods that take into account costs based on elements of economic analysis. "One of the methods of economic risk analysis for the implementation of ERP-system projects is the so-called ABC (Activity Based Costing) – a functional-cost analysis, in the framework of which differentiated calculation and distribution of the costs of operating the system are carried out by type of activity, product and organization functions. The application of this approach involves the use of a system of financial indicators [17].

The given indicators and methods constitute the traditional existing and used set of risk assessment methods for reducing the effectiveness of implementation projects of commercial OTS.

Given the specifics of the activities of nonprofit OTS, these approaches (indicators and methods) can't be considered as comprehensive in assessing the risks of implementation projects of AIS of state institutions. Effectively they can be used only in combination, when the elements of one of the approaches allow to overcome the shortcomings in others.

The aim of the article is to substantiate an approach to improve the risk management efficiency of non-commercial OTS implementation AIS projects based on the improvement of the risk assessment method for such projects.

To achieve this goal it is necessary to solve the following tasks:
– explore methods for assessing the risks of AIS implementation projects;
– improve the method of assessing the risks of AIS implementation projects;
– practically introduce and experimentally test the improved method.

2. The method of risk assessment of projects for the implementation of automated information components of non-commercial organizational and technical systems

Below is a method for assessing the risks of AIS implementation projects using the example of a public institution AIS implementation project based on the model presented in [13]. One of the promising projects for providing OTS, which will allow a significant positive effect, is the AIS implementation. This postulate allows to formulate a system of indicators for assessing the risks of reducing the effectiveness of the implementation of AIS of non-commercial OTS (state institutions):

1) total costs of the projects and the costs of completing tasks using the project results (increase/decrease of these costs);

2) duration of the project and the duration of the tasks using the project results (increase/decrease time);

3) quality of the performance (official) tasks;

4) effectiveness (effect) of the project and the like.

The initial data for assessing the risk of a decrease in the effectiveness of AIS implementation projects (for example, material and technical support for state institutions) is poorly formalized, so adequate tools should be used. For this, an approach is proposed that is presented in [18–20] and developed and tested in [21] and others.

An approach is proposed to improve the method of risk assessment of implementation projects of AIS of non-commercial OTS, providing for this (**Fig. 1**). In the process of a qualitative assessment of project risks, it is necessary, if possible, to determine as many different indicators as possible.

Risk identification, calculation of initial data for project risk assessment	Definition of risk assessment indicators of implementation projects of AIS of non-commercial OTS	The selection of indicators that have the highest rating
Building a tree of input linguistic risk variables for the AIS project (a_i)	**Project risk assessment** using hierarchical fuzzy inference	Obtaining a project risk assessment result (b), **risk management**

Fig. 1. Scheme of an improved method of risk assessment of projects for the implementation of automated information systems of non-commercial organizational and technical systems

In addition, the essence of the proposed improvement of the method is to obtain and compare indicators that determine various aspects of the activities and effectiveness of the OTS automated information system. In this case, an expert assessment of their predicted values after the implementation of the project is applied.

Formal interpretation of the risk assessment of AIS projects is necessary for a meaningful interpretation of the fuzzy approach. First of all, it involves the activities of the researcher in the selection of input and output linguistic variables of the fuzzy logical inference system that is being developed. Each input variable should influence the final result. For example, the level of the indicator for increasing the volume of performance of official tasks – a_1.

Obviously, the higher the score, the more attractive the project is, and the risks are small. The output variable b is formalized as the risk level for the implementation of the AIS project of non-commercial OTS. To do this, let's construct a tree of fuzzy inference based on the results of a study of a description of indicators and expert assessments on the risk assessment of the implementation of the AIS project, for example

1) a_1 – success indicators:

a_{11} – indicator of the success of the project as a whole (the project is completed on time, within the budget and with a positive effect);

2) a_2 – performance indicators of individual (service) tasks:

a_{21} – indicator of the volume of completed tasks;

a_{22} – indicator of the share of qualitatively completed tasks;

a_{23} – indicator of the share of completed tasks on time;

3) a_3 – performance indicators:

a_{31} – time for the implementation of the project;

a_{32} – time for organizational activities for the implementation of the project (installation and trial operation of the AIS, time for making complaints, time for staff training, etc.);

a_{33} – time to complete tasks using the project results;

4) a_4 – expense indicators:

a_{41} – indicator of the cost of implementing the project;

a_{42} – indicator of personnel costs;

a_{43} – indicator of the cost of completing tasks and paperwork.

For this case, 10 input variables are selected. For other cases, the number and content of input variables may be different.

Let b denote the result of the risk assessment of the implementation of the AIS project. The initial variable is the level of risk of reduced efficiency (failure to achieve the desired effectiveness) of AIS projects – b: management efficiency, staff training level, provision efficiency, and the like.

In the improved method of fuzzy inference regarding the assessment of the risk of reduced efficiency (failure to achieve the desired effectiveness) of the AIS implementation project, all vari-

ables are linguistic in nature with a universal set $M_u = \{m_1, m_2, \ldots m_n\}$. According to [13], these variables can be measured in the range of numbers from 0 to 10 or in the range from 0 to 1 by participants project based on their knowledge and experience. As a term-set of input and output variables, for simplification it is proposed to use the set L_1={"low", "medium", "high"} (level) of the variable. The construction of the membership functions of the terms, which is suggested for linguistic variables can be carried out using various methods, including the method of statistical processing of expert information, which is proposed in [19].

Next, it is necessary to build a fuzzy knowledge base (hereinafter – KB). The implementation of the task of assessing the risk of LAIS implementation projects (reducing efficiency, not achieving the desired LAIS project effectiveness) requires a significant number of rules ($R=10^3=1000$), which complicates the use of fuzzy inference (perception, editing and use). This situation is solved by constructing a hierarchical knowledge base [18] – a breakdown of a complex logical inference into several simple logical conclusions. This is facilitated by the hierarchical structure of the process of non-commercial OTS (state institutions). A hierarchical representation of the input variables and the construction of a "tree" of output are necessary, which defines a system of lower-dimensional knowledge statements embedded in each other. Such a tree is proposed for fuzzy inference after 10 input variables (**Fig. 2**).
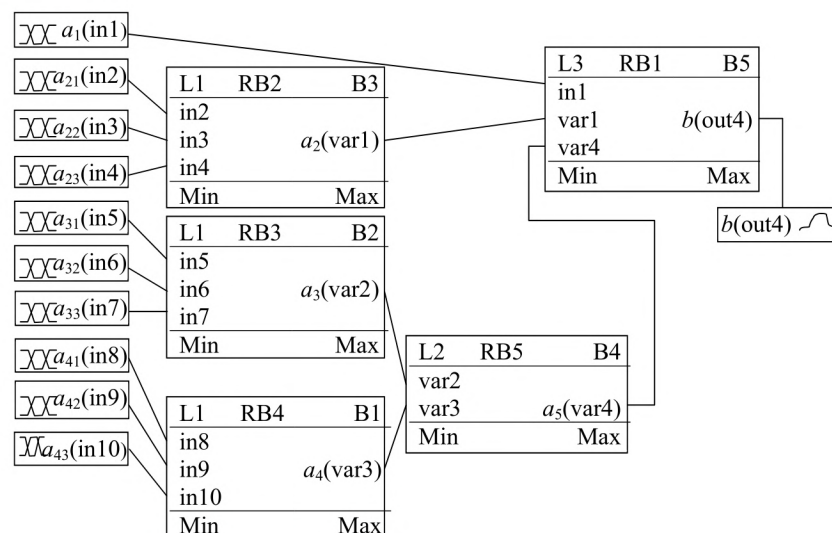
Fig. 2. The system of fuzzy hierarchical derivation of risk assessment of the implementation of projects of automated information systems in the notation of the program fuzzyTech 6.0

Applying the hierarchical structure of fuzzy inference, one can take into account a significant number of input variables that affect the overall risk assessment of AIS implementation projects. These projects are not a permanent system, so the number and content of input variables can vary. At the same time, the knowledge of experts (project participants) is changing.

According to [13], for each level of fuzzy inference, the activation method is min. This is due to the fact that all the rules as a logical connection for a subcondition apply only a fuzzy conjunction (operation "AND"). As a result, the aggregation method provides for the use of the min-conjunction operation. The accumulation of rule endings uses max-disjunction. As a defuzzification method, various approaches can be applied, for example, the center of gravity method, which has proven itself well.

Another advantage of the hierarchical fuzzy inference is the absence of defuzzification operations and fuzzification for the intermediate variables a_2, a_3, a_4 and a_5 (**Fig. 2**). This is due to the fact that the intermediate result of fuzzy inference in a certain form is direct to the machine of fuzzy inference of the next level of the system. As a result, to describe intermediate variables in hierarchical fuzzy knowledge bases, it is sufficient to specify only term sets; membership functions are not required.

52

3. Implementation and experimental evaluation of the method

The implementation of the method of risk assessment of the implementation projects of non-commercial AIS based on hierarchical fuzzy inference was carried out using the fuzzyTech 6.0 package. For a set of input variables, the value of the output variable b was not once calculated. The obtained results coincide with the intuitively obtained ones. For some of the data sets, the risk is quite high, therefore, additional measures are required to manage risks or cancel this version of the project in general.

The adequacy of the improved method for assessing the risks of non-commercial AIS implementation projects is verified using experiments conducted by the authors on various non-commercial OTSs. So in [21] and [22] it is carried out it with respect to the OTS for the management of law enforcement units; in [23], this is carried out in relation to systems for teaching students and students in a foreign language.

Let's consider in more detail the experiment conducted by V. Melenchuk [13] on the basis of the Department of Repair and Maintenance of Automotive and Special Equipment of the Military Academy (Odesa). For the experiment, let's select data on the use of AIS logistics, which occurred during the performance of official tasks at different times. During the experiment, the following project risk indicators are evaluated: the time that is spent on project risk assessment; the quality of the decision – the risk assessment coincides with the known (correct decision), the assessment does not match (incorrect decision).

The results of the time experiment for risk assessment are presented in **Fig. 3**, *a* by the quality of decisions made – in **Fig. 3**, *b*.

The results of the experiment indicate that the program module "Project Risk Assessment", which implements an improved method for assessing the risks of AIS projects of material and technical support of motor units of state institutions, provides the opportunity:

– reduce the time for project risk assessment by 1.23 times and increase the reliability of decisions by 1.68 times in comparison with the implementation of the project risk assessment in a "manual" way;

– reduce the time to evaluate the project risk by 1.14 times and increase the reliability of project management decisions by 1.32 times compared with the use of another method.

The development of a software module based on the algorithm of the method as part of automated information systems of government institutions will reduce the time to assess the risks of AIS implementation projects.
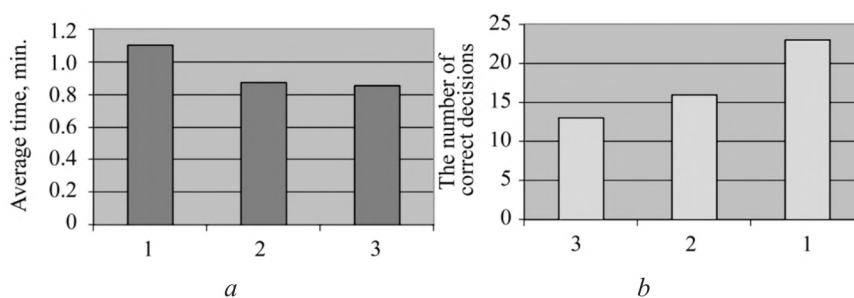
Fig. 3. The results of the experimental verification:
1 – "manual" method; 2 – automation (statistical approach); 3 – automation (developed approach);
a – verification of time for risk assessment, *b* – verification of the quality of decisions

4. Discussion of research results

The studies presented in the article are primarily theoretical-analytical in nature, based on the results of experiments described in the available literature. The improved method for assessing the risks of AIS implementation projects is the basis for improving the risk management method of AIS implementation projects.

The basis of improvement is the use of hierarchical fuzzy inference. Let's believe that this study is an extension of its application in a new subject area – project risk assessment. The ad-

equacy of this approach is confirmed by other studies in other subject areas when it comes to weak formalization or not the possibility of formalization in general. In most cases, the situation is complicated by uncertainty. As a result, the application of the apparatus of probability theory and mathematical statistics here gives the worst results.

However, it should be noted that the use of fuzzy logic apparatus requires the creation of additional components as part of the OTS:

a) unit that carries out a number of actions to perform the fuzzy logic algorithm (working with statistics, working with knowledge, building a fuzzy inference system, etc.);

b) presence of highly qualified personnel in the field of mathematics, analytics and work with knowledge and the like;

c) construction in OTS of a system for formalizing, accumulating, processing and applying statistical data, knowledge, and the like.

5. Conclusions

So, the article presents an improved method for assessing the risks of the implementation of AIS for non-commercial OTS by the example of a study of the projects for introducing AIS of material and technical support for motor units of state institutions. It is found that:

a) the apparatus of probability theory and mathematical statistics does not allow to assess the risks of projects for the implementation of automated information systems of non-commercial OTS, the activities of which are carried out in conditions of uncertainty;

b) improved method differs from the known ones by using a hierarchical fuzzy inference system. An increase in the number of input variables leads to an increase in complexity (an increase in the number of rules) for constructing a fuzzy inference system. The construction of a hierarchical system of fuzzy inference and knowledge bases can reduce complexity (the number of rules);

c) the method makes it possible to quantify, reduce the time to assess the risks of projects and improve the quality of decisions on projects for the implementation of AIS of non-commercial OTS. The practical implementation of an improved method requires the development of new or adaptation of existing methods of working with explicit and implicit knowledge. It is also necessary to formalize the experience gained by experts, in which all project participants (developers, users, etc.) can be involved, is the prospect of further research in this direction;

d) studies are given that can be developed to assess the risk of other projects and the entire class of automated information systems of the OTS in the face of uncertainty.

References

[1]   A Guide to the Project Management Body of Knowledge (PMBOK® Guide) (2017). Project Management Institute, 760.

[2]   Chimshir, V. (2013). Matters of projects classification and ranking by applicable technical systems. Eastern-European Journal of Enterprise Technologies, 5 (2 (65)), 44–48. Available at: http://journals.uran.ua/eejet/article/view/18441/16180

[3]   Altwies, D., White, D. (2018). Achieve PMP Exam Success: A Concise Study Guide for the Busy Project Manager. J. Ross Publishing, 526.

[4]   Microsoft Solutions Framework. Distsiplina upravleniya riskami MSF ver. 1.1. Available at: https://www.microsoft.com/ru-ru

[5]   DeMarko, T., Lister, T. (2005). Val'siruya s medvedyami: upravlenie riskami v proektah po razrabotke programmnogo obespecheniya. p.m Office, 190.

[6]   Ageev, A. E. (2006). Modelirovanie organizatsionnyh struktur i protsessov upravleniya riskami proekta. Otkrytye informatsionnye i komp'yuternye integrirovannye tehnologii, 32, 110–113.

[7]   Bedriy, D. I., Polshakov, V. I. (2012). Research projects budgeting with an allowance for risks. Eastern-European Journal of Enterprise Technologies, 1 (12 (55)), 47–49. Available at: http://journals.uran.ua/eejet/article/view/3626/3399

[8]   Danchenko, O. B. (2014). Ohliad suchasnykh metodolohiy upravlinnia ryzykamy v proektakh. Upravlinnia proektamy ta rozvytok vyrobnytstva, 1, 16–25.

[9]   Latkin, M. A. (2008). Informatsionnaya model' upravleniya riskami proektov predpriyatiya. Otkrytye informatsionnye i komp'yuternye integrirovannye tehnologii, 39, 210–214.

[10]   Fillips, D. (2006). Upravlenie proektami v oblasti informatsionnyh tehnologiy. Moscow: Lori, 374.

[11]   Bushuev, S. D., Yaroshenko, N. P., Yaroshenko, Yu. F. (2013). Upravlenie proektami i programmami razvitiya organizatsiy na osnove predprinimatel'skoy energii. Upravlenie proektami i programmami, 4, 300–311.

[12]   Head, G. L., Horn, I. I. (1994). Essentials of Risk Management. Insurance Institute of America, 230.

[13]   Melenchuk, V. M. (2016). Model of Risk Assessment in Transport Logistic Projects / Programs / Portfolios Using Fuzzy Inference. Visnyk Lvivskoho derzhavnoho universytetu bezpeky zhyttiediyalnosti, 13, 48–55.

[14]   Pleskach, V. L., Zatonatska, T. H. (2011). Informatsiyni systemy i tekhnolohiyi na pidpryiemstvakh. Kyiv: Znannia, 718.

[15]   Ganesh, K., Mohapatra, S., Anbuudayasankar, S. P., Sivakumar, P. (2014). Enterprise Resource Planning: Fundamentals of Design and Implementation. Springer, 170. doi: https://doi.org/10.1007/978-3-319-05927-3

[16]   Rybydailo, A. A., Poryvai, O. V., Levshenko, O. S. et. al. (2015). Analiz zarubizhnoho ta vitchyznianoho dosvidu upravlinnia proektamy z vprovadzhennia informatsiynykh tekhnolohiy. Zbirnyk naukovykh prats Tsentru voienno-stratehichnykh doslidzhen Natsionalnoho universytetu oborony Ukrainy imeni Ivana Cherniakhovskoho, 1 (53), 55–64.

[17]   Davis, W. S., Yen, D. C. (1998). The Information System Consultant's Handbook: Systems Analysis and Design. CRC-Press, 800.

[18]   Leonenkov, A. V. (2005). Nechetkoe modelirovanie v srede MatLab i FuzzyTECH. Sankt-Peterburg: BHV-Peterburg, 736.

[19]   Shtovba, S. D. (2007). Proektirovanie nechetkih sistem sredstvami MatLab. Moscow: Goryachaya liniya-Telekom, 288.

[20]   Cao, B.-Y. et. al. (Eds.) (2014). Fuzzy Systems & Operations Research and Management. Springer, 402.

[21]   Androshchuk, O. S., Mykhailenko, O. V. (2014). Model vyiavlennia porushnykiv zakonodavstva na derzhavnomu kordoni iz zastosuvanniam ierarkhichnoho nechitkoho lohichnoho vyvodu. Suchasni informatsiyni tekhnolohiyi u sferi bezpeky ta oborony, 1, 5–10.

[22]   Lemeshko, V. (2016). The usage of border units for specific tasks: retrospective analysis and development prospects. Zbirnyk naukovykh prats Natsionalnoi akademiyi Derzhavnoi prykordonnoi sluzhby Ukrainy. Seriya: viyskovi ta tekhnichni nauky, 4 (70), 101–117.

[23]   Lemeshko, O. V., Yankovets, A. V., Bets, I. O., Isaieva, I. F. (2019). Peculiarities of the English Language Training of Military Administration Masters. Revista Romaneasca Pentru Educatie Multidimensionala, 11 (2), 160. doi: https://doi.org/10.18662/rrem/123

COMPARISON OF DT& GBDT ALGORITHMS FOR PREDICTIVE MODELING OF CURRENCY EXCHANGE RATES

Maan Y. Anad Alsaleem
Directorate of Education in Nineveh
Tenahî, Duhok, Ramy Land B9, Iraq
Maanyounis1983@gmail.com

Safwan O. Hasoon
College of Computer Science and Mathematics
Mosul University
Almajmoa, Mosul, Ninavah, Iraq, 41002
Dr.safwan1971@uomosul.edu.iq

Abstract

Recently, many uses of artificial intelligence have appeared in the commercial field. Artificial intelligence allows computers to analyze very large amounts of information and data, reach logical conclusions on many important topics, and make difficult decisions, this will help consumers and businesses make better decisions to improve their lives, and it will also help startups and small companies achieve great long-term success. Currency exchange rates are important matters for both governments, companies, banks and consumers. The decision tree is one of the most widely artificial intelligence tools used in data mining. With the development of this field the decision tree and Gradient boosting decision tree are used to predicate through constructed intelligent predictive system based on it. These algorithms have been used in many stock market forecasting systems based on global market data. The Iraqi dinar exchange rates for the US dollar are affected in local markets, depending on the exchange rate of the Central Bank of Iraq and the features of that auction. The proposed system is used to predict the dollar exchange rates in the Iraq markets Depending on the daily auction data of the Central Bank of Iraq (CBI). The decision tree and Gradient boosting decision tree was trained and testing using dataset of three-year issued by the CBI and compare the performance of both algorithms and find the correlation between the data. (Runtime, accuracy and correlation) criteria are adopted to select the best methods. In system, the characteristic of artificial intelligence have been integrated with the characteristic of data mining to solve problems facing organization to use available data for decision making and multi-source data linking, to provide a unified and integrated view of organization data.

Keywords: decision trees, gradient boosting decision tree, correlation, accuracy, run times, exchange rates.

1. Introduction

The increases use of data in digital form and databases in a wide range in different fields led to the large quantity of these data, it was necessary to develop tools and algorithms to help extract information from these data and find useful information. Therefore new field in artificial intelligence, called data mining, it has emerged as a technique aimed for extracting knowledge [1]. This technique has become more popular in the information age through the exploration of large quantities of data using the techniques of (Pattern Recognition, integration of mathematical methods and statistical information technology) led to possibilities to predict future behavior that helps in decision-making. One method widely used in data mining is Decision trees which is one of the methods used for the purpose of classification and finding a regression to predict the value of a variable object In addition a more accurate prediction method was proposed [2, 3], in this paper introduced view of boosting algorithm as iterative functional gradient descent algorithms. To improve machine learning methods at an acceptable cost for increased learning and accuracy of results in Decision trees. The proposed system is used gradient boosting decision tree (GBDT) as a way to predict the exchange rates of dollar based on the CBI's annual reports of auction daily auction price, quantity and cash for the market price and comparison results for the use of decision trees.

2. Decision Tree (DT)

It is one of the most popular machine learning algorithms and has been widely used in various modern machine learning and data mining applications [4]. General structure consist of root, branches and leaves typically upside down the leaves are at the bottom. There are two main type of it Classification tree and used depends on the desired results of the algorithm. The tree is built in the same way as building ID3 where the contract is chosen based on the concept of entropy which is based on the following equation:

$$Entropy(t) = -\sum_{i=0}^{c-1} p(i\,|\,t) \log_2 p(i\,|\,t),$$ (1)

where c is the number of class and $p(i|t)$ Indicates the probability of records belonging to that class.

3. Gradient boosting decision tree

It is method used to produce a strong learner and data mining applications [5]. Let $xi \in R$ is the dataset and have n examples, m features and k ensemble learning, what want to predict is $y(x)^k$. The output of this method is the sum of the prediction values of these trees Using the following equation [6].

$$y(x)^k = \sum_{i=1}^{k} f(x),$$ (2)

where f is output of regression tree.

4. Implementation and Result

Proposed System was based on data published by the Central Bank of Iraq for the daily auction of dollars for the years (2015–2016–2017), respectively, which amounted to 479 auction sessions after the deletion of the holidays where there is no auction. As these indicators reflect the comprehensive views of currency exchange rates at the official auction price, market price and quantity offered. The algorithms (GBDT)&(DT) was adopted to predict the market price and compare the result for the same data. The steps of workflow as show in **Fig. 1**.
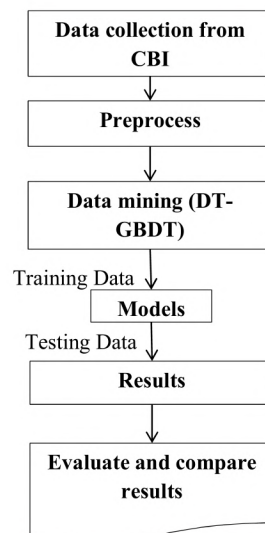
Fig. 1. Proposed Frame Work

The result of two methods were compared for selected the best technique to apply for predictively of proposed system.

4. 1. Data collection

At this stage was adopted data of the Central Bank of Iraq, which published on its official site for the years (2015–2016–2017), **Table 1.** Available on the site https://www.cbi.iq/.

Table 1

A subset of the year dataset

No. Session	Date	MarketPrice	AuctionPrice	Volume	Cash	Credits
2924	06-Apr	1,292	1,166	119,020,000	12,200,000	106,820,000
2925	07-Apr	1,292	1,166	108,540,000	14,950,000	93,590,000
2926	08-Apr	1,321	1,166	116,044,000	15,050,000	100,994,000
2927	09-Apr	1,327	1,166	104,770,000	10,650,000	94,120,000
2928	12-Apr	1,302	1,166	161,241,189	34,200,000	127,041,189
2929	13-Apr	1,297	1,166	165,852,225	38,475,000	127,377,225
2930	14-Apr	1,297	1,166	117,789,137	11,800,000	105,989,137
2931	15-Apr	1,297	1,166	110,948,963	36,500,000	74,448,963
2932	16-Apr	1,290	1,166	140,522,917	32,100,000	108,422,917
2933	19-Apr	1,295	1,166	126,470,740	28,850,000	97,620,740

4. 2. Preprocess

In preprocess the configure of data should be standardizing by applying normalization , delete the empty and duplicate values for fields of various years adopted and converting these into a formula (CSV) dataset for use in data mining.

4. 3. Data mining (DT-GBDT)

An exploration program was applied using both methods (DT) ,(GBDT) on the same dataset, which was configured to measure execution time and accuracy of results to make comparison between two method and choses the best depended on.

The results of this research are divided into two sections, first that commercial price forecast and a second that includes comparing the performance of two algorithms for these data.

As a result of the market price of the dollar for the Iraqi dinar for the data approved were according as showing in **Fig. 2.**

The market price of the us dollar against the Iraq dinar

Fig. 2. A diagram of the process

As shown in the **Fig. 2**, the trade exchange rate of the US dollar compared to the Iraqi dinar for the sample of the research is 1264.985.

58

4. 4. Correlation

Correlation is a statistical term that refers in general use to the proximity of the two variables and relationship with each other [7–15]. The correlation between fields and their effects as showing in **Table 2**.

Table 2
The correlation table between the fields

Attribute	Auction price	Cash	Credits	Market price	Volume
Auction price	1	−0.276	−0.711	0.255	−0.581
Cash	−0.276	1	0.407	−0.089	0.580
Credits	−0.711	0.407	1	−0.535	0.867
Market price	0.255	−0.089	−0.089	1	−0.365
Volume	−0.581	0.867	0.867	−0.365	1

The weights of each fields used as shown in **Fig. 3**.
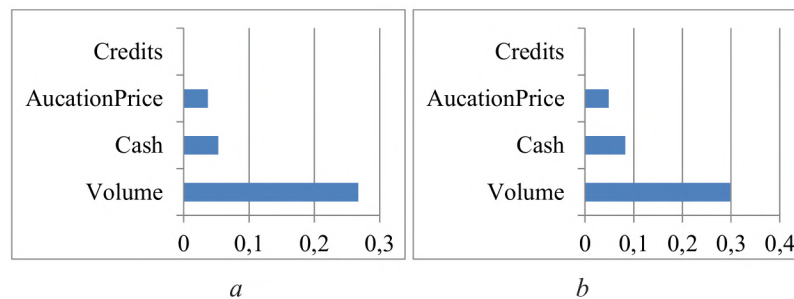
Fig. 3. Weights of each field: *a* – DT; *b* – GBDT

Runtimes is the time consumed for each algorithm used for prediction is shown in **Fig. 4**.
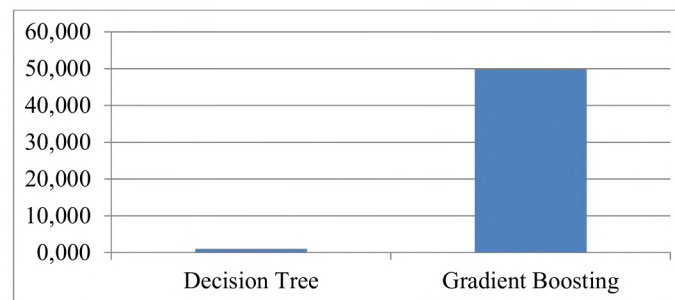
Fig. 4. Runtimes (MS)

From **Fig. 4** let's note that the time consumed for GBDT is more than the DT because GBDT is generates several sub-trees and calculates the sum of the main tree and sub-trees. These processes can't be implemented in parallel to reduce the runtime Because of the serial operations that the algorithm calculates.

4. 5. Prediction of DT & GBDT

The prediction chart is one of important tools that give visibility to the distribution of the samples and the predictive values as shown in **Fig. 5**, **6**, **Table 3**.

59
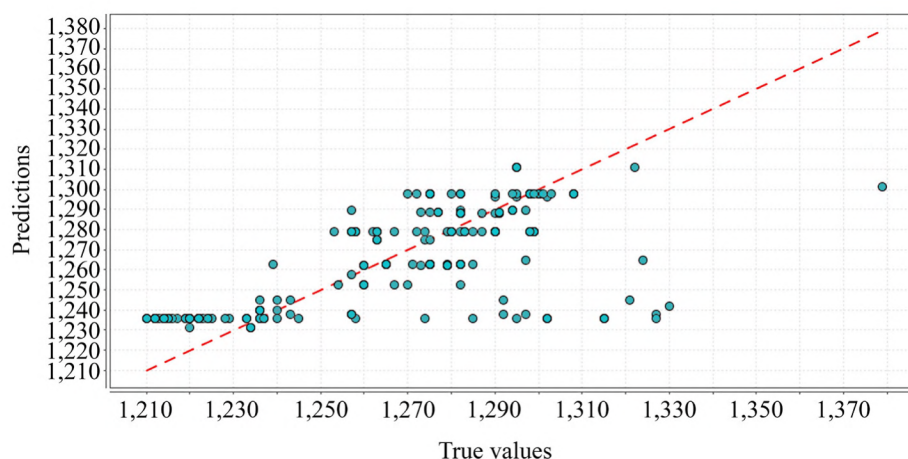
Fig. 5. Prediction chart of DT
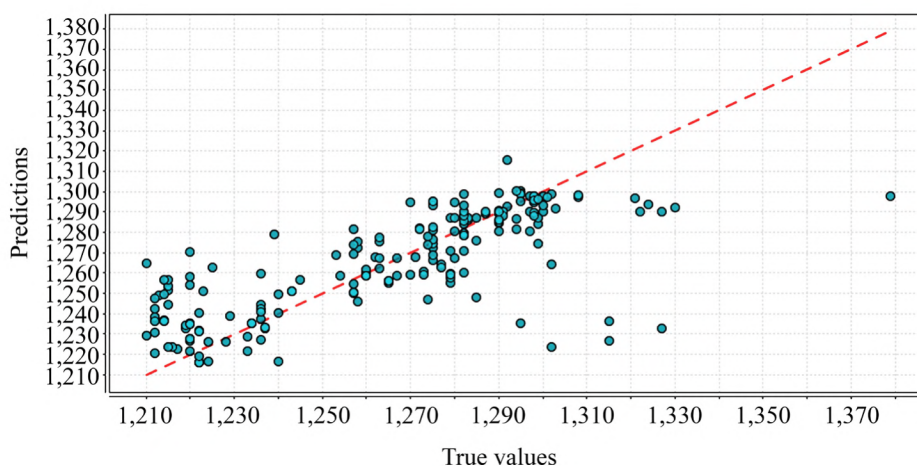
Fig. 6. Prediction chart of GBDT

Table 3

Comparison of error ratio

	Gradient Boosting Trees	Decision tree
Root mean squared error	22.078+/–1.167 (micro average: 22.106+/–0.000)	23.608+/–1.873 (micro average: 23.667+/–0.000)
Absolute error	14.645+/–0.828 (micro average: 14.636+/–16.568)	16.349+/–1.459 (micro average: 16.354+/–17.107)
Relative error lenient	1.14 %+/–0.06 % (micro average: 1.14 %+/–1.27 %)	1.28 %+/–0.12 % (micro average: 1.28 %+/–1.30 %)
Squared error	488.546+/–51.614 (micro average: 488.697+/–1197.970)	560.157+/–87.500 (micro average: 560.112+/–1286.439)
Correlation	0.744+/–0.039 (micro average: 0.736)	0.693+/–0.087 (micro average: 0.692)

5. Conclusion

The integration of intelligent techniques and data mining of prosed system is used for predicting currency rates based on bank records of exchange rates, which reflected the result in terms of time and accuracy compared with traditional methods. The DT and GBDT are good tools for decision making to predicate currency rate taking in consideration the DT is a best method to compare with GBDT in term of time (**Fig. 3**), on the other hand the GBDT is best methods in term of accuracy see **Table 3.**

60

References

[1] Koncz, K., Hilovská, S. P. (2012). Application of Artificial Intelligence and Data Mining Techniques to Financial Markets. Acta všfs, 6, 62–76.

[2] Friedman, J. H. (2001). Greedy function approximation: A gradient boosting machine. Annals of Statistics, 29 (5), 1189–1232. doi: http://doi.org/10.1214/aos/1013203451

[3] Friedman, J. H. (2002). Stochastic gradient boosting. Computational Statistics & Data Analysis, 38 (4), 367–378. doi: http://doi.org/10.1016/s0167-9473(01)00065-2

[4] Gupta, B., Rawat, A., Jain, A., Arora, A., Dhami, N. (2017). Analysis of Various Decision Tree Algorithms for Classification in Data Mining. International Journal of Computer Applications, 163 (8), 15–19. doi: http://doi.org/10.5120/ijca2017913660

[5] Feng, Z., Xu, C., Tao, D. (2018). Historical Gradient Boosting Machine. EPiC Series in Computing, 55, 68–80. doi: http://doi.org/10.29007/2sdc

[6] Anghel, A., Papandreou, N., Parnell, T., Palma, De. A., Pozidis, H. (2018). Benchmarking and Optimization of Gradient Boosting Decision Tree Algorithms. Available at: https://arxiv.org/abs/1809.04559

[7] Mu, Y., Liu, X., Wang, L. (2018). A Pearson's correlation coefficient based decision tree and its parallel implementation. Information Sciences, 435, 40–58. doi: http://doi.org/10.1016/j.ins.2017.12.059

[8] Guolin, K., Qi, M. et. al. (2017). LightGBM: A highly efficient gradient boosting decision tree. NIPS, 3149–3157.

[9] Frenkel, J. A.; Bilson, J. F. O., Marston, R. C. (Eds.) (1984). Tests of Monetary and Portfolio Balance Models of Exchange Rate Determination. Exchange Rate Theory and Practise. Chicago: University of Chicago Press, 239–260.

[10] Gençay, R. (1999). Linear, non-linear and essential foreign exchange rate prediction with simple technical trading rules. Journal of International Economics, 47 (1), 91–107. doi: http://doi.org/10.1016/s0022-1996(98)00017-8

[11] Béreau, S., Villavicencio, A. L., Mignon, V. (2010). Nonlinear adjustment of the real exchange rate towards its equilibrium value: A panel smooth transition error correction modelling. Economic Modelling, 27 (1), 404–416. doi: http://doi.org/10.1016/j.econmod.2009.10.007

[12] Wong, W. K., Xia, M., Chu, W. C. (2010). Adaptive neural network model for time-series forecasting. European Journal of Operational Research, 207 (2), 807–816. doi: http://doi.org/10.1016/j.ejor.2010.05.022

[13] Anders, U., Hann, T. H., Nakaheizadeh, G.; Weigend, A. S., Abu-Mustafa, Y., Refens, A. P. N. (Eds.) (1997). Testing for Nonlinearity with Neural Networks. Decision Technologies for Financial Engineering. Singapore: World Scientific.

[14] Low, A. H. W., Muthuswamy, J.; Dunis, C. (Ed.) (1996). Information Flows in High Frequency Exchange Rates., Forecasting Financial Markets. Exchange Rates and Asset Management. Chichester: John Wiley & Sons.

[15] Lemeshko, O., Yevdokymenko, M., Anad Alsaleem, N. Y. (2018). Development of the tensor model of multipath qoe-routing in an infocommunication network with providing the required quality rating. Eastern-European Journal of Enterprise Technologies, 5 (2 (95)), 40–46. doi: http://doi.org/10.15587/1729-4061.2018.141989

APPLICATION OF KOHONEN SELF-ORGANIZING MAP TO SEARCH FOR REGION OF INTEREST IN THE DETECTION OF OBJECTS

Victor Skuratov
All-Russian Research Institute of Radio Engineering
22 Bol'shaya Pochtovaya str., Moscow, Russian Federation, 105082
viktor.skuratov@gmail.com

Konstantin Kuzmin
Department of Mathematical and instrumental methods in economics
University of Russian Innovation Education
10 Krasnobogatyrskaya str., Moscow, Russia, 107061
konstantin.alexandrovich@yahoo.com

Igor Nelin
Department of Radiolocation, radio navigation and on-board radio electronic equipment
Moscow Aviation Institute
4 Volokolamskoe highway, Moscow, Russian Federation, 125993
nelin.iv@yandex.ru

Mikhail Sedankin
State Research Center – Burnasyan Federal Medical Biophysical Center of
Federal Medical Biological Agency
23 Marshala Novikova str., Moscow, Russia, 123098
Fundamentals of Radio Engineering Department
National Research University "Moscow Power Engineering Institute"
14 Krasnokazarmennaya str., Moscow, Russian Federation, 111250
msedankin@yandex.ru

Abstract
Today, there is a serious need to improve the performance of algorithms for detecting objects in images. This process can be accelerated with the help of preliminary processing, having found areas of interest on the images where the probability of object detection is high. To this end, it is proposed to use the algorithm for distinguishing the boundaries of objects using the Sobel operator and Kohonen self-organizing maps, described in this paper and shown by the example of determining zones of interest when searching and recognizing objects in satellite images. The presented algorithm allows 15–100 times reduction in the amount of data arriving at the convolutional neural network, which provides the final recognition. Also, the algorithm can significantly reduce the number of training images, since the size of the parts of the input image supplied to the convolution network is tied to the image scale and equal to the size of the largest recognizable object, and the object is centered in the frame. This allows to accelerate network learning by more than 5 times and increase recognition accuracy by at least 10 %, as well as halve the required minimum number of layers and neurons of the convolutional network, thereby increasing its speed.
Keywords: pattern recognition, Kohonen self-organizing maps, search and recognition of objects in the image, satellite and radar images, region of interest.

1. Introduction

Currently, the low speed of detecting objects in images is one of the main problems of modern systems for processing various visual data. An increase in the speed of search and recognition of objects can lead to a significant increase in the performance of systems for analyzing satellite and radar images, medical images, data from robotic and military systems, unmanned vehicles, etc., having both technological and serious economic effects.

62

One of the ways to increase the accuracy and speed of recognition algorithms is the use of neural networks (NN), and the most modern type of NN used in pattern recognition is convolutional neural network (CNN) [1]. For the high-quality operation of this type of network, it is necessary that the size of the recognized object and the sizes of the objects in the training set be comparable. If, in addition to the various types of desired objects, there is also a variation in the scale of the object in the image, the creation of a training sample and training of such a network will take considerable time and computational resources, the number of errors in recognition will increase, and the speed will be low. The presented algorithm allows to reduce the amount of data analyzed when searching and recognizing objects in the image by 15–100 times, increase accuracy and save computing resources. This is achieved through the use of Kohonen maps to determine areas of interest in the input image, in which there is a high probability of finding the desired object.

2. Literature review and problem statement

Today, there are a number of works where the use of the self-organizing map of Kohonen (Self-organizing map, SOM) for image recognition has been investigated. Some authors use Kohonen maps to prepare input data with subsequent analysis by other NNs, while others use it to directly recognize objects in images. In [2], image segmentation by Kohonen maps is first applied, and then analysis in a hybrid NN. Kohonen maps were used to reduce the training set for hybrid NN and to speed up the analysis. The disadvantage of [2] is that the input image is classified as a whole, without the ability to search for an object. Therefore, when zooming in on the desired fragment in the input image, recognition will not be performed. In [3], Kohonen maps were used to solve clustering problems with a large number of objects and to distinguish among them those that have unusual characteristics.

Articles [4–8] describe the evolution of the R-CNN (Region-based Convolutional Network) algorithm for searching and recognizing objects in images. In [4, 5], the initial version of the R-CNN algorithm is described. The algorithm extracts about 2000 regions on the input image, each of which is scaled using the affine transformation, and fed to the input of the convolution network, which extracts the feature vector (map). The article [5] describes the linear regression training to refine the coordinates of the object window. R-CNN has several drawbacks, mainly due to the high time spent on training the network, as well as on direct image processing by the algorithm, so that processing one image takes about 47 seconds. The following describes the development of this algorithm (Fast R-CNN [6] and Faster R-CNN [7]) up to Mask R-CNN [8] in which the ability to predict the position of the mask covering the found object is added.

The article [9] describes the YOLO algorithm (You Only Look Once), which allows searching and recognizing objects in images 103 times faster than R-CNN and 102 times faster than Fast R-CNN, but with lower accuracy. This algorithm superimposes a grid on the input image and divides it into cells. Around each cell, the algorithm determines the bounding box of the zone of the possible location of objects with an assessment of the accuracy of detection and the probability of belonging to classes. Then, the accuracy estimate for each zone is multiplied by the probability of the class and the final value of the probability of detection is obtained. In [10], the SSD: Single Shot MultiBox Detector algorithm is presented, which is comparable in accuracy and speed to YOLO. The algorithm overlaps the entire area of the input image with bounding frames, the size of which varies within the set limits, allowing the detection and recognition of objects of various sizes. Both algorithms perform analysis from several thousand to several tens of thousands of parts of the input image.

When detecting and recognizing objects in images, it is necessary to apply algorithms that divide the input image into a set of images suitable in size for analysis in a convolutional NN. To save time and resources, the applied algorithm should reduce the amount of data needed for further analysis. Such an algorithm can be implemented in the following ways:

1) sequentially splitting the input image into frames of the required size with a frame shift of a certain number of pixels relative to the previous one;

2) using the algorithms R-CNN, Fast and Faster R-CNN, Mask R-CNN, YOLO, as well as SSD.

Both of the presented methods require significant time and computational resources. In one case, several thousand frames are submitted to the subsequent convolutional NN for analysis, into which each input image is divided [4, 5], and in the other case, the image is analyzed as a whole, with enumeration of the possible boundaries of regions of interest and without preliminary screening of areas of no interest [6–10].

Thus, there is an obvious need for algorithms that can reduce the amount of data being analyzed, and thereby increase the speed of search and recognition systems for objects in images.

3. The aim and objectives of research

Interesting objects and the possibility of recognizing its type in a convolutional NN.

To achieve the aim, the following tasks are set:

– highlight the boundaries of the objects present in the image;

– perform a search for centers of objects;

– check the selected algorithms on real input data.

4. The algorithm for distinguishing the boundaries of objects located on the underlying surface

This scientific work is based and is a continuation of the previous study [11], in which the possibility and prospect of using neural networks and Kohonen maps to determine the centers of objects in images are investigated, and the performance of these two types of neural networks is compared.

Before transferring the input image for analysis to the convolutional NN, it is necessary to carry out preliminary processing.

Between the object in the image and the underlying surface there is always an interface, which is formed due to the difference in brightness or light levels, because the reflectivity of, for example, airplanes is usually higher than that of the underlying surface. Also, in most cases, the bodies of objects such as tanks or planes cast a shadow on the underlying surface, which also forms the interface. If to select these boundaries around the objects with dots in the input image, then the center of the cluster will actually coincide with the center of the object.

The algorithm for extracting the boundaries of objects located on the underlying surface, given in [11], has been finalized and now looks like this:

1) input color image is converted to shades of gray;

2) resulting image is contrasted;

3) application of the Sobel operator – a differential operator that calculates the approximate value of the image brightness gradient;

4) conversion to a binary image, using clipping by the brightness threshold. The resulting luminance separation boundaries take values 1, all the rest – 0;

5) removal of small objects;

6) filling inside closed borders;

7) removal of the boundaries of the desired object of the selected image parts that are not characteristic of geomeric forms.

5. Methodology for determining centers of interest

To increase the speed of analysis and reduce the necessary computing resources when objects of interest are detected in the input image, it is proposed to identify the areas of their possible location with further sequential analysis of the found areas in the convolutional NN.

To highlight the centers of zones of interest in the input image, it is necessary to train NN without a teacher, i. e. lack of training sample, as processing of each input image is carried out independently of the previous ones. The main types of Kohonen networks that use teaching without a teacher are [12, 13]:

– Kohonen network for vector quantization of signals;

– self-organizing maps of Kohonen.

In this paper, let's describe the SOM application to solve the problem of determining the centers of zones of interest, which is a development [11].

The main goal of SOM is to convert input vectors of arbitrary dimension into a one- or two-dimensional discrete map with a topologically ordered shape [13]. Kohonen maps are based on competitive learning. The neurons of the output layer compete for the right to activate, as a result of which only one output neuron, the winner neuron, is active. One way to organize this kind of competition between neurons is to use negative feedbacks between them. In the general case, neurons in SOM are located at the nodes of a two-dimensional grid with rectangular or hexagonal cells (**Fig. 1**). The magnitude of the interaction between neurons in the network is determined by the distance r_n between them. The distance between the individual neurons is more consistent with the Euclidean distance for the hexagonal grid. The more neurons in the grid, the higher the degree of detail of the SOM result.
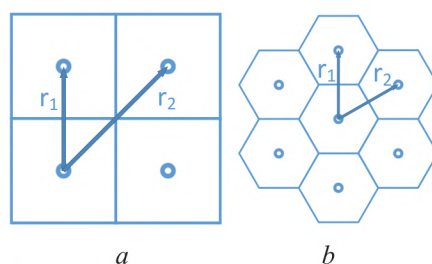
Fig. 1. The initial arrangement of neurons in the nodes of a two-dimensional grid with cells:
a – quadrangular; b – hexagonal

The location of the winning neurons determined during the competitive process is ordered in relation to each other, then ask the ones in the grid a significant coordinate system in which the coordinates of the neurons are an indicator of the statistical features contained in the input images.

The work of the SOM algorithm usually begins with the initialization of the synaptic network weights and, after the correct initialization, three main processes are launched to form the map: competition, cooperation and synaptic adaptation.

The principle of operation of the SOM algorithm is considered in more detail in [11].

6. Description of the area of interest search algorithm

A satellite or radar image of the underlying surface with a known scale is fed to the input. Next, pre-processing is carried out, which is carried out in several stages:

1. Highlighting the boundaries of objects present in the image. For this, the algorithm described in paragraph 4 is used, based on the use of the Sobel operator.

2. Search for centers of objects. SOM is used for this.

3. Identification of areas of interest. Around the found centers, an expanded zone of interest is formed, within which parts of the original image are extracted with a certain "window". The selected parts of the image should contain the point of the center of the cluster and overlap the vicinity of the zone of interest. The dimensions of the "window" are selected based on the given dimensions of the largest detectable object and change when the image scale is changed.

4. In the presence of closely located relative to the scale of the desired object network nodes, the zone of interest expands so as to overlap the common area for these nodes, instead of looking for the region of interest for each node separately.

5. Analysis in the convolution network. The obtained parts of the input image are submitted for analysis to the convolution network, where the presence of the object on and its type is determined.

The algorithm for the search for zones of interest is shown in **Fig. 2**.

This algorithm can be used to search and recognize in the input image not only various types of armored vehicles and aircraft, but also other objects of interest, for example, when analyzing the visual data of unmanned vehicles or when testing robotic systems. For this, it is necessary

to set the maximum and minimum sizes of objects of interest for the algorithm to search for zones of interest, compose a training sample for these objects and train the convolutional NN.
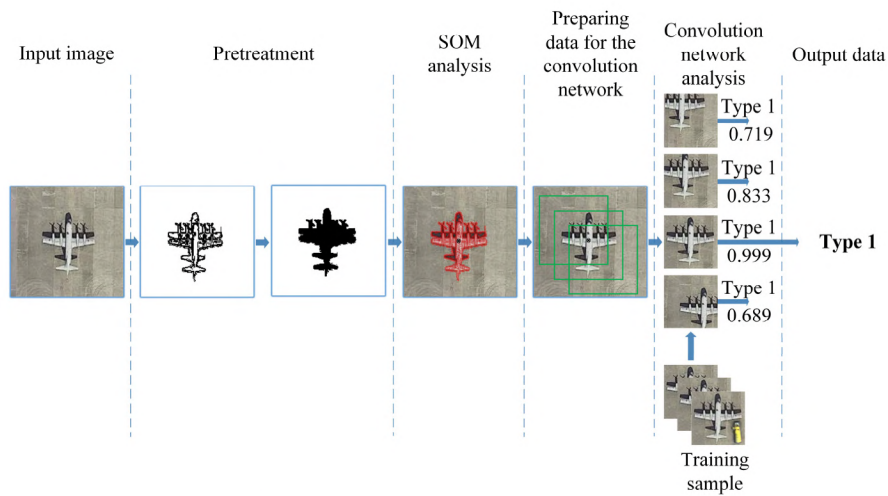
Fig. 2. The algorithm of the search for zones of interest and determining the type of object

7. Demonstration of the algorithm on real input data

To search for several objects in the input image, it is necessary to take into account the real scale of the image and their relative dimensions. In order to avoid missing objects, it is necessary that the determined number of cluster centers in the image coincides with the number of smallest objects that can fit on the input image with a known scale. **Fig. 3** shows an example of the algorithm for determining zones of interest in a real color satellite image measuring 671×493 pixels, which contains several types of aircraft, various underlying surfaces and structures. After preliminary processing, the input image is submitted for analysis to SOM with the initial arrangement of neurons at the nodes of a two-dimensional grid with hexagonal cells. SOM needs about 150 learning eras. Based on the scale of the input image, the number of smallest aircraft that can fit on the image is 6×4. Therefore, at the output of the neural network, 24 cluster centers must be defined. If the centers of the clusters are located relatively close to each other, then their combination into one located in the center between them is possible. The same applies to "windows" around neighboring cluster centers if they overlap more than 90 % of the area. It is also possible to exclude from the analysis the centers located in the immediate vicinity of the edge of the image, since they can't be the center of the aircraft, which the convolutional network could recognize during further processing.
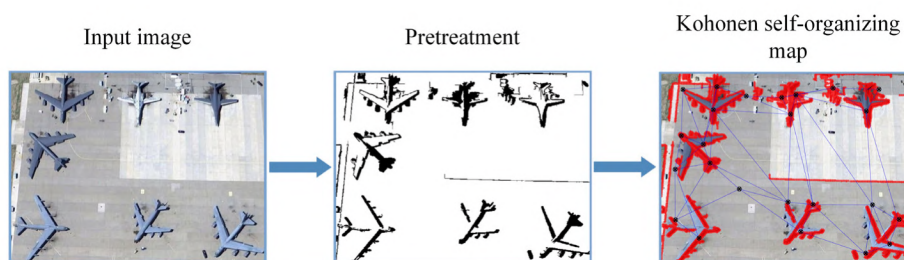
Fig. 3. Input image processing with SOM analysis

As can be seen from **Fig. 3**, the Kohonen map identified the centers of the clusters in such a way that all aircraft will be highlighted with a "window" and will be used for further analysis in the convolution network. The minus of the map is the dependence of the position of the centers of the clusters on neighboring neurons, which leads to the presence of centers in areas with no differences in brightness. In this case, after the "window" identifies zones of interest around the centers of the clusters, about 100 cut frames the size of the maximum aircraft are sent for

66

further analysis. This is 1000 times less than when using sequential splitting of the input image into frames or 15–100 times less than when using algorithms similar to RCNN, YOLO and SSD. Also, the application of this algorithm significantly reduces the required number of training images of the aircraft for the convolution network, because the size of the "window" is tied to the image scale and is equal to the size of the largest detectable aircraft. This means that there is no need to vary the size of the aircraft in training images.

Table 1 shows the performance of the Kohonen map depending on the resolution of the input image and the number of possible objects of minimum size. The calculations фre performed in a program of our own design without the use of a GPU (graphics processor), acceleration and optimization algorithms on a personal computer with the parameters specified in paragraph 4.

Table 1
Kohonen map performance

The size of the input image, pix.	Number of search objects	SOM processing, sec.
120×230	3	0,1
200×400	10	0,3
671×493	24	3,3

As can be seen from the **Table 1**, the image processing speed of the Kohonen map has a non-linear dependence on the image size and the number of search objects, so the size of the input image should be selected based on the required speed of the algorithm.

According to the results of [11], the main drawback of the SOM algorithm was the frequent location of network nodes between objects, and not inside them. This drawback is eliminated using the algorithm for initializing the network weights according to random examples and changing the communication function between neurons in such a way that with increasing distance between them, the interaction quickly decreased. This allows to reduce the number of network nodes outside the facilities by about 4.7 times.

8. Discussion of the results of the created algorithm for the search for zones of interest on the underlying surface

Existing algorithms for searching and recognizing objects select several thousand or even hundreds of thousands of parts on the input image and submit them to the convolution network for analysis. The algorithm proposed in this article allows one to reduce the number of analyzed portions of the input image and to reduce the training sample for the convolution network, which can significantly reduce the time for searching and recognizing objects. This is achieved through a preliminary search for areas of interest in the image with further analysis of only the selected areas. The size of the "window" scanning certain areas of interest is determined based on the image scale and the given dimensions of the largest detectable object. Highlighting the boundaries of objects and applying SOM allow to determine the centers of objects in the image and create zones of interest around them. These solutions make it possible to eliminate variations in scale and center the desired object, due to which the training sample size of the terminal convolution network is reduced several times, its training is accelerated, and recognition accuracy is increased.

The disadvantage of the created algorithm is a significant increase in the recognition speed only when analyzing images on which the boundaries of objects do not occupy most of the space. For example, in satellite and radar images, when the desired objects are located on a homogeneous underlying surface of great length. When analyzing images occupied by small objects, the algorithm will determine the entire image as the zone of interest, while still reducing the number of analyzed portions of the input image. The analyzed parts will be 300–500 times less than when using sequential partitioning or 3–10 times less than when using algorithms similar to RCNN, YOLO and SSD. In the future, it is planned to identify unique features of the shape of the boundaries of the de-

sired objects, which will help to distinguish these objects against the background of the underlying surface and the boundaries of objects of no interest.

The pre-processing algorithm shows a high speed of extracting the boundaries of the objects of the input image. The search for cluster centers using a Kohonen self-organizing map allows to process images with sizes up to 500×500 pixels at high speed. and the number of search objects about 40 pcs. In the future, it is planned to use Kohonen map acceleration and optimization algorithms for GPU calculations, as well as consider other options for searching for cluster centers, for example, the Kohonen neural network.

Compared with the previous work [11], the following is done:

– the algorithm for highlighting the boundaries of objects by performing image contrasting, filling the space inside closed borders, and filtering selected objects in the image which geometric shape does not match the shape of the boundaries of the desired objects has been improved;

– the algorithm for determining the zone of interest for closely located, relative to the scale of the desired object, network nodes has been changed. Now the zone of interest is expanded in such a way as to cover the common area for these nodes, instead of looking for the region of interest for each node separately;

– improving the initialization algorithm of the initial network weights and the function of reducing the connections between neurons with increasing distance between them, allows to significantly reduce the number of network nodes that are between objects, and not inside them.

In further work, it is planned to improve the presented algorithm due to a better allocation of the boundaries of objects and the search for their centers. It is also planned to create and optimize a convolutional neural network for object recognition, which will create a complete system for searching and recognizing objects on radar or satellite images of the underlying surface.

9. Conclusions

1. To highlight the boundaries of objects present in the image, an algorithm based on the use of the Sobel operator is used. The algorithm has high speed, highlighting the boundaries of the objects of the input image in 0.008–0.03 sec.

2. SOM is used to search for centers of objects, as this is one of the fastest algorithms for determining the centers of input data clusters.

3. The developed algorithm is tested on real satellite images. Its application allows to reduce the amount of data analyzed by the convolution network by 15–100 times, which accordingly reduces the time of searching and recognition of necessary objects. Also, the use of this algorithm reduces the required number of training images for the convolution network, since the size of the "window" is related to the image scale and corresponds to the size of the largest detected object. This fact and the centering of the object on training images can accelerate network learning by more than 5 times and increase recognition accuracy by at least 10 %, as well as halve the required minimum number of layers and neurons of the convolutional network, thereby increasing its speed.

References

[1] Simard, P. Y., Steinkraus, D., Platt, J. C. (2003). Best practices for convolutional neural networks applied to visual document analysis. Proceedings of the Seventh International Conference on Document Analysis and Recognition. doi: https://doi.org/10.1109/icdar.2003.1227801

[2] Novikova, N. M., Dudenkov, V. M. (2015). Modelirovanie neyronnoy seti dlya raspoznavaniya izobrazheniy na osnove gibridnoy seti i samoorganizuyuschihsya kart Kohonena. Aspirant, 2, 31–34.

[3] Narushev, I. R. (2018). Neural network on the basis of the self-organizing kochonen card as a means of detecting anomalous behavior. Ohrana, bezopasnost', svyaz', 2 (3 (3)), 194–197.

[4] Girshick, R., Donahue, J., Darrell, T., Malik, J. (2014). Rich Feature Hierarchies for Accurate Object Detection and Semantic Segmentation. 2014 IEEE Conference on Computer Vision and Pattern Recognition. doi: https://doi.org/10.1109/cvpr.2014.81

[5] Girshick, R., Donahue, J., Darrell, T., Malik, J. (2016). Region-Based Convolutional Networks for Accurate Object Detection and Segmentation. IEEE Transactions on Pattern Analysis and Machine Intelligence, 38 (1), 142–158. doi: https://doi.org/10.1109/tpami.2015.2437384

[6]   Girshick, R. (2015). Fast R-CNN. 2015 IEEE International Conference on Computer Vision (ICCV). doi: https://doi.org/10.1109/iccv.2015.169

[7]   Ren, S. et. al. (2015). Faster R-CNN: Towards real-time object detection with region proposal networks. Advances in neural information processing systems, 91–99.

[8]   He, K., Gkioxari, G., Dollar, P., Girshick, R. (2017). Mask R-CNN. 2017 IEEE International Conference on Computer Vision (ICCV). doi: https://doi.org/10.1109/iccv.2017.322

[9]   Redmon, J., Divvala, S., Girshick, R., Farhadi, A. (2016). You Only Look Once: Unified, Real-Time Object Detection. 2016 IEEE Conference on Computer Vision and Pattern Recognition (CVPR). doi: https://doi.org/10.1109/cvpr.2016.91

[10]   Liu, W., Anguelov, D., Erhan, D., Szegedy, C., Reed, S., Fu, C.-Y., Berg, A. C. (2016). SSD: Single Shot MultiBox Detector. Computer Vision – ECCV 2016, 21–37. doi: https://doi.org/10.1007/978-3-319-46448-0_2

[11]   Skuratov, V., Kuzmin, K., Nelin, I., Sedankin, M. (2019). Application of kohonen neural networks to search for regions of interest in the detection and recognition of objects. Eastern-European Journal of Enterprise Technologies, 3 (9 (99)), 41–48. doi: https://doi.org/10.15587/1729-4061.2019.166887

[12]   Haykin, S. (2008). Neyronnye seti: polniy kurs. Moscow: Izdatel'skiy dom Vil'yams.

[13]   Kohonen, T. (2001). Self-organizing maps. Vol. 30. Springer Science & Business Media, 502. doi: https://doi.org/10.1007/978-3-642-56927-2

ALGORITHM FOR SOLVING THE INVERSE PROBLEMS OF ECONOMIC ANALYSIS IN THE PRESENCE OF LIMITATIONS

Ekaterina Gribanova
Department of Automated Control System
Tomsk state university of control systems and radioelectronics
40 Lenina str., Tomsk, Russia, 634050
geb@asu.tusur.ru

Abstract

The solution of inverse problems is considered taking into account the restrictions using inverse calculations. An algorithm is proposed for solving the inverse problem, taking into account restrictions while minimizing the sum of the absolute values of the changes in the arguments. The problem of determining the increments of the function arguments is presented as a linear programming problem. The algorithm includes solving the inverse problem with the help of inverse calculations while minimizing the sum of the absolute changes in the arguments, checking the correspondence of the obtained arguments to the given restrictions, adjusting the value of the argument if it goes beyond the limits of acceptable values, and changing the varied arguments to achieve the given value of the resulting indicator. The solution of two problems with the additive and mixed dependence between the arguments of the function is considered. It is shown that the solutions obtained in this case are consistent with the result of using an iterative procedure based on changing the resulting value to a small value until a given result is achieved, and the results are compared with solving problems using the MathCad mathematical package. The advantage of the algorithm is a smaller number of iterations compared to the known method, as well as the absence of the need to use coefficients of relative importance. The presented results can be used in management decision support systems.

Keywords: inverse calculations, inverse problem, linear programming, economic analysis, optimization algorithm.

1. Introduction

Tasks to be solved in the field of economics can be divided into direct and reverse in the direction of causal relationship. The direct task is establishing an investigation for well-known reasons, i. e., to calculate the result based on the available values of its values and the type of dependence between them. This allows to evaluate the current state of the investigated object, make a forecast for future periods, and study the influence of factors on the output value. An example of solving a direct problem can be the determination of the profit of an enterprise for given values of income and expenses, the determination of revenue for given values of price and quantity.

The inverse problem is to establish the causes leading to the corollary of interest, i. e., such a selection of initial values that would ensure a given value of the result. Such problems are considered incorrect [1] and have become widespread in various fields, including the economy [2–6].

In [7], an inverse computation apparatus is proposed that allows solving an inverse problem using expert information. Solving problems of this kind is relevant, because it allows to answer the question "how to do it so that ...?", determine the control actions to achieve the desired state of the economy, which is an integral function of decision support systems. The inverse computing apparatus has found practical application in various sectors of the economy [8–11].

Solving inverse problems using inverse calculations is to obtain the point values of the growth of the arguments of a function based on its given value and additional information coming from the person who forms the solution. In particular, the coefficients of the relative importance of the argument and the direction of their change (increase or decrease) can be indicated as such information.

The relationship of indicators can be represented in the form of a tree, at the first level of which the resulting indicator is located, at the second – indicators that form it. **Fig. 1** shows a graphical illustration of the direct and inverse problems in the case of multiple dependence for the function of two arguments: profitability (r) is equal to the ratio of profit (p) to cost (c) [12].

70

$$r=p/c. \tag{1}$$

Let's consider the solution of the inverse problem. Initial data: $r=0.2$, $p=10$ (c.u.), $c=50$ (c.u.). It is necessary to determine the values of profit and costs that will ensure a profitability of 0.3. Without additional information, this problem can have set of solutions.
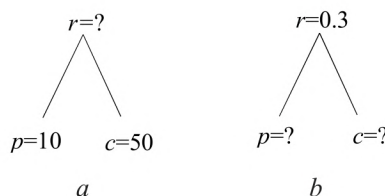
Fig. 1. Graphical representation of the problem: a – direct; b – indirect

Let x_i – i-th argument of the function $f(x)$ ($i=1..n$, n – the number of arguments), and α_i – the coefficient of relative priority of the i-th argument. Then the solution of the problem using inverse calculations can be obtained by solving the system of equations:

$$\begin{cases} y \pm \Delta y = f\left(\begin{array}{l} x_1 \pm \Delta x_1\left(\alpha_1\right), x_2 \pm \\ \pm \Delta x_2\left(\alpha_2\right),...,x_n \pm \Delta x_n\left(\alpha_n\right) \end{array} \right); \\ \dfrac{\Delta x_1}{\Delta x_2} = \dfrac{\alpha_1}{\alpha_2};... \dfrac{\Delta x_1}{\Delta x_n} = \dfrac{\alpha_1}{\alpha_n}; \\ \sum\limits_{i=1}^{n} \alpha_i = 1, \end{cases}$$

where Δx_i – the increment of the i-th argument; x_i – the initial value of the i-th argument; y, Δy – the initial value and the increment of the resulting function.

So, for problem (1), let's set the values of the coefficients of relative priority of the function arguments: $\alpha_1=0.6$ and $\alpha_2=0.4$, and an increase in profit and a decrease in costs should occur.

Then the solution to the problem can be obtained as follows:

$$\begin{cases} r + \Delta r = \dfrac{\left(p + \Delta p\right)}{\left(c + \Delta c\right)}; \\ \dfrac{\Delta p}{\Delta c} = -\dfrac{\alpha_1}{\alpha_2}. \end{cases}$$

$$(p-1.5\Delta c)/(c+\Delta c)=0.3;$$

$$\Delta c=-2.78;$$

$$\Delta p=-1.5\cdot2.78=4.17.$$

The values of profit and costs are equal: $p=10+4.17=14.17$, $c=50-2.78=47.22$.

The binding to the expert opinion has its positive aspects: several possible solutions to the problem can be considered, the best change in indicators is indicated from the point of view of available resources, the coefficients can be set taking into account the real possibility of the direction of the change in the arguments and their interdependence. The resulting decision can subsequently be adjusted taking into account additional conditions. However, sometimes it becomes necessary to obtain a result without involving expert information. The decision obtained using the coefficients of relative priority of the arguments is subjective and based on the opinion of a specialist, the determination of which may be difficult. The tasks, the solution of which can be found

without involving expert information, in particular, include tasks of searching as close as possible to the original solution, i. e., with a minimum change in the arguments. Earlier, two methods for solving such problems were considered.

The first method is considered in [13]; the problem of determining the increments of arguments is represented as the optimization problem of quadratic programming: the sum of the squares of the increments of the arguments acts as the objective function. Using geometric constructions, a method for solving such a problem using a system of equations is determined. However, the scope of this method is limited due to the fact that the dependence function between the arguments can't always be formed. In addition, this method minimizes the sum of the squares of the changes in the arguments, while the absolute values of the arguments can be considered as easier to understand the characteristics of their changes. The sum of the absolute values of the increments of the arguments can be considered as an alternative to the Euclidean distance and suggests a decrease in the influence of large deviations.

The second method is presented in [14] and is based on the concept of a gradient vector, showing the direction of the greatest increase in the function. Therefore, moving in this direction, it is possible to achieve a given value of the function (if necessary, increase it) with a smaller change in the arguments. This method does not require the formation of a function of dependence between arguments, however, it is heuristic and in the problem under study does not guarantee an optimal solution from the point of view of the chosen criterion.

In addition, when solving problems, restrictions on the values of the arguments can be imposed. Restrictions on the values of indicators can be determined by the area of their acceptable values, the features of doing business (for example, the amount of resources used by an enterprise can't be more than the available stock), forecast values of indicators established by an expert, etc.

In [15], an algorithm is proposed for solving the problem in the presence of restrictions, including the gradual change of the resulting indicator to a small step value and the determination of the argument values using inverse calculations using the coefficients of the relative priority of the arguments. If the values of the arguments do not satisfy the constraints, then, if possible, the deficit is filled by other resources. The algorithm ends when the objective function is equal to the specified value or all resources are exhausted.

In [16], stochastic algorithms for solving the inverse problem under constraints were considered. In the first version, the global optimization problem is considered, in which the integral function of the degree of correspondence of the resulting value to the established one and the growth of arguments to the given importance factors acts as the objective function. An algorithm is also proposed based on the sequential change of the resulting indicator by a small amount and the choice of the argument with a probability corresponding to the priority coefficient, due to which a new value of the resulting indicator is achieved. The algorithm stops when it reaches the set value of the function or if all arguments are assigned markers, according to which their further change is impossible.

The disadvantage of the considered work is the need for multiple iterations, therefore, to solve the problem requires a lot of computing resources. In addition, in the case of stochastic algorithms, the resulting solution will be suboptimal.

The presented work is devoted to the development of an algorithm for solving the inverse problem with a minimum total absolute change in the arguments, taking into account the limitations. Unlike existing works, this algorithm will not require multiple solutions to the inverse problem with a sequential approximation of the initial value of the resulting indicator to the given one, the maximum number of iterations will be equal to the number of arguments whose values are constrained.

The aim of research is development of an algorithm for solving inverse problems while minimizing the sum of the absolute values of the arguments, taking into account the limitations that differ from the existing ones, using the approach based on the choice of variable arguments, solving the inverse problem and adjusting the values of the arguments in accordance with the restrictions.

To achieve the aim, the following objectives are set:
– develop a method for solving the inverse problem while minimizing the sum of the absolute values of the arguments;

– develop an algorithm for solving the inverse problem, taking into account restrictions;

– to compare the solutions obtained as a result of the implementation of the algorithm with the results of using the methods presented in the literature and the mathematical package MathCad.

Thus, the proposed algorithm is based on the use of the inverse computing apparatus proposed in [7, 15]. It is modified to solve problems without involving expert information (with a minimum amount of absolute values of the arguments), taking into account restrictions on the values of the arguments.

2. Solution of the problems of economic analysis, taking into account the limitations

The problem of determining a solution with a minimum sum of the absolute values of the argument changes in the presence of restrictions has the form:

$$\left| \Delta x_1 \right| + \left| \Delta x_2 \right| + \ldots \to \min,$$

$$f\left(x + \Delta x \right) = y,$$

$$l_i \leq x_i + \Delta x_i \leq h_i, \tag{2}$$

where i – the number of the argument, the value of which is constrained ($i=1..m$, m – the number of arguments the value of which is constrained); l_i and h_i – the lower and upper bounds of the interval to which the values of the i-th argument must belong.

To solve this problem, let's consider an approach that consists in solving the linear programming problem with one constraint ($f(x+\Delta x)=y$) and then adjusting the solution in accordance with the established boundaries l_i and h_i.

Let's consider a solution to the linear programming problem with one restriction. Depending on the type of model and the increase in the result, the arguments of the objective function (2) will show either a positive or negative sign when the module is opened. So, for example, in the case of the additive model ($f(x)=x_1+x_2$), an increase in the result with a smaller amount of absolute changes in the arguments will be achieved with positive changes in the arguments.

After the module is expanded in the case of a linear constraint ($f(x+\Delta x)=b_1(x_1+\Delta x_1)+$ $+b_2(x_2+\Delta x_2)+\ldots+b_n(x_n+\Delta x_n)$) ($b$ – the numerical values for the arguments in the constraint) the problem (2) is a linear programming problem [17]. The classic method for solving it is the simplex method. However, with the only restriction and equality of numerical values for arguments in the objective function to unity, the problem can be solved by a simpler method. Its solution is reduced to finding an element with a large absolute numerical value b with an increase in the argument in the constraint and solving the equation for this argument [18].

If there are several such maximum values, then when solving the problem, either a uniform change of these arguments can be performed to achieve a given value of the result, or their change in accordance with the coefficients of relative importance specified by the expert, or a change in one of the arguments chosen randomly. When implementing software systems, the equation is solved using classical methods for finding roots (for example, by the Newton method), the article discusses the analytical solutions to such problems.

If the restriction has a nonlinear form, the considered problem relates to nonlinear programming problems [19]. To convert the constraint into a linear one, Taylor series expansion can be used (the initial values of the increments are zero):

$$f\left(\Delta x_1, \Delta x_2, \ldots, \Delta x_n \right) = \sum_{i=1}^{n} \frac{\partial f}{\partial \Delta x_i} \Delta x_i. \tag{3}$$

Consequently, the value of the partial derivatives $\left(b_i = \dfrac{\mathrm{d}f}{\mathrm{d}\Delta x_i} \right)$ at the zero point is considered as numerical values in increments of the arguments.

73

Thus, the algorithm for determining the solution of the inverse problem using inverse computation, if there are restrictions on the values of the arguments, includes the following steps.

Step 1. Solving the problem of determining the increments Δx_i of variable arguments in such a way that the sum of their absolute values is minimal:

$$\left| \Delta x_1 \right| + \left| \Delta x_2 \right| + \ldots \rightarrow \min,$$

$$f(x + \Delta x) = y. \tag{4}$$

Change the argument values by the obtained increment value: $x_i = x_i + \Delta x_i$.

Step 2. Verify compliance of mutable arguments with given constraints. If all values satisfy the constraints, then the algorithm stops. If there is at least one argument that does not satisfy the restrictions, then the value of the nearest boundary is assigned to it, and such an argument is excluded from the list of mutable arguments. If the list of mutable arguments is empty, then the algorithm ends.

In the presented algorithm, in step 1, the solution of problem (4) occurs, however, minimization of the sum of the squares of the increments and the change in the increments of the arguments in accordance with the elements of the gradient vector can be considered. This algorithm will allow to find a solution to such problems in the presence of restrictions.

3. The results of solving inverse problems with restrictions

Let's consider the application of the described algorithm for the additive and mixed dependence between the arguments of a function. Relative priority coefficients are excluded from the tasks.

The volume of delivery Q of products to the outlet consists of the delivery volume of the first, second and third type of product:

$$Q = Q_1 + Q_2 + Q_3, \tag{5}$$

where Q_1, Q_2, Q_3 – the volume of delivery of products of the first, second and third kind, respectively.

The initial values of the arguments are: $Q_1 = 15$ kg, $Q_2 = 17$ kg, $Q_3 = 20$ kg. The initial value of the resulting indicator Q is 52 kg. It is necessary to determine the volume of delivery of products of the first, second and third type so that the total volume is 60 kg of products.

At the same time, the following restrictions are set for argument values:

$$0 \leq Q_1 \leq 25;$$

$$0 \leq Q_2 \leq 17.5;$$

$$0 \leq Q_3 \leq 25.$$

Let's carry out the solution of the inverse problem with the help of inverse calculations under given constraints. Since the value of the resulting function needs to be increased, this can be achieved with positive gains in these arguments. The task has the form:

$$\Delta Q_1 + \Delta Q_2 + \Delta Q_3 \rightarrow \min;$$

$$(Q_1 + \Delta Q_1) + (Q_2 + \Delta Q_2) + (Q_3 + \Delta Q_3) = 60;$$

$$\Delta Q_1, \Delta Q_2, \Delta Q_3 \geq 0.$$

The numerical values for ΔQ_1, ΔQ_2 and ΔQ_3 are equal. Let's consider the case when the change in the growth of arguments occurs evenly.

74

The system of equations has the form:

$$\begin{cases} \dfrac{\Delta Q_1}{\Delta Q_2} = 1, \\[2mm] \dfrac{\Delta Q_1}{\Delta Q_3} = 1, \\[2mm] \left(15 + \Delta Q_1\right) + \left(17 + \Delta Q_2\right) + \left(20 + \Delta Q_3\right) = 60. \end{cases}$$

System solution:

$$\Delta Q_1 = \Delta Q_2 = \Delta Q_3 = 2.667.$$

Therefore,

$$Q_1 = 15 + 2.667 = 17.667,$$

$$Q_2 = 19.667, \; Q_3 = 22.667.$$

The argument Q_2 does not satisfy the restrictions; let's assign this argument the value of the boundary 17.5 ($Q_2 = 17.5$). The list of mutable arguments left Q_1 and Q_3.
The system of equations has the form:

$$\begin{cases} \dfrac{\Delta Q_1}{\Delta Q_3} = 1, \\[2mm] \left(17.667 + \Delta Q_1\right) + 17.5 + \left(22.667 + \Delta Q_3\right) = 60. \end{cases}$$

System solution:

$$\Delta Q_1 = \Delta Q_3 = 1.083.$$

Therefore,

$$Q_1 = 17.667 + 1.083 = 18.75, \; Q_2 = 17.5,$$

$$Q_3 = 22.667 + 1.083 = 23.75.$$

The solution corresponds to the obtained solution using the MathCad program (**Fig. 2**).

$$\Delta Q1 := 0 \quad \Delta Q2 := 0 \quad \Delta Q3 := 0 \quad Q1 := 15 \quad Q2 := 17 \quad Q3 := 20$$

$$f(\Delta Q1, \Delta Q2, \Delta Q3) := \left|\Delta Q1\right| + \left|\Delta Q2\right| + \left|\Delta Q3\right|$$

  Given

$$14 \le Q1 + \Delta Q1 \le 25 \;\; 16 \le Q2 + \Delta Q2 \le 17.5 \;\; 18 \le Q3 + \Delta Q3 \le 25$$

$$(Q1 + \Delta Q1) + (Q2 + \Delta Q2) + (Q3 + \Delta Q3) = 60$$

  $$\Delta Q := \text{Minimize}(f, \Delta Q1, \Delta Q2, \Delta Q3)$$

$$Q1 := Q1 + \Delta Q_0 = 18.75$$

$$Q2 := Q2 + \Delta Q_1 = 17.5$$

$$Q3 := Q3 + \Delta Q_2 = 23.75$$

Fig. 2. Problem solution in MathCad

Fig. 3 shows the change in the values of the arguments during ten iterations when solving the problem using the iterative procedure presented in [15]. The result obtained corresponds to the solution in **Fig. 2**.
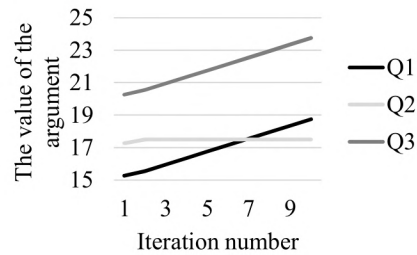
Fig. 3. Changing argument values over ten iterations

Let's consider the mixed dependency between function arguments. Profit (M) of an enterprise is defined as the difference between income and costs [20, 21]:

$$M=Num(Price-Cu), \qquad (6)$$

where *Price* – the unit price of a product; *Num* – amount of product sold; *Cu*– unit cost of a product.

The initial value of the profit from the sale of products of the type in question is 4,018 c.u., the unit price is 60 c.u., the quantity is 98 units, the unit cost of production is 19 c.u. It is necessary to determine the value of the price, cost and quantity in this way so that the profit is equal to 4500 c.u.

Constraints for variables: $80 \leq Num \leq 130$, $50 \leq Price \leq 62.5$, $18.5 \leq Cu \leq 25$.

Let's calculate the partial derivatives of the constraint function $f(\Delta Num, \Delta Price, \Delta Cu)= =(98+\Delta Num)\cdot(60+\Delta Price-19-\Delta Cu)-4500$:

$$\frac{\partial f}{\partial \Delta Num} = 41,$$

$$\frac{\partial f}{\partial \Delta Price} = 98,$$

$$\frac{\partial f}{\partial \Delta Cu} = -98.$$

The absolute value of the partial derivative is greater for price and cost increment. Let's consider the uniform change in these indicators:

$$\begin{cases} \dfrac{\Delta Price}{\Delta Cu} = -1; \\ 98 \cdot \left(60 + \Delta Price - 19 - \Delta Cu\right) = 4500. \end{cases}$$

System solution: $\Delta Price=2.459$, $\Delta Cu=-2.459$, $Price=62.459$, $Cu=16.54$. The cost value does not satisfy the limit. Consequently, $Cu=18.5$, $\Delta Price=4500/98-62.459+18.5=1.959$.

The value of the price does not satisfy the restriction, therefore,

$$Price=62.5,$$

$$Num=4500/(62.5-18.5)=102.273.$$

The resulting value satisfies the constraint, the calculations are completed.

76

The solution also coincided with the solution of problem (1) in the MathCad program.

Table 1 presents the results obtained using the considered algorithm in the case of minimizing the sum of the squares of the changes in the arguments.

Table 1
Argument values while minimizing the squared argument changes

Iteration number	Num	Price	Cu
	98	60	19
1	99.02	62.223	16.777
2	99.667	63.65	18.5
3	102.273	62.5	18.5

4. Discussion of the results of the development of an algorithm for solving inverse problems with constraints

An algorithm is proposed for solving the inverse problem using inverse calculations while minimizing the sum of the absolute changes in the arguments, taking into account restrictions on the values of the arguments. The results of applying the algorithm are consistent with the solutions obtained using the mathematical package and applying the iterative procedure presented in [15].

The advantage of the proposed algorithm is that, unlike the approaches considered in [15, 16], it does not require multiple iterations, during which the resulting indicator is successively changed until a given value is reached. In the proposed algorithm, the number of iterations is determined by the number of arguments that do not satisfy the constraints. The algorithm, in contrast to the method proposed in [13], which considers minimizing the sum of the squares of the arguments, does not require the formation of a function of dependence between the arguments and suggests finding a solution while minimizing the absolute deviations of the arguments (a task in such a formulation may be more understandable for a specialist).

The disadvantages of the proposed method include the need to calculate partial derivatives of the function in the case of a nonlinear dependence between the arguments of the function.

The presented algorithm does not require the use of the simplex method and can be used to solve linear programming problems of the considered type in other areas of research. The disadvantage of the proposed algorithm is the requirement that the number of constraints that include different variables should be equal to unity, which narrows the range of tasks.

The directions of further research are related to the modification of this algorithm for the case of discrete data, i. e., if there is a requirement that the arguments of the function are integer.

5. Conclusions

1. An algorithm is proposed for solving the inverse problem while minimizing the sum of the absolute increments of the arguments, taking into account restrictions on the values of the arguments. The application of the algorithm allows one to obtain results that are consistent with the results of using mathematical packages and an iterative method, which involves changing the resulting indicator by a small amount until the specified value is reached. Confirmation of this is given in the results of the numerical solution of two inverse problems in which the additive and mixed dependence between the arguments is considered. A feature of the algorithm is the absence of the need for multiple iterations, as well as the ability to determine a solution with a minimum total absolute change in the arguments. This is achieved by presenting the problem as a linear programming problem with one restriction. Its solution reduces to determining the maximum absolute numerical values for the arguments in the constraint and solving the inverse problem using inverse calculations.

2. The presented algorithm can be implemented in decision support systems, providing organization specialists with the opportunity to solve inverse problems using inverse calculations if there are restrictions without using expert information. The approach will allow to determine the solution to problems with a minimum total absolute change in the arguments, i. e., the one closest to the current one, and ensure the speed of such software systems.

References

[1] Colton, D., Engl, H. W., Louis, A. K., McLaughlin, J. R., Rundell, W. (Eds.) (2000). Surveys on Solution Methods for Inverse Problems. Springer. doi: https://doi.org/10.1007/978-3-7091-6296-5

[2] Ekeland, I., Djitté, N. (2006). An inverse problem in the economic theory of demand. Annales de l'Institut Henri Poincare (C) Non Linear Analysis, 23 (2), 269–281. doi: https://doi.org/10.1016/j.anihpc.2005.10.001

[3] Barbagallo, A., Mauro, P. (2014). An Inverse Problem for the Dynamic Oligopolistic Market Equilibrium Problem in Presence of Excesses. Procedia - Social and Behavioral Sciences, 108, 270–284. doi: https://doi.org/10.1016/j.sbspro.2013.12.837

[4] Shananin, A. A. (2018). Inverse Problems in Economic Measurements. Computational Mathematics and Mathematical Physics, 58 (2), 170–179. doi: https://doi.org/10.1134/s0965542518020161

[5] Klemashev, N. I., Shananin, A. A. (2016). Inverse problems of demand analysis and their applications to computation of positively-homogeneous Konüs–Divisia indices and forecasting. Journal of Inverse and Ill-Posed Problems, 24 (4). doi: https://doi.org/10.1515/jiip-2015-0015

[6] Beck, A., Teboulle, M. (2009). A Fast Iterative Shrinkage-Thresholding Algorithm for Linear Inverse Problems. SIAM Journal on Imaging Sciences, 2 (1), 183–202. doi: https://doi.org/10.1137/080716542

[7] Odintsov, B. E., Romanov, A. N. (2014). How to create business performance management (BPM) system. Bulletin of the University of Finance, 6, 22–36.

[8] Barmina, E. A., Kvjatkovskaja, I. Yu. (2010). Monitoring the quality of a commercial organization. Structuring indicators. The use of cognitive maps. Bulletin of the Astrakhan State Technical University, 2, 15–20.

[9] Blumin, S. L., Borovkova, G. S. (2018). Application of analysis of finite fluctuations and reverse computations in control systems and decision support systems. Control Sciences, 6, 29–34. doi: https://doi.org/10.25728/pu.2018.6.4

[10] Borshchuk, I. V., Odintsov, B. E., Shkvir, V. D. (2013). Inverse calculations in prevent crisis phenomenon of socio-economic systems. International conference on application of information and communication technology and statistics in economy and education. Bulgaria, 140–143.

[11] Dik, V. V., Urintsov, A. I., Odintsov, B. Ye., Churikanova, O. Yu. (2014). Decision support methods in balanced ScoreCard. Naukovyi visnyk Natsionalnoho hirnychoho universytetu, 4, 120–126.

[12] Ali, H. A. E. M., Al-Sulaihi, I. A., Al-Gahtani, K. S. (2013). Indicators for measuring performance of building construction companies in Kingdom of Saudi Arabia. Journal of King Saud University - Engineering Sciences, 25 (2), 125–134. doi: https://doi.org/10.1016/j.jksues.2012.03.002

[13] Gribanova, E. B. (2018). Methods for solving inverse problems of economic analysis by minimizing argument increments. Proceedings of Tomsk State University of Control Systems and Radioelectronics, 21 (2), 95–99. doi: https://doi.org/10.21293/1818-0442-2018-21-2-95-99

[14] Gribanova, E. (2019). Development of a price optimization algorithm using inverse calculations. Eastern-European Journal of Enterprise Technologies, 5 (4 (101)), 18–25. doi: https://doi.org/10.15587/1729-4061.2019.180993

[15] Odincov, B. E., Romanov, A. N. (2014). Iterative method of optimization of enterprise management by means of inverse calculations. Bulletin of the Financial University, 2, 60–73.

[16] Gribanova, E. B. (2016). Stochastic algorithms to solve the economic analysis inverse problems with constraints. Proceedings of Tomsk State University of Control Systems and Radioelectronics, 19 (4), 112–116. doi: https://doi.org/10.21293/1818-0442-2016-19-4-112-116

[17] Vanderbei, R. J. (2014). Linear programming. Foundations and Extensions. Springer. doi: https://doi.org/10.1007/978-1-4614-7630-6

[18] Ganicheva, A. V. (2019). Method of the solution of some classes optimising tasks. Modeling, optimization and information technology, 7 (2), 43–54. doi: https://doi.org/10.26102/2310-6018/2019.25.2.002

[19] Trunov, A. (2015). Modernization of means for analyses and solution of nonlinear programming problems. Quantitative Methods in Economics, XVI (2), 133–141.

[20] Shen, B., Shen, Y., Ji, W. (2019). Profit optimization in service-oriented data market: A Stackelberg game approach. Future Generation Computer Systems, 95, 17–25. doi: https://doi.org/10.1016/j.future.2018.12.072

[21] O'Neill, B., Sanni, S. (2018). Profit optimisation for deterministic inventory systems with linear cost. Computers & Industrial Engineering, 122, 303–317. doi: https://doi.org/10.1016/j.cie.2018.05.032

EVALUATION OF THE INTER-REPAIR OPERATION PERIOD OF ELECTRIC SUBMERSIBLE PUMP UNITS

Habibov Ibrahim Abulfaz[1]
h.ibo@mail.ru

Abasova Sevinj Malik[1]
seva-abasova@mail.ru

[1]*Department of Engineering and Computer Graphics*
Azerbaijan State Oil and Industry University
20 Azadliq ave., Baku, Azerbaijan, AZ 1010

Abstract

In recent years, in the oil and gas industry of Azerbaijan, the use of electric submersible pumps (SEP) as one of the effective way to increase the level of production of well products. Currently, electric centrifugal pumping units (ECPU) are widely used both on land and in offshore fields. Currently, a total of about 15 % of SOCAR's oil wells are produced using electric submersible pumping units.

ECPU effectiveness is largely determined by both the period of their operation and the frequency of repair and restoration work.

It is established that the use of ECPUs contributes to an increase in the service life of equipment and the effectiveness of a mechanized method of oil production. To assess the benefits of the latter, the most important factor is the inter-repair period (Tir) of the equipment.

Existing methods for determining the inter-repair period of oilfield equipment are accompanied by large errors, which significantly reduce their reliability.

In this regard, the article is tasked with developing a more practical and reliable method for determining the inter-repair period, where the point of change in the nature of the failure rate is adopted as the determining parameter.

Keywords: electric submersible pumping units, oil well, repair frequency, failure rate.

1. Introduction

Oil and gas sectors of Azerbaijan are the determining factors of the fuel and energy complex (FEC) of the republic. More than 60 % of the country's budget is formed here and therefore, issues related to improving the efficiency of technological processes and equipment resources used in this industry are relevant.

At present, in the republic's oil producing fields, along with fountain and rod-pumping methods, a production method using electric submersible pumping units is also used. About 15 % of SOCAR's oil wells produce oil using electric submersible pumps (ESP) [1].

Prediction of the time between ESP failures before launching into the well, as well as assessment of its residual life during operation, will determine the operating time to failure, plan repair measures and prevent the maximum wear of their components. One of the main parameters characterizing the performance of oil pumping equipment is their inter-repair period.

The aim of research is development of a new solution in the determination of the inter-repair period (T_{ir}) of electric submersible pumps, using the point of change in the nature of the intensity of their failures.

2. Theoretical background of the problem

Field data on malfunctions and premature failure of parts and assemblies of ESPs shows that the nature of their occurrence varies in time and a sharp fracture occurs at a certain point (**Fig. 1**), which leads to dangerous failures [2].
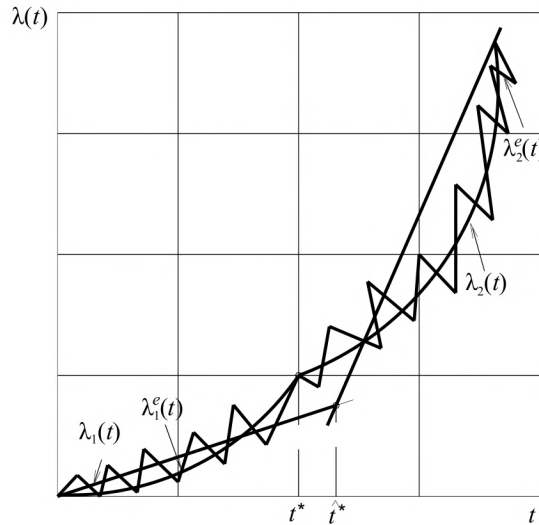
Fig. 1. The nature of the change in the frequency of failures occurring in electric submersible pumps: $\lambda_1(t)$, $\lambda_2(t)$ – theoretical and $\lambda_1^e(t)$, $\lambda_2^e(t)$ – empirical failure rates

In the main period of operation, the physics of failures contains elements of both wear-out and sudden failures, but with a large predominance of wear-out gradual failures with some characteristic increasing function of the failure rate $\lambda(t)$. In fact, if the pump element has almost no hidden defects, but it quickly is "aging", then the failure rate and the reliability function $P(t)$, that is, the probability of failure-free operation, should be well approximated by Weibull law with a parameter of >1 or a normal law [6].

In the case when the consequences of failures can be the occurrence of dangerous situations and injuries of staff, existing in the theory of reliability methods for determining the inter-repair period (IRP), based on the analysis and minimization of operating losses, for example [3–5], become unacceptable.

The results of numerous experiments and analysis of the evaluation data for the operation of electric submersible pumps (ESP) allow to divide the nature of their intensity into two cases: before the point of intensity breakdown and after. In this work, the intensity tipping point t^* is determined using the nonlinear corrosion-regression approximation of the empirical intensity functions $\lambda_1^e(t)$ and $\lambda_2^e(t)$, respectively, to the fracture point and after. The point t^* obtained in [7] using a linear approximation of the above empirical functions is taken as the initial approximation.

After the fracture point, the failure rate increases sharply due to the physico-mechanical and physico-chemical processes occurring in the nodes and parts of the equipment. The frequency of these deviations is described as follows:

$$\lambda(t) = \frac{f(t)}{1 - F(t)} = -\frac{1}{P(t)}\frac{dP(t)}{dt},\tag{1}$$

where $\lambda(t)$ – the failure rate; $P(t)$ – the probability of failure-free operation associated with the distribution function $F(t)$ and the distribution density $f(t)$ of the time between failures by the ratios:

$$F(t) = 1 - P(t),$$

$$f(t) = \frac{dF(t)}{dt} = -\frac{dP(t)}{dt}.$$

The appearance of dangerous failures is considered to be possible [2], if the ratio of neighboring (at intervals) values of the empirical failure rate satisfies the relation

80

$$\lambda_2^e(t) / \lambda_2^e(t) \geq 2, \tag{2}$$

where $\lambda_1^e(t)$ and $\lambda_2^e(t)$ – the empirical failure rate before and after the fracture point.

To estimate the value of the point of a breakdown in the failure rate, as a first approximation, it is enough to find the intersection of straight lines, which are linearization of the curves $\lambda_1^e(t)$ and $\lambda_2^e(t)$ in the vicinity of the point "suspicious" of the presence of a fracture in the intensity of the failure. Such a point (let's denote it by $\ll \hat{t}* \gg$) must, first of all, satisfy relation (2) and is defined as the intersection point of two linear regressions

$$\hat{\lambda}_1(t) = a_1 t + b_1, \quad \hat{\lambda}_2(t) = a_2 t + b_2 \tag{3}$$

coefficients a_1, b_1 and a_2, b_2 are estimated by the method of least squares (OLS).

Equating the left and right sides of equations (3), let's obtain:

$$\hat{t}^* = \left(\hat{b}_1 - \hat{b}_2 \right) \Big/ \left(\hat{a}_2 - \hat{a}_1 \right).$$

Substituting the last least-squares equation $\hat{a}_j$, $\hat{b}_j$ into the last equation of the coefficient a_j, b_j $(j = 1, 2)$, let's reduce to the following formula [7]:

$$\hat{t}^* = \frac{m_{\lambda_1} - m_{\lambda_2} + \left(\dfrac{k_{\lambda_2}}{D_2} \cdot m_2 - \dfrac{k_{\lambda_1}}{D_1} \cdot m_1 \right)}{\dfrac{k_{\lambda_2}}{D_2} - \dfrac{k_{\lambda_1}}{D_1}}. \tag{4}$$

Here

$$m_j = \frac{1}{n_j} \sum_{n=1}^{n_j} t_n^{(j)}, \quad m_{\lambda_j} = \frac{1}{n_j} \sum_{n=1}^{n_j} \lambda_j^e \left(t_n^{(j)} \right), \tag{5}$$

$$D_j = \frac{1}{n_j} \sum_{n=1}^{n_j} \left(t_n^{(j)} - m_j \right)^2, \quad k_{\lambda_j} = \frac{1}{n_j} \sum_{n=1}^{n_j} \left(t_n^{(j)} - m_j \right) \left[\lambda_j^e \left(t_n^{(j)} \right) - m_{\lambda_j} \right], \quad (j = 1, 2),$$

$\left\{ t_n^{(1)} \right\}_{n=\overline{1,n_1}}$ and $\left\{ t_n^{(2)} \right\}_{n=\overline{1,n_2}}$ – points from the left-side and right-sided neighborhood of the "suspicious" point $\hat{t}^*$; $\left\{ \lambda_1^e \left(t_n^{(1)} \right) \right\}$ and $\left\{ \lambda_2^e \left(t_n^{(2)} \right) \right\}$ – the values of the intensities $\lambda_1^e(t)$ and $\lambda_2^e(t)$ at the points $t = t_n^{(1)}$ and $t = t_n^{(2)}$, respectively. The value $\hat{t}^*$ found by formula (4) is taken in [8] as the value of the inter-repair period T_{ir}.

The refinement of estimate (4) is achieved by smoothing the intensity curves $\lambda_1^e(t)$ and $\lambda_2^e(t)$ by the nonlinear regressions. Let $\tilde{\lambda}_1(t)$ and $\tilde{\lambda}_2(t)$ be the best nonlinear approximations of functions $\lambda_1^e(t)$ and $\lambda_2^e(t)$, obtained using the 2D program. The solution to the t equation

$$\tilde{\lambda}_1(t) = \tilde{\lambda}_2(t) \tag{6}$$

for a given initial approximation $t_0 = \hat{t}^*$, where $\hat{t}^*$ is determined by formula (4), it gives a more accurate estimate of the inter-repair period T_{ir}. The solution of nonlinear equation (6) for a given initial approximation is easily found using the corresponding program in the MATHCAD or MATLAB system.

It should be noted that when crossing the fracture point t^*, the form of the distribution function may also change. Then, with the known distribution functions $f_1(t)$ and $f_2(t)$ before and after the fracture point, the corresponding intensity functions $\lambda_1(t)$ and $\lambda_2(t)$ are found by formula (1), and instead of equation (6), the equation is solved concerning t

$$\lambda_1(t) = \lambda_2(t), \tag{7}$$

at the initial approximation $t_0 = \hat{t}*$, where $\hat{t}*$ is determined by formulas (4)–(6), in which $\lambda_j^y(t)$ is replaced by $\lambda_j(t)$ $(j = 1, 2)$.

In particular, for the exponential distribution law with distribution density

$$f(t) = \begin{cases} 0 & \text{at} \quad t < 0, \\ \lambda e^{-\lambda t} & \text{at} \quad t \geq 0, \end{cases} \tag{8}$$

failure rate

$$\lambda(t) \equiv \lambda. \tag{9}$$

For a truncated normal distribution law with a distribution density

$$f(t) = \frac{C}{\sigma\sqrt{2\pi}} \exp\left\{-\frac{(t - a_0)}{2\sigma^2}\right\}, \quad C = 1 / \Phi\left(\frac{a_0}{\sigma}\right),$$

where

$$\Phi(x) = \int_{-\infty}^{x} \frac{1}{\sqrt{2\pi}} e^{-\frac{1}{2}\xi^2} d\xi$$

is the distribution function of the standard normal law, the failure rate is determined by the formula

$$\lambda(t) = \phi\left(\frac{t - a_0}{\sigma}\right) \Big/ \left[\sigma\Phi\left(\frac{a_0 - t}{\sigma}\right)\right], \quad \varphi(x) = \frac{1}{\sqrt{2\pi}} e^{-\frac{1}{2}x^2}; \tag{10}$$

for Weibull distribution with distribution density

$$f(t) = \lambda b t^{b-1} \exp\left\{-\lambda t^b\right\}, \quad \lambda = \frac{1}{a},$$

failure rate

$$\lambda(t) = \lambda b t^{b-1}. \tag{11}$$

3. Research results

In this case, statistics $v = \dfrac{r}{N}$, are used where r – the number of failed samples for the running time t of the N samples put to the test, and the probability of failure-free operation $P(t)$ is related to v by the ratio $P(t) = 1 - v$.

The reliability characteristic determined by the value v is sufficient statistics [6]. This means that knowledge of any other statistics (that is, a random variable depending on the sampled data) does not add anything to the knowledge of probability $P(t)$, obtained on the basis of statistics v [10, 13].

Statistical processing of volume data $n = 12$ from the last column of **Table 1** shows that they obey the truncated normal distribution law (*N*) with $a_0 = 0.636$ and $\sigma = 0.336$ or the Weibull distribution (*W*) with $\hat{a} = 1.2969$ and $\hat{b} = 1.9470$.

Let's denote $\beta = 1/b$ and $\hat{\beta} = 1/\hat{b}$, where $\hat{b} = 1.9470$ – the parameter b estimate obtained in [9] using nonlinear regression. Confidence limits for the true value of the parameter b can be obtained using statistics $W = \hat{\beta}/\beta$, from the table of values of which are given in [11]. It is possible to select such statistics W, values for example, $W_{1-\alpha/2}$ and $W_{\alpha/2}$, that

$$P\left\{W_{1-\alpha/2} \le \frac{\hat{\beta}}{\rho} \le W_{\alpha/2}\right\} = 1 - \alpha.$$ (12)

Table 1
Statistical indicators of submersible ESP failures

Operating interval, days	The number of failures by category of wells					The number of failures in the operating time interval
	normal «N»	sand «S»	corrosion «C»	corrosion-sand		
				«CS»	«CS'»	
0–15	–	–	22	38		60
15–30	–	–	28	87	10	125
30–45	–	19	30	90	30	169
45–60	15	23	26	70	36	170
60–75	20	30	12	40	44	146
75–90	35	34	–	8	28	105
90–105	45	29	6	5	15	100
105–120	60	22	–	–	4	86
120–135	48	18	–	–	–	66
135–150	43	12	–	–	–	55
150–165	37	5	4	–	–	46
165–180	24	–	–	–	–	24
180–195	327	192	128	338	–	1,152

This inequality can be rewritten in the form

$$\frac{\hat{\beta}}{W_{\alpha/2}} \le \beta \le \frac{\hat{\beta}}{W_{1-\alpha/2}},$$

where the $100 - (1 - \alpha)\%$ two-sided confidence boundaries for the parameter b of the Weibull distribution are:

$$\hat{b} \cdot W_{1-\alpha/2} \le b \le \hat{b} \cdot W_{\alpha/2}.$$ (13)

Assuming $\alpha = 0.1$, from [11] let's find for $n = 12$ and $r = 12$ and $W_{0.95} = 1.60$. Therefore, for the example under consideration with a confidence probability $P = 0.9$, the true value of the parameter satisfies the inequality

$$0.60 \cdot 1.9470 \le b \le 1.35 \cdot 1.9470,$$

so

$$1.1682 \le b \le 2.6284.$$ (14)

The failure rate, obeying the Weibull distribution c $b > 2$, tends to increase sharply. Since in our example the parameter b, according to (14) can have a value greater than 2, dangerous failures can occur.

83

4. Discussion of research results

Based on the experimental data, a series of failure values of submersible ESPs is constructed, which is presented below:

$$60; 125; 169; 170; 146; 105; 100; 86; 66; 55; 46; 24. \tag{15}$$

A series of statistics v corresponds to series (15) (the failure rate r among the total number of pumps N=1152).

$$0.0521; 0.1085; 0.1467; 0.1475; 0.1267; 0.0911;$$
$$0.0868; 0.0746; 0.0573; 0.0477; 0.0399; 0.0208. \tag{16}$$

Having ordered series (16) by increasing its members, let's obtain the so-called variational series:

$$0.90208; 0.0399; 0.0477; 0.0521; 0.0573; 0.0746;$$
$$0.0868; 0.0911; 0.1085; 0.1267; 0.1467; 0.1475. \tag{17}$$

As shown in [9], a number of developments (15) up to t=86 are rather well described by the normal distribution with parameters a_0=0.636 and σ=0.336, and after t=86 – by the Weibull distribution with parameters $\hat{a} = 1.2969$ and $\hat{b} = 1.9470$.

Let's take the point t=86 or, which is the same thing, v=0.673 for the suspicious point of fracture of the failure rate. Let's assume that up to the point v^*=0,673, the statistics v obeys the truncated normal law

$$f_1(v) = \phi\left(\frac{v - a_0}{\sigma}\right)\bigg/\left[\sigma\Phi\left(\frac{a_0}{\sigma}\right)\right] \tag{18}$$

with parameters a_0=0.636 and σ=0.336 and with intensity

$$\lambda_1(v) = \phi\left(\frac{v - a_0}{\sigma}\right)\bigg/\left[\sigma\Phi\left(\frac{a_0 - v}{\sigma}\right)\right], \tag{19}$$

and after the point v^*=0.673 – to the Weibull distribution with density

$$f_2(v) = \frac{b}{a}v^{b-1}\exp\left\{-\frac{b}{a}v^b\right\} \tag{20}$$

with parameters $\hat{a} = 1.2969$ and $\hat{b} = 1.9470$ and intensity

$$\lambda_2(v) = \frac{b}{a}v^{b-1}. \tag{21}$$

Regression equations for statistics v can be written as

$$\hat{\lambda}_1(v) = a_1 v + b_1, \quad \hat{\lambda}_2(v) = a_2 v + b_2. \tag{22}$$

For the left-sided neighborhood of the point v^*=0.673, points from the sequence are taken

$$\left\{v_n^{(1)}\right\}_{n=\overline{1,n_1}} = \{0.0521; 0.161; 0.303; 0.455; 0.582; 0.673\} \quad (n_1 = 6),$$

and for the right-hand neighborhood – points from the sequence

$$\left\{v_n^{(2)}\right\}_{n=\overline{1,n_2}} = \left\{0.673; 0.759; 0.839; 0.891; 0.939; 0.979; 1.0\right\} \ (n_2 = 7).$$

The function $\Phi(x)$ is calculated by the approximate formula [12]

$$\Phi(x) = 1 - \phi(x) \cdot \sum_{i=1}^{3} \alpha_i \xi^i, \tag{23}$$

where

$$\xi = 1/(1 + p \cdot x), \quad p = 0.33267, \quad \alpha_1 = 0.4361836, \quad \alpha_2 = -0.1201676, \quad \alpha_3 = 0.9372980.$$

The error of formula (23) is estimated as

$$|\varepsilon(x)| \le 10^{-5}.$$

Equation solution

$$\lambda_1(v) = \lambda_2(v), \tag{24}$$

where $\lambda_1(v)$ and $\lambda_2(v)$ are represented by formulas (19) and (21), respectively, under the initial condition $v_0 = v^* = 0.576$ gives

$$v^* = 0.612, \tag{25}$$

which corresponds to the operating time

$$t^* = 90. \tag{26}$$

Since $t^* = 90$ is the end of the time interval [75, 90], which corresponds to the intensity $v=0.582$, the closest to the value $v^* = 0.612$ and not exceeding v^* the value t^*, determined by value (26) is taken as the value of the inter-repair period T_{ir}.

Table 2 shows the data on the average (T_{av}) and maximum (T_{max}) inter-repair periods for the operation of ESP-type submersible units in various oil and gas production units for Azneft. As can be seen from the **Table 2** experimental data on the average T_{av} value of the inter-repair period for Azneft Production Association of the Azerbaijan Republic using ESP in difficult operating conditions, the T_{av} is in the range 63 ... .100, which is consistent with our calculated value $t^*=90$ days.

Table 2
Data on the average (T_{av}) and maximum (T_{max}) inter-repair period of operation of EDP-type submersible units in various oil and gas production units for Azneft

Name of «Azneft» oil and gas production units	Standard sizes of ECPU submersible units and information on T_{av} and T_{max} (in days)											
	ECPU-5-200			ECPU-6-160			ECPU-6-250			ECPU-6-350		
	n	T_{cp}	T_{max}	n	T_{av}	T_{max}	n	T_{av}	T_{max}	n	T_{cp}	T_{max}
«Balakhanyneft» OGPU	–	–	–	–	–	–	–	–	–	–	–	–
A. D. Amirov OGPU	–	–	–	–	–	–	–	–	–	–	–	–
«Surakhanyneft» OGPU	1	63	100	2	54...67	89...92	–	–	–	–	–	–
G. Z. Tagiyev OGPU	–	–	–	–	–	–	–	–	–	–	–	–
«Bibieybatneft» OGPU	–	–	–	–	–	–	1	66	78	–	–	–
Total:	1	63	100	2	54...67	89...92	1	66	78	–	–	–

85

4. Conclusions

1. The use of electric submersible pump units in oil production is promising and is highly efficient.

2. The indicator of the inter-repair period (T_{ir}) of equipment is a generalizing parameter characterizing the performance of electric submersible pumps.

3. The proposed method for assessing the inter-repair period of operation of electric submersible pump units is practical and can be used in engineering tasks related to the analysis of the reliability of technical equipment.

References

[1] Lea, J. F., Rowlan, L. (2019). Electrical submersible pumps. Gas Well Deliquification, 237–308. doi: https://doi.org/10.1016/b978-0-12-815897-5.00012-3

[2] Stel, H., Sirino, T., Ponce, F. J., Chiva, S., Morales, R. E. M. (2015). Numerical investigation of the flow in a multistage electric submersible pump. Journal of Petroleum Science and Engineering, 136, 41–54. doi: https://doi.org/10.1016/j.petrol.2015.10.038

[3] Delou, P. de A., de Azevedo, J. P. A., Krishnamoorthy, D., de Souza, M. B., Secchi, A. R. (2019). Model Predictive Control with Adaptive Strategy Applied to an Electric Submersible Pump in a Subsea Environment. IFAC-PapersOnLine, 52 (1), 784–789. doi: https://doi.org/10.1016/j.ifacol.2019.06.157

[4] E Ofuchi, E. M., Stel, H., Vieira, T. S., Ponce, F. J., Chiva, S., Morales, R. E. M. (2017). Study of the effect of viscosity on the head and flow rate degradation in different multistage electric submersible pumps using dimensional analysis. Journal of Petroleum Science and Engineering, 156, 442–450. doi: https://doi.org/10.1016/j.petrol.2017.06.024

[5] Egidi, N., Maponi, P., Misici, L., Rubino, S. (2012). A three-dimensional model for the study of the cooling system of submersible electric pumps. Mathematics and Computers in Simulation, 82 (12), 2962–2970. doi: https://doi.org/10.1016/j.matcom.2012.05.014

[6] Gnedenko, B. V., Belaev, Yu. K., Solov'ev, A. D. (1965). Matemaicheskie metody v teorii nadezhnosti. Moscow: Nedra, 524.

[7] Babaev, S. G. (1987). Nadezhnost' neftepromyslovogo oborudovaniya. Moscow: Nedra, 264.

[8] Atnagumov, A. R., Ishemchuzhin, I. E. (2010). Prognozirovanie narabotki na otkaz elektrotsentrobezhnogo nasosa pered spuskom v skvazhinu i otsenka ego ostatochnogo resursa pri ekspluatatsii. Neftyanoe hozyaystvo, 6, 102–104.

[9] Gabibov, I. A., Abasova, S. M. (2012). Otsenka veroyatnosti bezotkaznoy raboty pogruzhnyh elektronasosov na osnove issledovaniya svoystv dostatochnoy statistiki. Uchenye zapiski Azerb. Gos. Morskoy Akademii, 2, 60–71.

[10] Kendall, M., Styuart, A. (1973). Statisticheskie vyvody i svyazi. Moscow: Nauka, 899.

[11] Kapur, K., Lamberson, L. (1980). Nadezhnost' i proektirovanie sistem. Moscow: Mir, 604.

[12] Ayvozyan, S. A., Enyukov, I. S., Meshalkin, L. D. (1983). Prikladnaya statistika: Osnovy modelirovaniya i pervichnaya obrabotka dannyh. Moscow: Finansy i statistika, 471.

[13] Kirvelis, R., Davies, D. R. (2003). Enthalpy Balance Model Leads to more Accurate Modelling of Heavy Oil Production with an Electric Submersible Pump. Chemical Engineering Research and Design, 81 (3), 342–351. doi: https://doi.org/10.1205/02638760360596892

RESEARCH OF MAGNETIC FIELD DISTRIBUTION IN THE WORKING AREA OF DISK SEPARATOR, TAKING INTO ACCOUNT AN INFLUENCE OF MATERIALS OF PERMANENT MAGNETS

Iryna Shvedchykova
Department of Energy management and Applied Electronics
Kyiv National University of Technologies and Design (KNUTD)
2 S. Nemyrovycha-Danchenka str., Kyiv, Ukraine, 01011
ishved@i.ua

Inna Melkonova[1]
inna.mia.lg@gmail.com

Julia Romanchenko[1]
romanchenkojulia321123@gmail.com

[1]*Department of Electrical Engineering*
Volodymyr Dahl East Ukrainian National University
59a S. Central ave., Severodonetsk, Ukraine, 93400

Abstract

Based on the results of a numerical-field analysis of the distribution of the magnetic force field in the working area of the disk magnetic separator, designed to clean bulk substances from ferromagnetic inclusions, the influence of the magnetic material of the poles of the magnetic system on the field distribution is determined. A consistent study of two magnetic systems assembled on the basis of magnetic materials of different classes is carried out. The finite element method implemented in the COMSOL Multiphysics software environment is used to calculate the distribution of magnetic induction in a disk magnetic separator with rare-earth and ferrite magnets. Due to the complexity of the spatial geometry of the force field in the working area of the disk magnetic separator, a three-dimensional model of the magnetic system is developed. A comparative analysis of the distribution of the magnetic force field in the working area of the disk separator with a highly coercive magnetic system and with a magnetic system based on ferrite blocks is carried out. As a result of the analysis, it is found that the indicators of the intensity and heterogeneity of the magnetic field for a highly coercive magnetic system significantly exceed the corresponding parameters of a ferrite magnetic system. It is proved that when choosing magnets for the magnetic system of a disk separator, preference should be given to highly coercive alloys, the magnetic properties of which significantly exceed the magnetic properties of ferrite magnets. To reduce the cost of the magnetic system of the disk separator, the use of a combined magnetic system assembled from magnetic materials of different classes is proposed. Studies of combined magnetic systems with various mass fractions of magnetic materials are done. The ratio of the mass fractions of magnets of various properties in the poles of the magnetic system is determined, at which sufficiently high magnetic characteristics are provided in the working area. It is shown that the presence of a ferrite fraction in the magnetic poles not only reduces the cost of the magnetic system of the separator, but also reduces the mass of the system. The tasks of further research are justified.

Keywords: disk separator, magnetic induction, permanent magnet, combined magnets, ferromagnetic inclusions.

1. Introduction

The widespread use of magnetic separators for cleaning bulk materials from ferromagnetic inclusions, primarily in the food and related industries, actualizes the task of increasing their efficiency, which is understood to ensure maximum reliability of removal. One of the ways to increase the efficiency of devices for magnetic separation is the use of permanent magnets [1–4]. To improve the quality of purification of raw materials and finished products from magnetic impurities, the permanent magnets of the separators must have high magnetic properties and stable magnetic parameters. Moreover, the layout of magnetic systems, including using various types of magnetic materials, to ensure the necessary distribution of the magnetic force field in the working area of the device.

Permanent magnets, in particular ceramic magnets based on barium or strontium ferrites, have been used in magnetic separators for many years to clean bulk substances from ferromagnetic impurities. Practical experience in operating magnetic systems of separators [5, 6] has shown that the widespread use of ferrite magnets is due to their relatively low cost, high stability of magnetic properties and corrosion resistance. Thus, the work [5] summarizes the experience of using ferrite magnetic systems of permanent magnet separators in the food, pharmaceutical, animal feed and other related industries for the purification of bulk substances from ferromagnetic inclusions. It has been shown that with sufficiently long-term use of such systems (about 30 years), the decrease in magnetic induction does not exceed 4 %. When developing magnetic systems for pulley separators, as shown in [6], it is advisable to use ferrite permanent magnets due to their relatively low cost.

In recent years, the construction of magnetic systems for separators has found application of highly coercive rare-earth permanent magnets based on a neodymium-iron-boron (Nd-Fe-B) alloy. Permanent magnets of this alloy are characterized by a sufficiently high residual magnetic induction B_r (up to B_r=1.44 T), temperature stability (up to 150 °C), have a small volume per unit of energy.

The disadvantages of magnets include the low operating temperature of some brands, as well as low corrosion resistance, which is eliminated by coating the surface of the magnets with protective layers of copper, zinc, nickel, chromium [7].

Today, Nd-Fe-B-based magnets have no analogues in magnitude of magnetic induction and its stability over time. It is advisable to use magnetic systems of separators with irreplaceable magnets where it is necessary to improve the quality of cleaning with the minimum dimensions of the separator. So, in [2], the prospects of using magnetic systems based on neodymium magnets for the purification of bulk substances from weakly magnetic impurities at food industry enterprises are justified. In [8], a method is presented for separating small metallic non-ferrous particles from two-component metallic non-ferrous mixtures using a new type of permanent magnet separator. It is also promising to use Nd-Fe-B alloy magnets in magnetic systems for high-gradient separation [9, 10], in particular in biomedicine, for targeted delivery and localization of magnetic nanoparticles in a given area of a biological object [11, 12].

When constructing magnetic systems of separators based on permanent magnets, a combination of various types of magnetic materials is also used. According to the results of experimental studies in [13], combined layout solutions of magnetic systems of drum-type separators are proposed, which provide for the use of both ferrite and rare-earth permanent magnets. Ferrite magnet blocks are recommended for magnetizing the extreme rows of Nd-Fe-B alloy magnets and for improving the conditions of the east of ore material from the surface of the drum. Moreover, at a distance of 20 mm from the surface of the drum, the magnetic induction is 0.2 T, and its gradient is 5 T/m.

In [14], the characteristics of combined magnets are analyzed, which are assembled from different types of magnets and are considered as a new class of permanent magnets. It is shown that the properties of such magnets are determined by both magnetic properties and the volume content of their components, and by the assembly scheme. It is concluded that the theoretical and experimental studies of combined magnets are promising for the purpose of their practical application.

Thus, as the analysis of publications [1–14] shows, a reasonable choice of material of permanent magnets and layout solutions of magnetic systems is an important stage in the design of new types of magnetic separators. At the same time, the question of the effect of the material of the magnets on the distribution of the magnetic field in the working zones of the magnetically separating devices requires attention.

The aim of research is analysis of the distribution of the magnetic force field in the working area of the disk magnetic separator and determination of the effect of the magnetic material of the poles of the magnetic system on this distribution.

To achieve this aim it is necessary:

1) to conduct a comparative analysis of the distribution of the magnetic force field in the working area of the disk separator for various types of magnetic materials of the poles of the magnetic system;

2) to substantiate the feasibility of using combined permanent magnets in the construction of the magnetic system of the disk separator.

2. Materials and methods

To clean bulk materials transported by belt conveyors from unwanted ferromagnetic impurities, a new design of a disk magnetic separator is designed, shown in **Fig. 1**. On the surface of the stationary ferromagnetic disk 1 there are permanent magnets 2 located in a spiral at the same distance from each other with alternating polarity of the poles, both in the direction of deployment of the spiral and in the radial direction. In the presence of a non-magnetic rotating discharge disk (not shown in **Fig. 1**), this configuration of the magnetic system ensures its self-cleaning.
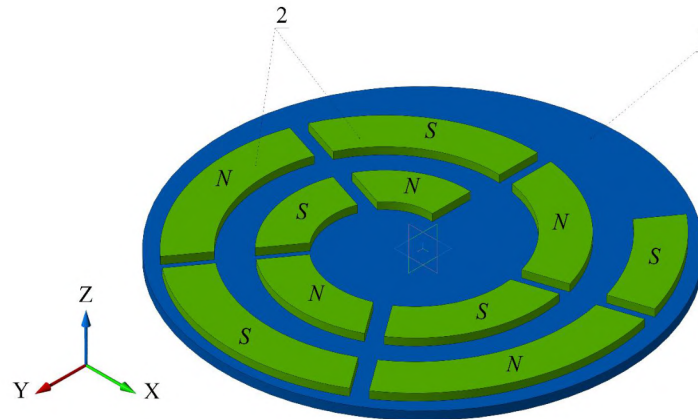

Fig. 1. The magnetic system of the disk separator: 1 – ferromagnetic disk; 2 – permanent magnets

In [15], the results of previous studies of the influence of the spiral geometry of the magnetic system (**Fig. 1**) on the distribution of the magnetic field in the working region of the separator are presented. An analysis of the spatial distribution of the magnetic field induction in the working area of the magnetic separator, presented in [15], shows that a sufficiently strong magnetic field (B_{max}=0.6...0.65 T) is formed in the working volume of the separator on the surface of the magnets, sufficient for extraction of ferromagnetic inclusions. Studies on the effect of magnetic materials and their layouts on the distribution of the magnetic force field are not conducted.

The magnetic field in a system with permanent magnets in the absence of electric current is described by the Maxwell system of equations, which in the magnetostatic approximation takes the form

$$\nabla \times \mathbf{H} = 0,$$

$$\nabla \cdot \mathbf{B} = 0, \tag{1}$$

where $\mathbf{H}$ – the magnetic field vector; $\mathbf{B}$ – the magnetic induction vector.

Equations for permanent magnets has the form

$$\mathbf{B} = \mu_0 \mu_r \mathbf{H} + \mathbf{B_r}, \tag{2}$$

where μ_r, $\mathbf{B}_r$ – the relative value of the magnetic permeability and residual induction of the permanent magnet material, respectively.

The equation of magnetic state for a ferromagnetic disk (pos. 1, **Fig. 1**) and the environment (air) can be written as

$$\mathbf{B} = \mu_0 \mu_r \mathbf{H}, \tag{3}$$

where μ_r – the relative value of the magnetic permeability for the ferromagnetic disk (μ_r=1000) and air (μ_r=1), respectively.

89

Based on expressions (2)–(4), a differential equation can be obtained for calculating the vector magnetic potential A $\left(\mathbf{B}=\nabla\times\mathbf{A}\right)$

$$\nabla(\mu_0\mu_r\nabla A - B_r) = 0. \tag{4}$$

Due to the complexity of the spatial geometry of the force field distribution in the working area of the disk magnetic separator, differential equation (4) is solved using the numerical finite element method in the COMSOL Multiphysics 3.5a 2008 software package.

To solve the first task of conducting a comparative analysis of the distribution of the magnetic force field in the working area of the disk separator using various types of magnetic materials, a computational experiment is conducted. A three-dimensional geometric model of the device's magnetic system with a finite element grid applied to it is shown in **Fig. 2, *a***. When constructing the finite element model, an arbitrary tetrahedral grid is selected. The number of grid points is 18191, the number of elements is 102,663, and the number of boundary elements is 10922, respectively. As the boundary conditions at the external borders of the computational domain, the magnetic isolation condition $A=0$ is used (**Fig. 2, *b***). At the same time, the continuity condition $A_1 - A_2 = 0$ is set at the internal boundaries, which is the standard setting of the boundary conditions in the COMSOL Multiphysics software environment.
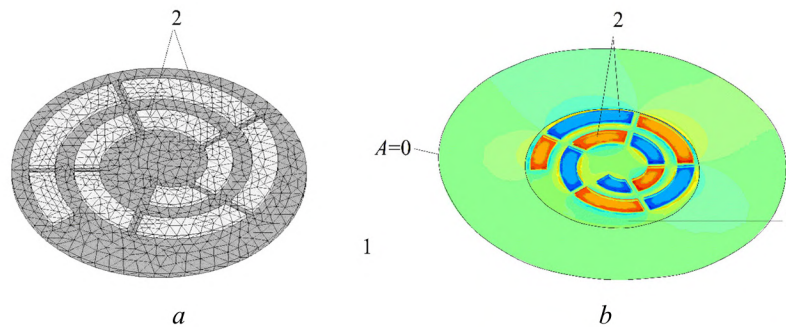

Fig. 2. Three-dimensional geometric model of the magnetic system
(1 – ferromagnetic disk, 2 – permanent magnets): *a* – with a applied grid from finite elements;
b – indicating the boundary conditions of the computational domain

In the study, the vertical component of the magnetization of the permanent magnets is directed along the Z axis (**Fig. 1**). The properties of the permanent magnets are set using equation (2) in the Subdomain Setting module of the COMSOL Multiphysics software environment. This equation makes it possible to better take into account the effects of demagnetization under the action of an external field directed against the vector of the current magnetization.

For ferromagnetic disk 1 (**Fig. 1**), made of soft magnetic structural steel, the assumption is made that the relative magnetic permeability μ_r of the disk material is constant (μ_r=1000). The design parameters of the magnetic system of the separator, taken as the base, are (**Fig. 3**): δ=25 mm, a=67.6 mm, b=51.7 mm, t=12.5 mm. The dimensions of the ferromagnetic disk 1 (**Fig. 1**), on which the permanent magnets are placed, are taken as follows: the disk diameter is 700 mm, and the thickness is 15 mm.
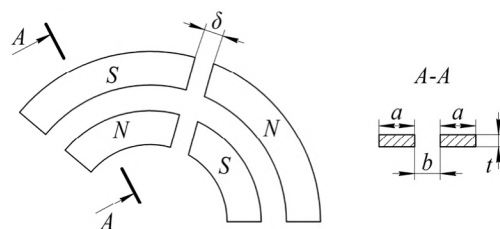

Fig. 3. Design parameters of the magnetic system of the separator

90

The influence of the magnetic material of permanent magnets on the distribution of magnetic induction B is studied in an arbitrarily selected air gap of the magnetic system of the separator for characteristic points 1 (or 3) and 2 (**Fig. 4**) along the vertical Z axis at a distance from the surface of the magnets up to 60 mm. It should be noted that for points 1 and 3, symmetrically located relative to the Z axis, the nature of the distribution of the magnetic field is identical.
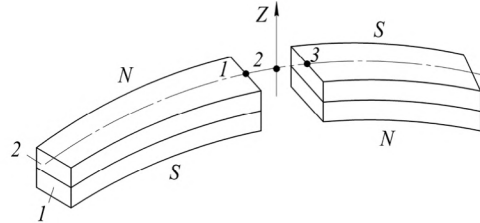

Fig. 4. The location of the characteristic points in the study area:
1 – ferrite magnets; 2 – magnets based on Nd-Fe-B alloy

In the research, it is assumed that the effect of the material is the same for any air gap of the magnetic system located both inside the disk and on its periphery.

3. Research results of the influence of the material of permanent magnets on the magnetic field distribution

At the first stage, two magnetic systems assembled on the basis of magnetic materials of different classes are sequentially investigated. For the first magnetic system, magnets based on barium ferrite Fe-Ba are chosen (relative magnetic permeability $\mu_r=1$, residual magnetic induction $B_r=0.4$ T, layer 2 in **Fig. 3** is absent), for the second – permanent magnets based on highly coercive Nd-Fe-B neodymium-iron-boron alloy (relative magnetic permeability $\mu_r=1.06$, residual magnetic induction $B_r=1.2$ T, layer 1 in **Fig. 4** is absent). The results of calculating the vertical component of magnetic induction B (along the vertical axis Z) for characteristic points 1 and 2 (**Fig. 4**) are presented in **Fig. 5**.
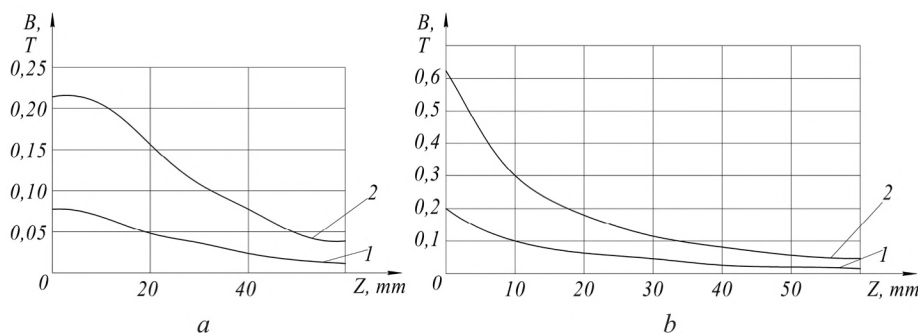

Fig. 5. The distribution of magnetic induction along the vertical Z axis (when constructing a magnetic system based on: 1 – barium ferrite, 2 – based on the Nd-Fe-B alloy):
a – for characteristic point 2; b – for characteristic point 1

To assess the heterogeneity degree of the magnetic field, the modulus of the magnetic induction gradient is $|\mathrm{grad}B|_i$ at i-th points ($i=2, \ldots, n, n=6$). Calculation of $|\mathrm{grad}B|_i$ is carried out at three points according to the formula

$$|\mathrm{grad}B|_i = \left|\left(B_{i+1} - B_{i-1}\right)/\left(2\nabla Z\right)\right|, \tag{5}$$

where ΔZ – the distance between the points where the magnetic induction is determined ($\Delta Z=10$ mm).

Magnetic induction gradient modulus calculation results $|\mathrm{grad}B|_i$ for characteristic point 2 (**Fig. 3**) are given in **Table 1**.

As can be seen from **Fig. 4**, the magnetic system based on the Nd-Fe-B alloy creates a magnetic field that is 2.75...4 times higher than the magnetic field intensity from ferrite magnets. Higher induction gradient $|\mathrm{grad}B|_i$ values should also be indicated in the working area of the magnetic system. For characteristic point 2, the gradient of magnetic induction $|\mathrm{grad}B|_i$ for poles based on Nd-Fe-B alloy exceeds, on average, 2 ... 4.3 times the corresponding indicator for ferrite magnets. These results are in good agreement with the results of studies obtained by other authors [2].

Table 1
$|\mathrm{grad}B|_i$ calculation results for characteristic point 2

Z, mm	Number of the point i	Nd-Fe-B alloy magnets		Barium ferrite magnets	
		B, T	$|\mathrm{grad}B|_i$, T/m	B, T	$|\mathrm{grad}B|_i$, T/m
0	1	0.220		0.080	
10	2	0.210	3	0.070	1.5
20	3	0.160	5	0.051	1.6
30	4	0.110	4	0.038	1.25
40	5	0.080	3	0.025	1.15
50	6	0.050	3	0.015	0.7
60	7	0.040		0.011	

Thus, when choosing magnets for the magnetic system of a disk separator, preference should be given to the Nd-Fe-B alloy, the magnetic properties of which significantly exceed the magnetic properties of ferrite magnets.

At the next stage, the magnetic systems of a separator of a combined type, built on the basis of magnets of different classes (combined magnets), are investigated. The layers of magnetic materials at the poles of the magnetic system are arranged as shown in **Fig. 3**: ferrite magnets are adjacent to the surface of the magnetic disk (**Fig. 1**) (layer 1 in **Fig. 2**), and the upper layer of the poles contains a highly coercive Nd-Fe-B alloy (layer 2 in **Fig. 2**). With this alternation of layers of magnetic materials, a certain magnetization of the upper layer of magnets from the Nd-Fe-B alloy occurs.

Magnetic induction is determined for characteristic points 1 and 2 (**Fig. 3**) along the vertical Z axis at a distance from the surface of the magnets to 60 mm, starting with a fraction of ferrite magnets of 50 % in each individual pole of the magnetic system. After that, the proportion of ferrite magnets gradually decreases, while the magnitude of the magnetic induction in the working gap of the combined magnet approaches the corresponding parameters of the magnetic system assembled entirely on the basis of the Nd-Fe-B alloy.

The results of calculating the magnetic induction B along the vertical Z axis for combined magnets compared to magnets based on the Nd-Fe-B alloy for point 1 are given in **Table 2**, and for point 2 – in **Table 3**, respectively.

As the **Tables 2, 3** show, the intensity of the magnetic field in the working zone of the separator depends on the proportion of ferrite magnets in the total mass of the combined magnetic system. So, with a ferrite magnet fraction of 50 %, magnetic induction in the corner zone on the surface of a permanent magnet (point 1 or 3 in **Fig. 3**) is even equal to the magnetic induction that the city has when using highly coercive blocks of magnets, and amounts to 0.62 T. At the same time, at a distance from the surface of the poles magnetic induction is significantly reduced.

With a proportion of ferrite magnets in the total mass of 25 %, combined magnets are inferior to Nd-Fe-B magnets at distances up to 40 mm. At the same time, at large distances (50 and 60 mm), such arrangements create the same magnesium field as Nd-Fe-B magnets. When the proportion of ferrite magnets in the total mass of the magnetic field is about 18–20 %, the magnetic

92

induction in the working area of the magnetic system with combined magnets approaches the values of magnetic induction in the Nd-Fe-B magnetic system.

Table 2

The results of calculating the magnetic induction B of the combined magnets compared to magnets based on the Nd-Fe-B alloy for point 1

Z, mm	Magnetic induction B, T			
	Nd-Fe-B alloy magnets	Combined magnets with a share of ferrite magnets in the total mass of the magnetic field, %		
		50	25	18
0	0.620	0.620	0.620	0.620
10	0.300	0.200	0.240	0.300
20	0.180	0.120	0.150	0.160
30	0.110	0.080	0.100	0.100
40	0.080	0.050	0.070	0.065
50	0.050	0.030	0.050	0.050
60	0.040	0.020	0.040	0.040

Table 3

The results of calculating the magnetic induction B of the combined magnets compared to magnets based on the Nd-Fe-B alloy for point 2

Z, mm	Magnetic induction B, T			
	Nd-Fe-B alloy magnets	Combined magnets with a share of ferrite magnets in the total mass of the magnetic field, %		
		50	25	18
0	0.220	0.160	0.210	0.220
10	0.210	0.150	0.200	0.210
20	0.160	0.110	0.150	0.150
30	0.110	0.080	0.100	0.100
40	0.080	0.050	0.070	0.070
50	0.050	0.030	0.050	0.050
60	0.040	0.020	0.040	0.040

Thus, the research results show that when constructing magnetic systems for disk separators, it is advisable to use combined magnets with such a fraction of the ferrite component in the total mass of poles of the magnetic system that does not exceed 20 %. Using this arrangement will also result in:

– to reduce the mass of the magnetic system of the separator by 10 % (the calculated mass value for the magnetic system based on Nd-Fe-B is 14.72 kg, and for the combined magnetic system – 13.25 kg, respectively);

– to reduce the cost of the magnetic system of the separator by 25 % (the estimated cost of the magnetic system based on Nd-Fe-B is 880 USD, and the combined magnetic system – 660 USD, respectively).

4. Discussion of research results

A comparative analysis of the distribution of the magnetic force field in the working area of the newly designed disk separator makes it possible to quantitatively evaluate the ad-

vantages of a highly coercive magnetic system over a magnetic system based on ferrite blocks. The main indicators characterizing the efficiency of the magnetic separator, that is, its ability to reliably remove and retain ferromagnetic inclusions, are indicators of the intensity and heterogeneity of the magnetic field in the working area. As calculations show, these indicators for a highly coercive magnetic system significantly exceed the corresponding parameters of a ferrite magnetic system.

In recent years, there has been a downward trend in the cost of rare earth magnets. However, the cost of ferrite magnets still remains significantly less than the cost of magnets based on a neodymium-iron-boron alloy. Therefore, to reduce the cost of the magnetic system of the disk separator, it is proposed to use a combined magnetic system assembled from magnetic materials of different classes. At the same time, it is important to select such a ratio of mass fractions of magnets of various properties in the poles of the magnetic system, at which sufficiently high magnetic characteristics are provided in the working area. In the research process, such a ratio is found. The presence of a ferrite fraction in the magnetic poles not only reduces the cost of a quarter of the magnetic system of the separator, but also reduces the mass of the system.

It should be noted that ferrite magnets of complex shape are not produced due to the difficulties of their manufacture. Therefore, certain difficulties may arise in the manufacture of ferrite poles of sector-like shape adopted in a disk separator. To justify the feasibility of using simpler forms of magnetic poles, for example, prismatic, additional studies of the distribution of the magnetic field in the working area of the magnetic separator are necessary.

5. Conclusions

When choosing magnets to build the magnetic system of a disk separator, preference should be given to the Nd-Fe-B alloy, the magnetic properties of which significantly exceed the magnetic properties of ferrite magnets. So, the magnetic system of a disk separator based on the Nd-Fe-B alloy creates a magnetic field that is 2.75...4 times higher than the magnetic field intensity from ferrite magnets. The magnetic induction gradient for a system based on the Nd-Fe-B alloy exceeds, on average, 2...4.3 times the corresponding indicator for ferrite magnets.

To reduce the cost of the design of the disk magnetic separator, it is advisable to use combined magnets with a fraction of the ferrite component in the total mass of the poles of the magnetic system not higher than 20 %. This arrangement of magnetic materials will lead to a decrease in the mass of the magnetic system of the separator by 10 % and to a decrease in its cost by 25 %.

References

[1] Li, Y., Yang, F. (2016). Research Progress and Development Trend of Permanent Magnetic Separators in China and Abroad. DEStech Transactions on Engineering and Technology Research. doi: https://doi.org/10.12783/dtetr/icvme2016/4873

[2] Slusarek, B., Zakrzewski, K. (2012). Magnetic properties of permanent magnets for magnetic sensors working in wide range of temperature. Przeglad elektrotechniczny, 88 (7), 123–126.

[3] Dimova, T., Aprahamian, B., Marinova, M. (2019). Research of the Magnetic Field Inside a Drum Separator With Permanent Magnets. 2019 16th Conference on Electrical Machines, Drives and Power Systems (ELMA). doi: https://doi.org/10.1109/elma.2019.8771679

[4] Hisayoshi, K., Uyeda, C., Terada, K. (2016). Magnetic separation of general solid particles realised by a permanent magnet. Scientific Reports, 6 (1). doi: https://doi.org/10.1038/srep38431

[5] Meshcheryakov, I. (2018). Spetsifika vybora magnitnyh materialov dlya magnitnyh separatorov. Kombikorma, 2, 22–24.

[6] Sayko, O. P., Drobchenko, V. I., Kofanov, A. S., Podolyuh, S. M. (2012). Shkivnye zhelezootdeliteli na postoyannyh magnitah. Ugol' Ukrainy, 7, 43–45.

[7] Romanyshyn, T. L. (2013). Obgruntuvannia vyboru materialu postiynykh mahnitiv dlia lovylnykh prystroiv. Rozvidka ta rozrobka naftovykh i hazovykh rodovyshch, 1 (46), 143–152.

[8] Lungu, M. (2009). Separation of small nonferrous particles using a two successive steps eddy-current separator with permanent magnets. International Journal of Mineral Processing, 93 (2), 172–178. doi: https://doi.org/10.1016/j.minpro.2009.07.012

[9] Zeng, S., Zeng, W., Ren, L., An, D., Li, H. (2015). Development of a high gradient permanent magnetic separator (HGPMS). Minerals Engineering, 71, 21–26. doi: https://doi.org/10.1016/j.mineng.2014.10.009

[10] Gómez-Pastora, J., Xue, X., Karampelas, I. H., Bringas, E., Furlani, E. P., Ortiz, I. (2017). Analysis of separators for magnetic beads recovery: From large systems to multifunctional microdevices. Separation and Purification Technology, 172, 16–31. doi: https://doi.org/10.1016/j.seppur.2016.07.050

[11] Karlov, A., Kondratenko, I., Kryshchuk, R., Rashchepkin, A. (2014). Magnetic system with permanent magnets for localization magnetic nanoparticles in a given region of the biological environments. Elektromekhanichni i enerhozberihaiuchi systemy, 4, 79−85.

[12] Chen, H., Bockenfeld, D., Rempfer, D., Kaminski, M. D., Liu, X., Rosengart, A. J. (2008). Preliminary 3-D analysis of a high gradient magnetic separator for biomedical applications. Journal of Magnetism and Magnetic Materials, 320 (3-4), 279–284. doi: https://doi.org/10.1016/j.jmmm.2007.06.001

[13] Myazin, V., Kilin, V., Yakubaylik, E. (2010). Perfection of methods and technology of highly magnetic iron ore concentration in connection with the innovations of the last years (by the example of the Siberian region). Vestnik ChitGU, 6 (63), 95–101.

[14] Kravchenko, A. Y., Bovda, A. M. (2003). Combined permanent magnets: expansion of permanent magnets classification. Elektrotekhnika i Elektromekhanika, 3, 37–39.

[15] Gerlici, J., Shvedchikova, I. A., Nikitchenko, I. V., Romanchenko, J. A. (2017). Investigation of influence of separator magnetic system configuration with permanent magnets on magnetic field distribution in working area. Electrical Electrical Engineering & Electromechanics, 2, 13–17. doi: https://doi.org/10.20998/2074-272x.2017.2.02

SYNTHESIS AND CHARACTERIZATION OF GREENER CERAMIC MATERIALS WITH LOWER THERMAL CONDUCTIVITY USING OLIVE MILL SOLID BYPRODUCT

Xenofon Spiliotis[1]

Vayos Karayannis
Department of Chemical Engineering
University of Western Macedonia
3 Ikaron str., Kozani, Greece, 50100
vkarayan62@gmail.com

Stylianos Lamprakopoulos[1]

Konstantinos Ntampegliotis[1]

George Papapolymerou[1]

[1]*Department of Environment*
University of Thessaly
Gaiopolis Campus, Larissa, Greece, 41110

Abstract

In the current research, the valorization of olive mill solid waste as beneficial admixture into clay bodies for developing greener ceramic materials with lower thermal conductivity, thus with increased thermal insulation capacity towards energy savings, is investigated. Various clay/waste mixtures were prepared. The raw material mixtures were characterized and subjected to thermal gravimetric analysis, in order to optimize the mineral composition and maintain calcium and magnesium oxides content to a minimum. Test specimens were formed employing extrusion and then sintering procedure at different peak temperatures. Apparent density, water absorption capability, mechanical strength, porosity and thermal conductivity were determined on sintered specimens and examined in relation to the waste percentage and sintering temperature. The experimental results showed that ceramic production from clay/olive-mill solid waste mixtures is feasible. In fact, the mechanical properties are not significantly impacted with the incorporation of the waste in the ceramic body. However, the thermal conductivity decreases significantly, which can be of particular interest for thermal insulating materials development. Furthermore, the shape of the produced ceramics does not appear to change with the sintering temperature increase.

Keywords: ceramics, green materials, circular economy, olive mill solid waste, porosity, thermal conductivity, thermal insulation.

1. Introduction

Innovative technologies that incorporate different forms of biomass and other alternative solid products (produced from various waste treatments) into red ceramics seem to develop rapidly at a global level. Actually, biomass energy potential is addressed to be the most promising among the renewable energy sources, due to its spread and availability worldwide [1–3]. The interesting points in these technologies are that they:

a) can act as an efficient disposal method;
b) exploit the biomass energy content into clay bodies for fuel savings;
c) use of materials with organic matter as pore-forming agents [4, 5].

Olive-mill solid waste is the main waste produced during the process of olive-pomace oil production. Particularly in Greece, approximately 250,000 tons of (olive stone wooden residue (OSWR) are produced annually [6, 7]. OSWR is mainly used as alternative fuel due to its high calorific value (18,828–20,577 MJ/Kg) [8, 9].

96

Introduction of olive-mill solid residue into clay-based ceramics can be considered as a promising alternative solution for the valorization of this solid residue. Effluent olive-mill waste-water sludge was already embedded into fired laboratory produced clay bricks by Hamza et al. [10]. Moreover, Cotes Palomino et al. [11, 12] have studied the influence of the amount of wet pomace (containing water, olive stone and pulp residue) into ceramics materials for optimization of their technological properties in order to meet the standards for use as structural construction bricks. Actually, the addition of olive-mill solid residue as a pore-forming agent into ceramic brick clays must be carefully controlled. High % addition into the ceramic body will liberate heat at an excessive rate and localized heating may cause defects in the products [13].

The aim of the present research is to provide broader insight into ceramic microstructures elaborated starting from standard industrial ceramic clays and OSWR powder, in the context of circular economy towards sustainable development. Emphasis is placed on the development of greener ceramic materials with lower thermal conductivity, thus focusing on the potential for improved thermal insulation capabilities with the beneficial utilization of this solid residue as admixture into ceramics. Particularly, the decomposition of OSWR in the ceramic body upon sintering is expected to influence the porosity and consequently the thermal conductivity of the produced ceramic material.

2. Materials and methods
2. 1. Raw Materials
2. 1. 1. Chemical Analysis
The 'Viokeral' clay mixture used in the present study is a blending at certain proportions of three clays collected from various locations of Central Greece and provided by "TERRA S.A.". **Table 1** contains chemical analysis results of these clays.

Table 1
Chemical analysis of clays*

PARAMETER	CONSTITUENT CLAY (%)		
	A	B	C
L.O.I.**	11.95	9.87	16.54
SiO_2	49.40	52.79	51.02
Al_2O_3	12.89	13.53	8.55
Fe_2O_3	7.10	7.57	4.66
CaO	8.58	6.29	11.62
MgO	4.86	4.31	3.89
K_2O	2.88	3.19	1.55
Na_2O	1.56	1.57	1.42
TiO_2	0.818	0.855	0.621
$CaCO_3$ (eq)	14.72	–	24.46
CO_2	6.47	–	10.75

Note: * – source: TERRA S. A.; ** – L.O.I.=Loss on Ignition

OSWR is the main residue of olive-pomace oil production processes. The OSWR used in the present study was obtained from a local olive press treatment plant after dewatering. **Table 2** presents physicochemical analysis results for this OSWR while **Table 3** shows a typical physicochemical analysis of OSWR.

97

Table 2

Physicochemical Analysis of OSWR*

Physical characteristics	
Net Calorific Value	17,818 MJ/kg
Gross Calorific Value	19,269 MJ/kg
Chemical characteristics	
Carbon	48.68 % w/w
Hydrogen	6.84 % w/w

*Note: * – source: TERRA S.A.*

Table 3

Physicochemical Analysis of OSWR*

Physical characteristics	
Gross Calorific Value**	20,962 MJ/kg
Moisture	12.3 % w/w
Ash	1.9 % w/w
Combustibles***	85.8 % w/w
Chemical characteristics	
Carbon	48.59 % w/w
Hydrogen	5.73 % w/w
Oxygen	44.06 % w/w
Nitrogen	1.57 % w/w
Sulphur	0.05 %w/w

*Note: * – Source: 1) Laboratory of Applied Thermodynamics; 2) Process design Laboratory, Aristotle University of Thessaloniki; ** – Dry basis; *** – Wet basis*

An advantage of OSWR is that CO_2 emissions for this additive come from the biomass (free of calcium carbonate), which means that, regarding CO_2 emission trading, this is a way to reduce the assigned quantities of CO_2 and lower the carbon footprint, because biomass is weighed with a zero emission factor [14].

2. 1. 2. Thermal Analysis

Fig. 1 shows the thermal analysis results, specifically TGA/DTA curves (Setaram STA 1600), for the "Viokeral" clay mixture. In these curves, it is observed that up to 150 °C, release of hygroscopic water is taking place and the process is endothermic. From 155 °C to 425 °C, loss of molecular water takes place and the process is also endothermic. From 425 °C to 775 °C, several endothermic and exothermic peaks are noticed due to combined dehydroxylation of the silicate lattice, combustion of organic matter and decomposition reactions [15]. From 775 °C to 858 °C, the process is endothermic due to the dissociation of carbonates. According to these results, the "Viokeral" mixture does not belong to the Kaolinitic group, since the characteristic peak of the kaolinic clays at about 980 °C is absent. The mass loss upon clay sintering at 1105 °C reaches 11.9 % w/w, which may be attributed to the elimination of organic matter by combustion, the elimination of water due to dehydroxylation, and the decomposition of carbonates.

In **Fig. 2**, the TGA/DTA curves for the OSWR used are presented. In these curves, the following endothermic and exothermic regions are noticed:

1) Up to 152.7 °C: Dehydration (endothermic);

2) 152.7–438 °C: Combustion of organic matter – Dehydration (endothermic);

3) 438–575 °C: Combustion of organic matter (exothermic);

4) 575–649 °C: Combustion of organic matter (endothermic);

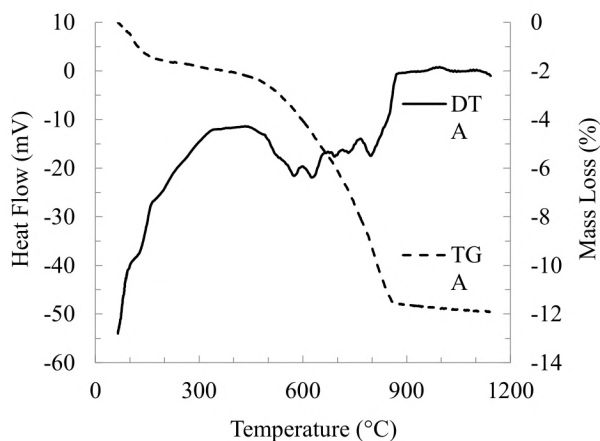5) 649–682.8 °C: Combustion of organic matter (strongly exothermic).

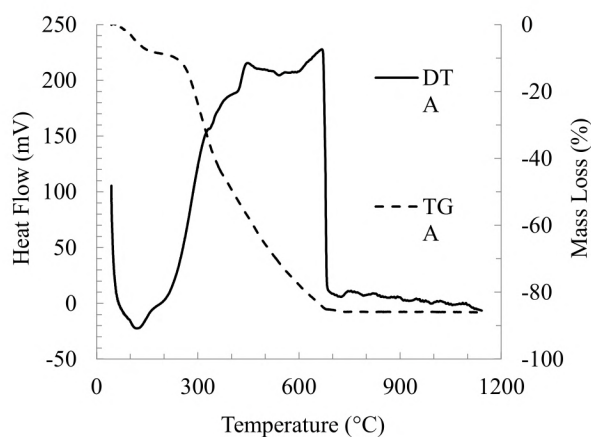**Fig. 1.** DTA/TGA curves for the "Viokeral" clay mixture

Fig. 2. TGA/DTA curves for OSWR

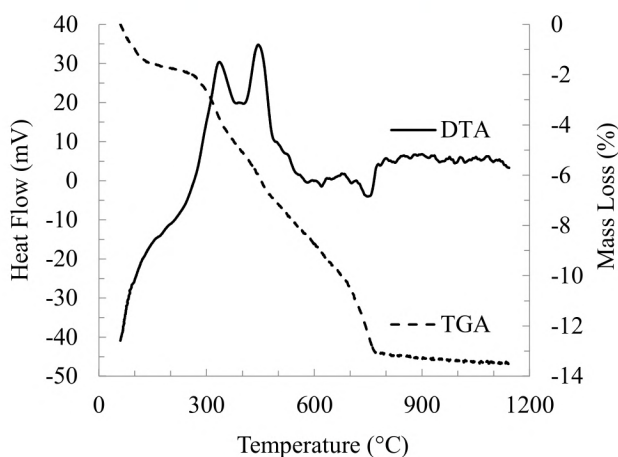In **Fig. 3,** the TGA/DTA curves for the "Viokeral"/6 %w/w OSWR mixture are provided.

Fig. 3. TGA/DTA curves for "Viokeral"/6 %w/w OSWR mixture

In these curves (**Fig. 3**), the following endothermic and exothermic regions are noticed:
1) Up to 110 °C: Dehydration (endothermic);
2) 110–322.27 °C: Loss of molecular water (endothermic);
3) 322.3–383.6 °C: Loss of molecular water – Combustion of organic matter (exo-thermic);

99

4) 383.6–434.3 °C: Loss of molecular water – Combustion of organic matter (endothermic);

5) 434.3–723.7 °C: Combustion of organic matter (exothermic);

6) 723.69–774 °C: Dissociation of carbonates (endothermic).

2. 2. Synthesis of ceramic specimens

Ceramic bodies were produced using each time 0, 3, 6 and 9 % w/w OSWR powder as an additive in the clay mixture. The various clay/OSWR mixtures were ground to particle size <1 mm. Then, they were kneaded with water and shaped into specimens using a laboratory pilot-plant vacuum extruder provided with manual cutter. The rectangular specimen cross section bars were 80×43.5×18 mm. Extruded test pieces were optically checked and weighed for moisture determination using a thermos-balance. Subsequently, the specimens were first dried at room temperature for 12 hours and then in an oven at 110 °C for at least 24 hours, until reaching a constant weight. Finally, the dried specimens were sintered in a programmable electric furnace following a protocol of gradual heating up to a peak temperature (850, 950, 1050 or 1150 °C).

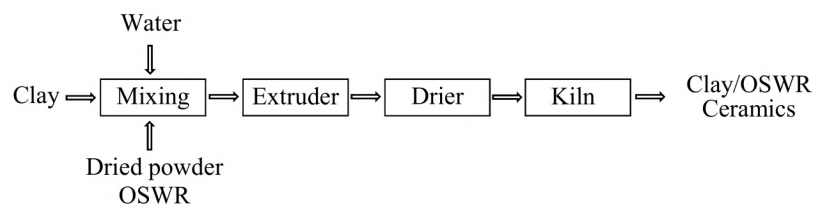A schematic diagram of the proposed method is shown in **Fig. 4.**

Fig. 4. Schematic diagram of the ceramic production process,
using OSWR powder as admixture

2. 3. Characterization of ceramic specimens

2. 3. 1. Water absorption capacity & open porosity

The specimens were immersed in water (25–30 °C) for 24 hours. Water absorption (WA) capacity and open porosity (OP) are obtained from the following equations:

$$WA\left(\%\right)=100\frac{W_{wet}-W_{dry}}{W_{dry}}, \qquad (1)$$

$$OP\left(\%\right)=100\frac{W_{wet}-W_{dry}}{\rho V_s}, \qquad (2)$$

where W_{wet} – weight of saturated with water samples (g); W_{dry} – weight of dry samples (g); ρ – density of water (1 g/cm³); V_s – volume of the samples (cm³).

2. 3. 2. Three-point bending strength (Modulus of Rupture)

Strength of sintered specimens was determined upon three-point bending using a Universal Testing Machine (UTM) type INSTRON MTS 3382, and the Modulus of Rupture (MOR) was calculated from the following equation [16]:

$$MOR\left(\text{MPa}\right)=\frac{3PL}{2bw^2}, \qquad (3)$$

where P – force (N); L – the opening width (36 mm); b – width of sample (mm); w – thickness of the sample (mm).

2. 3. 3. Thermal conductivity

Thermal conductivity coefficient (*k*) of sintered ceramics was measured at 25 °C by applying the guarded heat flow meter method using an Anter Unitherm Model 2022.

2. 3. 4. Scanning Electron Microscopy (SEM) characterization

SEM analysis of the ceramic specimens was conducted using a JEOL 6610LV microscope.

3. Results

3. 1. Mass loss on sintering and appearance color

Fig. 5 depicts the weight loss and the consequent change of the bulk density of the specimens, as a result of the sintering process.
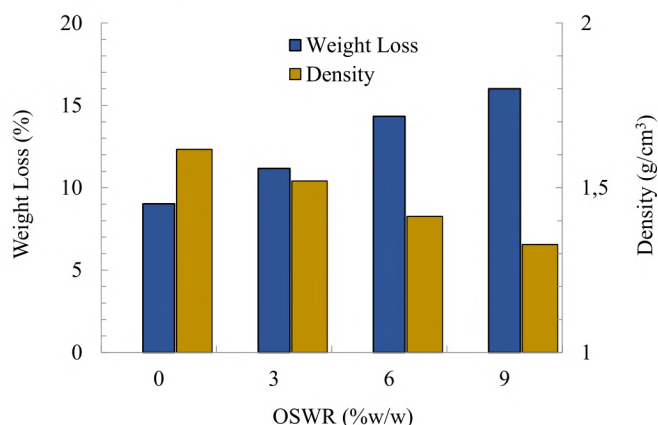
Fig. 5. Specimen weight loss and bulk density variation as a function of % OSWR content due to the sintering process (T_{sint}=950 °C)

3. 2. Water absorption capacity and open porosity

In **Fig. 6,** the influence of the OSWR proportion in the clay/OSWR mixtures on the water absorption (WA) capacity and open porosity (OP) is shown.
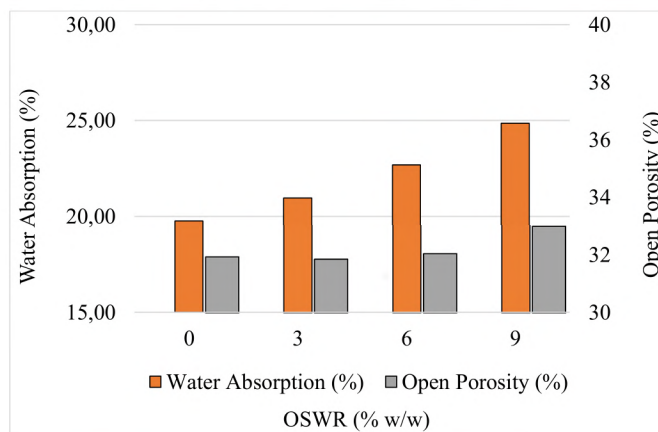
Fig. 6. Influence of the added OSWR percentage on Water Absorption (WA) and Open Porosity (OP) of sintered specimens (T_{sint}=950 °C)

3. 3. Mechanical Strength (Modulus of Rupture – MOR)

In **Fig. 7,** the dependence of mechanical strength calculated in terms of modulus of rupture (MOR) upon three-point bend testing of the specimens on the OSWR percentage in the clay/OSWR mixtures is presented.
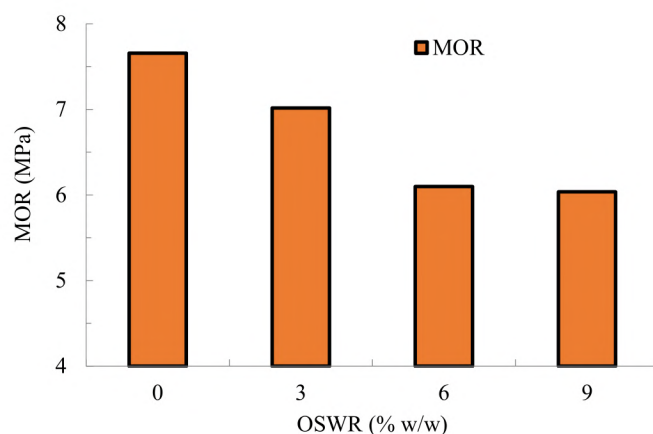
Fig. 7. Three-point bending strength (Modulus of Rupture – MOR) in relation to OSWR percentage in clay/OSWR mixtures, for sintered specimens (T_{sint}=950 °C)

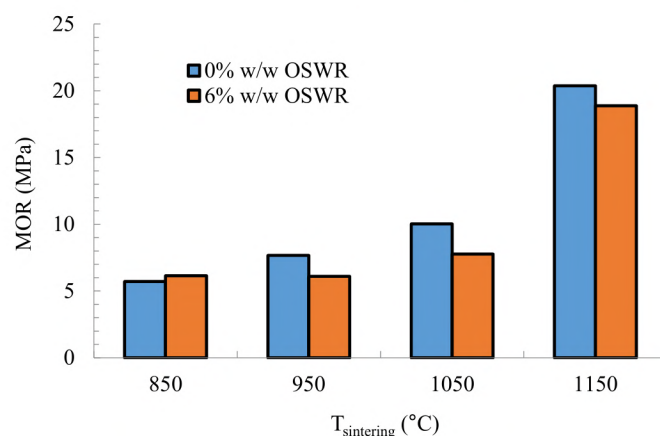In **Fig. 8,** the variation of MOR in relation to sintering temperature is shown.

Fig. 8. MOR in relation to sintering temperature (6 % w/w OSWR content)

3. 4. Thermal conductivity

In **Fig. 9** the change in thermal conductivity coefficient in relation to % w/w OSWR in the clay/OSWR mixture is presented.
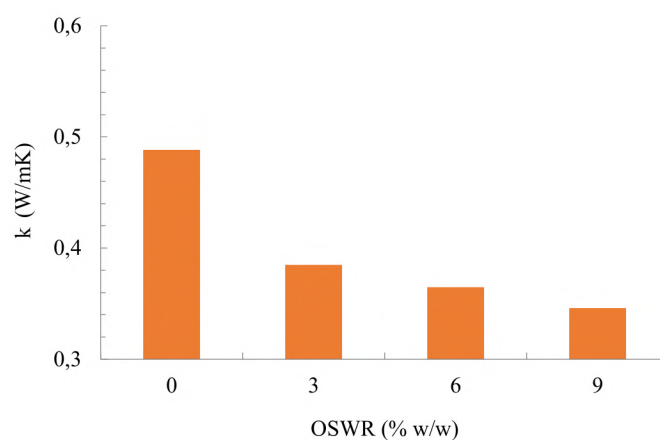

Fig. 9. Thermal conductivity coefficient (k) at 25 °C in relation to % OSWR addition, for sintered specimens (T_{sint}=950 °C)

102

Fig. 10 depicts the effect of sintering temperature on thermal conductivity.
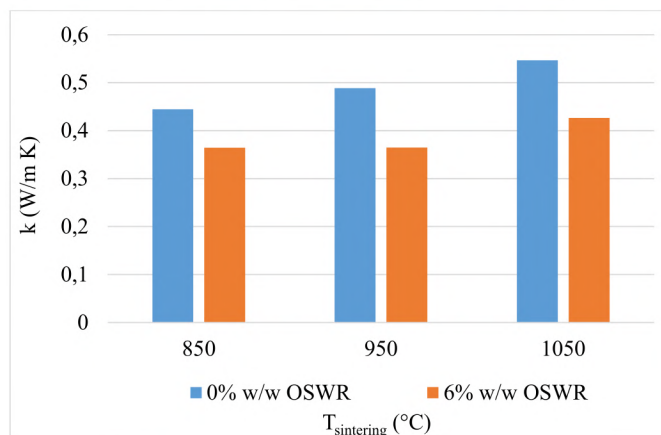

Fig. 10. Effect of sintering temperature on thermal conductivity coefficient (k) at 25 °C

3. 5. Microstructure

In **Fig. 11,** SEM micrographs of ceramic microstructures with 0–9 % w/w OSWR content, obtained at 950 °C, are presented. SEM micrographs of 6 % w/w OSWR content microstructures produced at 850–1,150 °C are given in **Fig. 12** to provide broader insight in the densification process.
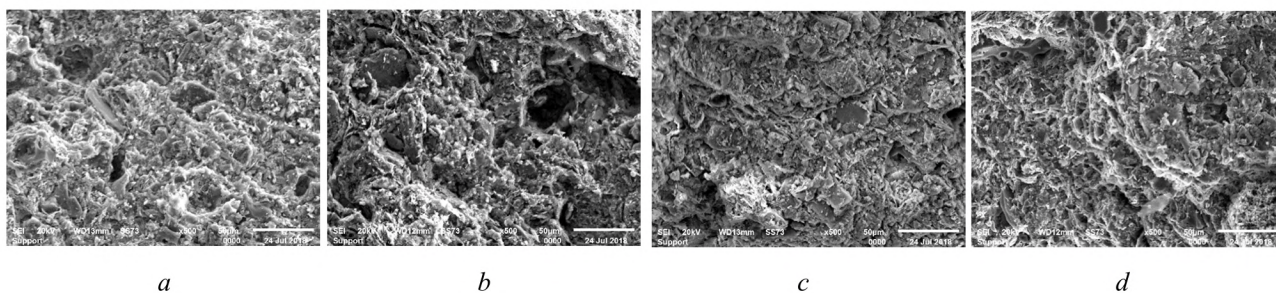

a   *b*   *c*   *d*

Fig. 11. Representative SEM micrographs of
ceramic microstructures obtained at 950 °C, incorporated with OSWR:
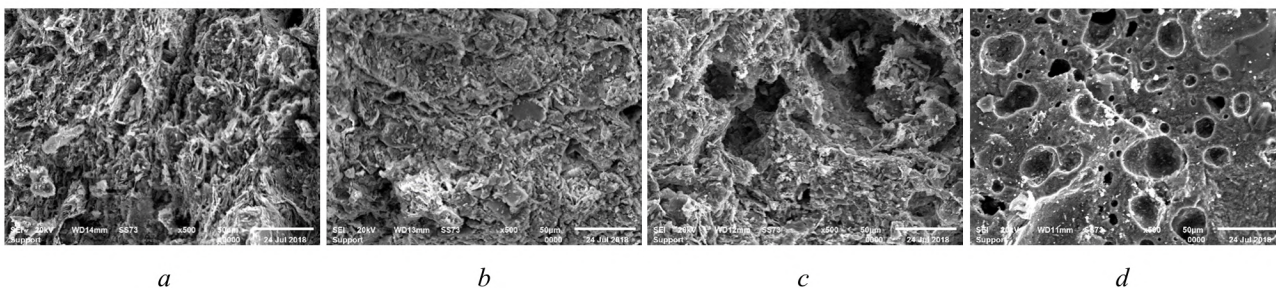*a* – 0 % w/w; *b* – 3 % w/w *c* – 6 % w/w; *d* – 9 % w/w

a   *b*   *c*   *d*

Fig. 12. Representative SEM micrographs of 6 % w/w OSWR
content ceramic microstructures obtained at:
a – 850 °C; *b* – 950 °C; *c* – 1050 °C; *d* – 1150 °C

In addition, photographs of real ceramic specimens, with OSWR (6 % w/w) and without OSWR (prototype) are provided in **Fig. 13**.
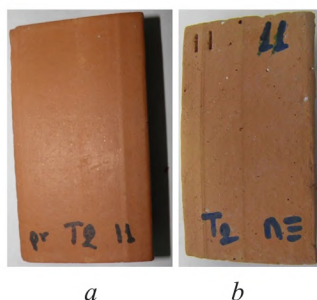
103

Fig. 13. Representative photographs of ceramic specimens obtained at 950 °C,
incorporated with OSWR: *a* – 0 % w/w (prototype); *b* – 6 % w/w

4. Discussion

The experimental results (**Fig. 5**) showed that the sintering process causes significant weight loss, without significant change of the volume of the specimens. This results in an almost linear depletion of density with OSWR content increase. Raising the sintering temperature (T_{sint}) from 850 °C up to 1050 °C does not affect either the outlook or the geometry of the specimens. At T_{sint}=1150 °C however, significant changes are observed: the color becomes dark brown, the texture vitreous and the samples almost waterproof (water absorption measurements confirm this observation), and also intense sample shrinkage occurs. Nevertheless, the specimen geometry is kept without any distortion, despite the large ratios of width/thickness (>2.3) and length/thickness (>4.3). The observed weight loss is attributed to the loss of the added OSWR. In particular, for clay/OSWR (6 % w/w) mixtures, the weight loss corresponds to more the 97 % of the OSWR mass (950 °C<T_{sint}<1050 °C) or more than 80 % of the OSWR mass (T_{sint}>1050 °C or T_{sint}<950 °C). The above observations confirm that OSWR can act as pore-forming agent. Moreover, increasing the OSWR content in the clay mixtures results in the weakening of the terracotta color of the specimens, which become paler.

Water absorption capacity (WA) and open porosity (OP) of the ceramic specimens obtained (**Fig. 6**) do not change significantly as far as the OSWR percentage in clay/OSWR mixture is up to 6 % w/w. A noteworthy increase in the parameters under study seems to occur for 9 % w/w OSWR use. It can, therefore, be assumed that, for clay/ OSWR mixtures with up to 6 % w/w OSWR content, formation of closed pores is possibly favored (significant weight loss but stable water absorption).

With regard to bending strength (**Fig. 7**), for OSWR up to 6 % w/w in the clay/OSWR mixture, the modulus of rupture (MOR) of the sintered specimens is reduced by approximately 20 % compared to those produced from clay (0 % w/w OSWR). This trend seems to decelerate significantly for OSWR percentages higher than 6 % w/w. Moreover, raising firing temperature from 850 °C to 950 °C (**Fig. 8**), the MOR remains stable. However, from 950 °C to 1050 °C, the MOR increases by approximately 27 %, while for sintering temperatures above 1050 °C, the MOR strongly increases (by approx. 140 % up to 1150 °C). For comparison, laboratory prepared samples of clay-bricks with us much as 6 % olive-mill wastewater sludge were also reported to successfully undergo mechanical and environmental tests [10]. Savings of raw materials into ceramic samples incorporated with wet pomace from olive oil industry are further referenced in the scientific literature, with the best results obtained for 3 wt % addition [11, 12].

In the present research, especially the reduction of thermal conductivity by approx. 20 % achieved for only 3 % w/w OSWR addition in the clay mixture (**Fig. 9**) should be underlined. Indeed, for more than 3 % w/w of OSWR, thermal conductivity is further decreased even to 30 % for 9 % w/w OSWR. This means that even small quantities of OSWR in the clay mixture lead to increased porosity thus improving considerably the heat transfer resistance of the ceramic material produced. For 6 % w/w OSWR in the clay mixture, ceramic specimen thermal conductivity is reduced (**Fig. 10**) by 18.1 % at T_{sint}=850 °C and by 25.3 % at T_{sint}=950 °C, while, at 1,050 °C, a more pronounced reduction in specimen thermal conductivity is observed. This means that the incorporation of the pore-making agent OSWR into ceramic bricks promotes the

insulating properties even at lower sintering temperatures and much more at higher temperatures. These findings can be of particular importance for the development of thermal insulating ceramic materials.

Beyond the beneficial effect of OSWR acting as pore-former in the bulk of the ceramic bodies, any possible impact on ceramics properties by using different sources and years of harvest of OSWR are rather considered negligible, given the limited residue percentages incorporated. In fact, the SEM examination of the specimens indicates a relatively limited effect of the incorporation of OSWR in the ceramic microstructures obtained, except of desirable increased porosity (**Fig. 11**). On the other hand, the microstructure becomes more compact by increasing the firing temperature from 850 °C to 1025 °C (**Fig. 12, *a–c***). Indeed, by further raising the sintering temperature up to 1150 °C (**Fig. 12, *d***) an extended diffusion involving viscous flow in the ceramic matrices produced is clearly shown, resulting in a certain decrease in porosity, thus, at least partially, explaining the above stated increase in modulus of rupture (MOR).

5. Conclusions

Adding OSWR (the main solid residue of olive-pomace oil production processes) into clay mixtures typically used by the ceramic industry for brick manufacturing does not hinder neither the extrusion, nor the drying and firing processes.

A decrease in the fired bulk density from approximately 1.62 g/cm^3 to 1.33 g/cm^3 is attained for an OSWR addition of 9 % at 950 °C. Mechanical (bending) strength is not modified significantly, when OSWR content does not exceed 3 %, while MOR is reduced by 20 % when OSWR percentage attains 6 %, and this trend seems to decelerate furthermore at higher % OSWR contents. Nevertheless, by sintering at 850 °C or 950 °C, the brick bending strength remains stable, while, at 1050 °C, it increases by approximately 27 %, and much more at 1150 °C.

Particularly, thermal conductivity of the produced ceramic bricks is reduced by as much as 21.2 % for only 3 % addition of OSWR into the clay mixture (0.385 Wm^{-1}K^{-1}), while the three point bending strength (M.O.R.) remains around 7 MPa.

In conclusion, beneficial utilization of OSWR can be attained in two ways:

a) production of high density bricks, at low % addition of OSWR as a body fuel;

b) production of lower density bricks at OSWR percentages greater than 3 %, both as a body fuel and pore-former agent.

Hence, the valorization of an olive-oil industry by-product can be achieved, while the fired clay brick industry can benefit from lower fuel consumption during the manufacturing process. The novel and greener ceramics so-produced are almost equivalent to the traditional ones, while also exhibiting lower thermal conductivity thus increased thermal insulation capability.

References

[1] Ducom, G., Gautier, M., Pietraccini, M., Tagutchou, J.-P., Lebouil, D., Gourdon, R. (2020). Comparative analyses of three olive mill solid residues from different countries and processes for energy recovery by gasification. Renewable Energy, 145, 180–189. doi: https://doi.org/10.1016/j.renene.2019.05.116

[2] Zabaniotou, A. (2018). Redesigning a bioenergy sector in EU in the transition to circular waste-based Bioeconomy-A multidisciplinary review. Journal of Cleaner Production, 177, 197–206. doi: https://doi.org/10.1016/j.jclepro.2017.12.172

[3] Mudhoo, A., Torres-Mayanga, P. C., Forster-Carneiro, T., Sivagurunathan, P., Kumar, G., Komilis, D., Sánchez, A. (2018). A review of research trends in the enhancement of biomass-to-hydrogen conversion. Waste Management, 79, 580–594. doi: https://doi.org/10.1016/j.wasman.2018.08.028

[4] Wang, A., Zheng, Z., Li, R., Hu, D., Lu, Y., Luo, H., Yan, K. (2019). Biomass-derived porous carbon highly efficient for removal of Pb(II) and Cd(II). Green Energy & Environment, 4 (4), 414–423. doi: https://doi.org/10.1016/j.gee.2019.05.002

[5] Demir, I. (2008). Effect of organic residues addition on the technological properties of clay bricks. Waste Management, 28 (3), 622–627. doi: https://doi.org/10.1016/j.wasman.2007.03.019

[6] Vlyssides, A. G., Barampouti, E. M. P., Mai, S. T. (2007). Physical characteristics of olive stone wooden residues: possible bulking material for composting process. Biodegradation, 19 (2), 209–214. doi: https://doi.org/10.1007/s10532-007-9127-5

[7] Federici, F., Fava, F., Kalogerakis, N., Mantzavinos, D. (2009). Valorisation of agro-industrial by-products, effluents and waste: concept, opportunities and the case of olive mill wastewaters. Journal of Chemical Technology & Biotechnology, 84 (6), 895–900. doi: https://doi.org/10.1002/jctb.2165

[8] De la Casa, J. A., Romero, I., Jiménez, J., Castro, E. (2012). Fired clay masonry units production incorporating two-phase olive mill waste (alperujo). Ceramics International, 38 (6), 5027–5037. doi: https://doi.org/10.1016/j.ceramint.2012.03.003

[9] Azbar, N., Bayram, A., Filibeli, A., Muezzinoglu, A., Sengul, F., Ozer, A. (2004). A Review of Waste Management Options in Olive Oil Production. Critical Reviews in Environmental Science and Technology, 34 (3), 209–247. doi: https://doi.org/10.1080/10643380490279932

[10] Hamza, W., Eloussaief, M., Mekki, H., Benzina, M. (2013). Physicochemical Characterization and Valorization of Tunisian Olive Oil Mill Wastewater Sludge in Ceramic Product. Transactions of the Indian Ceramic Society, 72 (4), 233–240. doi: https://doi.org/10.1080/0371750x.2013.870752

[11] Cotes Palomino, M. T., Martínez García, C., Iglesias Godino, F. J., Eliche Quesada, D., Corpas Iglesias, F. A. (2015). Study of the wet pomace as an additive in ceramic material. Desalination and Water Treatment, 57 (6), 2712–2718. doi: https://doi.org/10.1080/19443994.2015.1035678

[12] Cotes Palomino, M. T., Martínez García, C., Iglesias Godino, F. J., Eliche Quesada, D., Pérez Latorre, F. J., Calero de Hoces, F. M., Corpas Iglesias, F. A. (2015). Study of Waste from Two-Phase Olive Oil Extraction as an Additive in Ceramic Material. Key Engineering Materials, 663, 86–93. doi: https://doi.org/10.4028/www.scientific.net/kem.663.86

[13] Ruppik, M. (2006). Einsatz organischer und anorganischer Porosierungsstoffe in der Ziegelindustrie. Zi Ziegelindustrie international, 59 (8), 22–29.

[14] Commission Decision of 18 July 2007 establishing guidelines for the monitoring and reporting of greenhouse gas emissions pursuant to Directive 2003/87/EC of the European Parliament and of the Council (notified under document number C(2007) 3416) (Text with EEA relevance) (2007/589/EC). L229. Official Journal of the European Union. Available at: https://eur-lex.europa.eu/legal-content/EN/ALL/?uri=CELEX%3A32007D0589

[15] Smykatz-Kloss, W. (1974). Differential Thermal Analysis, Applications and Results in Mineralogy - (Minerals and Rocks, Vol. II). Springer-Verlag, 185.

[16] Karayannis, V. G. (2016). Development of extruded and fired bricks with steel industry byproduct towards circular economy. Journal of Building Engineering, 7, 382–387. doi: https://doi.org/10.1016/j.jobe.2016.08.003